Simona Colantonio

Applications of Mass Spectrometry in Proteomics and Pharmacokinetics

Thesis submitted
for the degree of *Philosophiæ Doctor*
Faculty of Pharmacy
Sapienza Università di Roma, Italy
2008

For my Father

Index

Acknowledgements

I have many people to thank for their help and assistence. In the first place Professor Francesco Gasparrini and Ilaria d'Acquarica for all the help they always have been giving me, from the early stages of my scientific adventure to these days.
I'd also love to thank Doctor Gordon Whiteley, director of the former Clinical Proteomic Reference laboratory (Advanced Technology Program, SAIC-Frederick, Inc., NCI-Frederick, Frederick, MD USA)*, where I learned everything I know about Proteomic Profiling. Doctor Robert Fisher has been so kind to accept me in his group Protein Chemistry Laboratory* (Advanced Technology Program, SAIC-Frederick, Inc., NCI-Frederick, Frederick, MD USA) *to complete my studies and I'll never be able to thank him enough.*
Last but not least my Family that supports me "no matter what" and my Father that gave me the courage to believe in myself and to follow my dreams, with his words and with the example of his own life. I wouldn't be here today, if it wasn't for Him.

Chapter I

PHARMACOKINETICS OF GEMCITABINE

Pharmacokinetics of Gemcitabine

Introduction

1. Pancreatic Cancer (PC)

In spite of advances made in the management of the other more common cancers of the gastrointestinal tract, significant progress in the treatment of pancreatic cancer (PC) remains elusive.

The pancreas is a coarsely lobulated yellowish gland that lies somewhat obliquely in the retroperitoneum, extending from the duodenal C loop and running cephalad to the splenic hilum. The gland is divided into somewhat arbitrary sections: the head (with a small, posterior uncinate process), neck, body, and tail. Tumors of the pancreatic head arise to the right of the superior mesenteric vein–portal vein confluence and include tumors of uncinate origin. Tumors of the pancreatic body arise between the superior mesenteric vein–portal vein confluence and the left lateral aspect of the aorta. Tumors of the pancreatic tail are located lateral to the aorta, extending out to the splenic hilum [1].

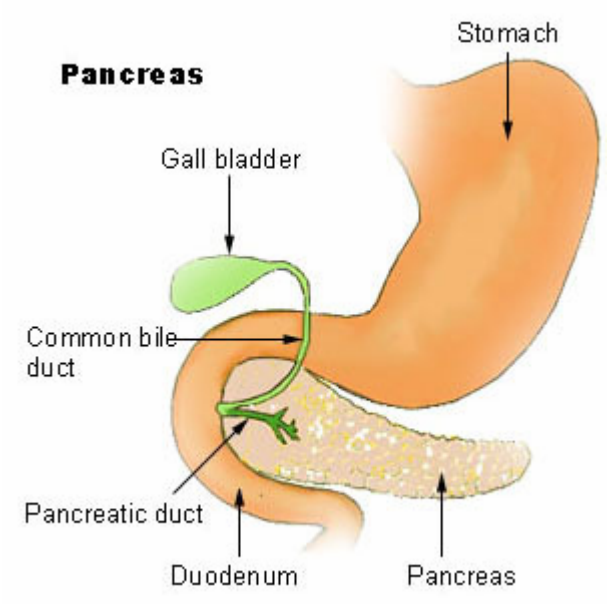

Fig. 1

The prognosis for pancreatic cancer is unfavorable in the most of the cases and pancreatic adenocarcinoma occurs in 80% of the diagnosed patients, in only the 10% of them the disease is confined to the pancreas. Of the remaining patients, 40% have regional involvement at diagnosis and 50% demonstrate metastasis [1]. The surgical resection is the only chance for long-term survival, but when the disease is metastatic or locally invasive, the surgery is no longer a feasible approach. Less than 20 % of the patients have resectable disease at diagnosis. Accurate preoperative staging is important in determining which patients will be able to undergo curative resection, because in many cases patients, who seemed to be operative candidates preoperatively, were subsequently found to have local spread or distant diseases.

Despite the continuous progresses in the imaging diagnosis and the availability of new therapeutic system, the mortality rate for pancreatic cancer is still constant, if not increasing. Including all the stages of the disease, only the 20% of the patients survive within the first year and the 5 years survival rate is only 5%. The number of new cases of pancreatic cancer in 2007 increased to 37,170 in the USA [2], with an almost identical rate of death, probably because most pancreatic cancer are advanced at the moment of the diagnosis, since many early symptoms often are no recognized. Some of the common symptoms are abdominal pain, jaundice, anorexia, weight loss, and depression and they depend on the size and the location of the tumor and of the metastasis as well. In general in patients with liver metastasis, the clinical state deteriorates rapidly.

Epidemiology, etiology and genetics aspects

In the United States, incidence rates of PC increased threefold between 1920 and 1978, an increase that has also been observed in other developed countries [3, 4].Rates for men and for women have modestly declined since 1978 and appear to have stabilized at the current rates. A portion of the increased incidence may have been attributable to more accurate disease

diagnosis and less disease misclassification. Additionally, improved surveillance may account for a small portion of the increased incidence.
A positive relationship exists between certain environmental exposures and cases of PC, including personal cigarette smoking, environmental tobacco smoke (ETS), and chemical exposures. [3, 4]
It has been proved that tobacco smoke exposure plays a significant role in the development of PC. It has been estimated that tobacco smoking contributes to the development of 20% to 30% of PCs.[4] The strongest associations between cigarette smoking and PC have been observed when the pack-years smoked were within the previous 10 years.[3] Smoking cessation can reduce this risk. Indeed, Mulder et al. [5] have estimated that moderate reduction in smoking in Europe could save almost 68,000 lives that would otherwise be lost to PC by the year 2020.
Also a certain number of demographic risk factors have been associated with the development of PC worldwide and they included are older age (most PCs occur between the ages of 60 and 80), African American race, low socioeconomic status, and Ashkenazi Jewish heritage (related to germline mutations) [4].
Several conditions such as a history of diabetes mellitus (DM), chronic cirrhosis, pancreatitis, a high-fat/cholesterol diet, and prior cholecystectomy [3, 4] have been associated with an increased risk of PC. The association between DM, pancreatitis, and the development of PC is complex because PC, by destroying the pancreatic parenchyma, can itself cause DM and pancreatitis.
Metaanalysis of 20 epidemiologic studies on the association between DM and PC confirms that the pooled relative risk of PC in persons with DM for 5 years is double (relative risk, 2.0; confidence interval, 1.3 to 2.2) the risk of persons without DM [3]. The analysis further suggested that impaired glucose tolerance, insulin resistance, and hyperinsulinemia are involved in the etiology of PC.
Ojajarvi, I.A., et al. performed a metaanalysis of 20 population studies of occupational exposures and PC from journal publications during the period

1969 to 1998 [6]. Exposure to chlorinated hydrocarbon solvents, nickel and nickel compounds, chromium compounds, polycyclic aromatic hydrocarbons, organochlorine insecticides, silica dust, and aliphatic solvents conveyed elevated risk ratios. Overall, the occupational etiologic fraction for PC was estimated at 12%, but it increased to 29% when the chlorinated hydrocarbon solvents were considered in a subpopulation.

Elevated serum levels of organochloride compounds (dichlorodiphenyltrichlorethane, dichlorodiphenyldichloroethylene, and polychlorinated biphenyls), are also associated with the development of PC [7]. Approximately 90% of PC patients have an acquired K-ras oncogene mutation. In a case-control study, PC patients with K-ras mutations had significantly higher levels of dichlorodiphenyltrichlorethane, dichlorodiphenyldichloroethylene, and three polychlorinated biphenyl compounds compared to PC patients without the K-ras mutation and to those in the control group. These compounds are postulated to enhance the actions of K-ras rather than cause the mutation, suggesting a gene-environment interaction or effect modification. It may also be that these compounds interact with premalignant ductal precursor lesions and accelerate their malignant progression.

Other possible factors that have been repeatedly studied, with no consistent association with the development of PC, include moderate alcohol intake, nonhereditary and acute pancreatitis, and coffee drinking.

PC is characterized by inherited and acquired genetic mutations [8]. Genetic predisposition plays a small but significant role in PC risk. Activation of the oncogene K-ras plus inactivation of tumor suppressor genes (p53, DPC4, p16, and BRCA2) are associated with the development of PC. Nearly 90% of all cases of PC have p16 mutations, 75% have p53 mutations, and 55% have DPC4 mutations. Fewer than 4% of PC cases appear to involve dysfunction of the various DNA mismatch repair genes [microsatellite instability (MIN)].

It is estimated that 10% to 20% of PCs are hereditary or have a familial link. Multiple lines of evidence support this. Cohort studies have shown an increased risk of developing PC among individuals who report a family history

of PC. Tersmette et al. [9] have shown that this risk increases with the number of affected members in the family.

Pathology aspects of PC

PC is not a single disease, in fact, an array of biologically and clinically distinct neoplasms can arise in the pancreas. Neoplasms of the pancreas can be broadly grouped into those with predominantly exocrine differentiation and those with endocrine differentiation. The vast majority of malignancies of the pancreas are solid infiltrating ductal adenocarcinomas, and the term PC is therefore often used synonymously with infiltrating ductal adenocarcinoma. *Exocrine neoplasms* of the pancreas can be further subdivided into cystic and solid tumors.

- *Solid neoplasms of the exocrine pancreas* – The most common solid neoplasms of the exocrine pancreas are the infiltrating ductal adenocarcinoma and variants of ductal adenocarcinoma, acinar cell carcinoma, and pancreatoblastoma. Infiltrating ductal adenocarcinomas are malignant epithelial neoplasms that show glandular or ductal differentiation [10]. Most arise in patients between the ages of 60 and 80 years, and men outnumber women (male-female ratio, 1.35:1.0). The majority of ductal adenocarcinomas arise in the head of the gland, but they can also arise in the body or in the tail or even diffusely involve multiple parts of the pancreas. Grossly, infiltrating ductal adenocarcinomas form firm, poorly defined white-yellow masses. These carcinomas often extend beyond the grossly identifiable tumor, and invasion into large vessels and adjacent organs is common.
- *Cystic neoplasms of the exocrine pancreas* – The most common cystic neoplasms of the pancreas include mucinous cystic neoplasms, intraductal papillary mucinous neoplasms (IPMNs), serous cystic neoplasms, and solid and pseudopapillary neoplasms. Mucinous cystic neoplasms are much more common in women (90%) than in men [11]. These distinctive neoplasms arise in the tail of the gland more

frequently than in the head of the gland. Grossly, mucinous cystic neoplasms are composed of large cysts that contain thick tenacious mucin [10, 11]. The cysts are separated by thick septae and do not communicate with the larger pancreatic ducts. These cysts are lined by a columnar mucin-producing epithelium, and the stroma surrounding the cysts has a histologic appearance similar to ovarian stroma. The epithelium can show varying degrees of cytologic and architectural atypia, and one-third of mucinous cystic neoplasms are associated with an invasive carcinoma, usually an invasive ductal adenocarcinoma.

Endocrine pancreatic cancer, also known as islet cell cancer, is a rare cancer. Only about 5 percent of the total of the cases of pancreatic cancers begin in the islet cells. Endocrine pancreatic tumors are defined "functioning" or "non-functioning" depending on their ability to secrete hormones. Most functioning islet cell tumors are benign, while non-functioning tumors are more likely to be malignant. Malignant tumors are called islet cell cancers or islet cell carcinomas. The three most common types are:

- *Gastrinoma*, which causes a hypersecretion of the gastrin hormone, causing increased stomach acid and leading to ulcers.
- *Insulinoma*, in which the excess of the production of insulin leads to hypoglycemia.
- *Glucagonoma*, in which the excessive glucagons hormone causes the opposite condition, hyperglycemia.

2. Gemcitabine

Pancreatic cancer was the first disease for which the Food and Drug Administration (FDA) approved a treatment on the basis of improved quality of life (QOL) rather than response rate to prolonged survival [11]. A three-way randomized clinical trial (RTC) in 1985 had shown that the treatment of metastatic pancreas cancer with bolus 5-fluorouracil (5-FU) was as effective as the association of 5-FU with doxorubicin or as the combination plus mitomycin (MMC) [12]. Bolus 5-FU remained the standard therapy for 12 years, until there was the evidence the gemcitabine treatment improved QOL in a prospectively randomized study that started in 1995 [13]. Even though there was no difference in survival between the two treatment the FDA approved gemcitabine hydrochloride for the palliative treatment of pancreatic cancer in May 1996, affirming the importance of QOL as a legitimate clinical end point in cancer chemotherapy [14].

Gemcitabine is a synthetic nucleoside analog in which the hydrogens on the 2' carbons of deoxycytidine are replaced by fluorines (Figure 1). It is marketed as Gemzar by Eli Lilly.

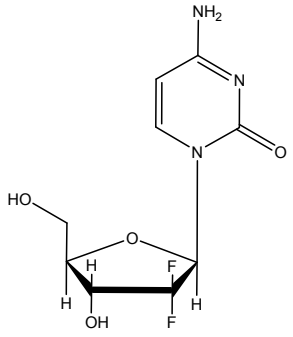

Figure 2

Mechanism of action

Gemcitabine (or 2´,2´-difluorodeoxycitidine, dFdC) is a prodrug. After intravenous injection, it enters cells via active nucleoside transporters [15]. Then, plasma and liver cytidine deamidase convert gemcitabine to 2´,2´-difluorodeoxyuridine (dFdU), a compound which has little cytotoxic activity.

Gemcitabine undergoes intracellular metabolism by deoxycytidine kinase to form the mono-phosphate, di-phosphate and tri-phosphate metabolites (Figure 2).

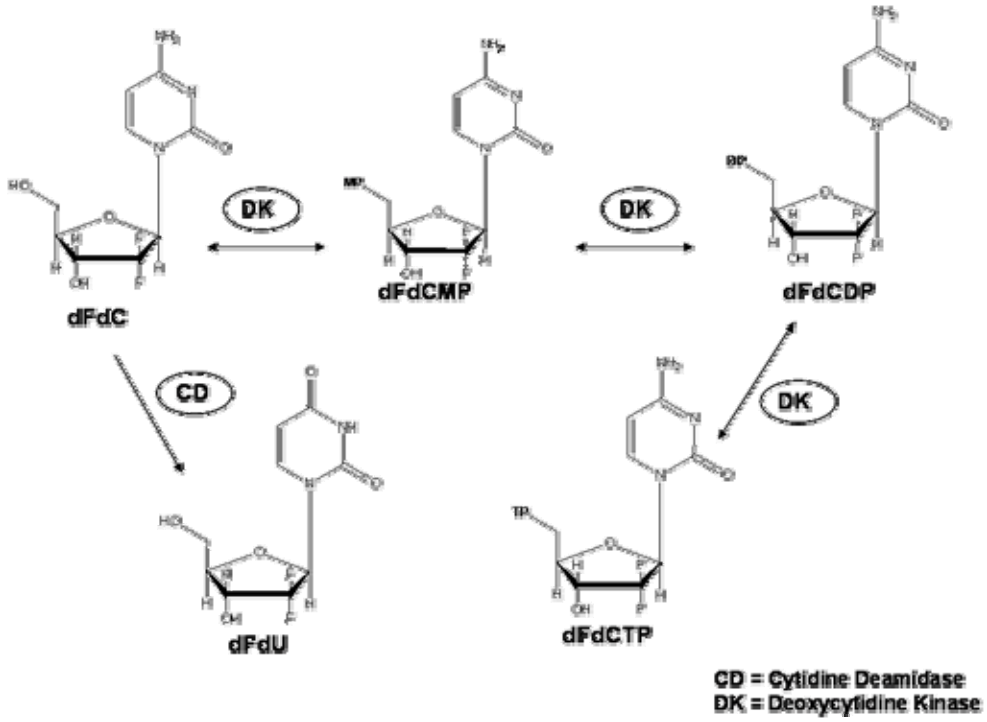

Figure 2

Metabolic scheme for gemcitabine showing conversion to its active and inactive metabolites.

As with fluorouracil and other analogues of pyrimidines, the drug replaces one of the building blocks of nucleic acids, in this case cytidine, during DNA replication and reparation [16]. The process arrests tumor growth, as new nucleosides cannot be attached to the "faulty" nucleoside, resulting in apoptosis (cellular "suicide").

The active nucleosides are di-phosphate (dFdCDP) and tri-phosphate (dFdCTP) 2´,2´-difluorodeoxycytidine and they show a combined action which results in an effective cytotoxic effect at the tumor site. dFdCDP inhibits ribonucleotide reductase, the enzyme that catalyzed the generation of deoxynucleoside tri-phosphates for DNA synthesis. The result of this action is the reduction of the tri-phosphate deoxycytidine (dCTP) concentration. The triphosphate metabolite (dFdCTP) competes with dCTP for incorporation DNA

and the dFdCDP induced reduction of the dCTP concentration enhances the incorporation of dFdCTP into the DNA which causes chain termination with a mechanism known as masked chain termination [17], in which after the drug metabolite incorporation into the DNA chain, only one more deoxynucleotide is added [18]. This "extra" nucleotide may be important in hiding the dFdCTP from DNA repair enzymes, as the incorporated dFdCMP appears to be resistant to repair, so the ability of cells to incorporate dFdCTP into DNA is critical for gemcitabine-induced apoptosis [17]. The result is that DNA polymerase is unable to eliminate gemcitabine nucleotide and repair the DNA strain. It has been proved that in CEM T lymphoblastoid cells, gemcitabine induces internucleosomal DNA fragmentation which induces apoptosis [19]. Gemcitabine exhibits cell phase specificity, primarily killing cells undergoing DNA synthesis (S-phase) and also blocking the progression of cells through the G1/S-phase boundary. Furthermore, the unique actions that gemcitabine metabolites exert on cellular regulatory processes serve to enhance the overall inhibitory activities on cell growth. This interaction is termed "self-potentiation" and is evidenced in very few other anticancer drugs [20].

Pharmacokinetics aspects

Gemcitabine is administered as an intravenous infusion. The pharmacokinetics of the parent compound is largely determined by deamination, and the predominant urinary elimination product is the inactive metabolite dFdU. Gemcitabine has a short plasma half-life of approximately 15 minutes, with women and elderly subjects having slower clearance [21]. Clearance is dose-independent but can vary widely among individuals.

Incorporation into DNA is time and concentration dependent [22] and other in vitro and in vivo studies confirmed that the amount of gemcitabine incorporated into cellular DNA affects the cytotoxicity of the drug. These studies proved that the effective plasma concentration for gemcitabine is in

the range of 10umol/L and 20umol/L (2.99-5.99 ug/mL): in this range there is the maximum intracellular concentration of gemcitabine triphosphate.

Conversion of gemcitabine to its active metabolite dFdCMP by deoxycytidine kinase is saturated at infusion rates of approximately 10 mg/m^2 per minute, which produce plasma drug concentrations in the range of 15 to 20 M [16, 23]. The fixed dose rate (FDR) infusion is based on studies demonstrating that gemcitabine was saturable in peripheral blood mononuclear cells when gemcitabine was administered at different doses during a standard 30-min infusion [16, 21].

In an attempt to increase dFdCTP formation, the duration of infusion at this maximum concentration has been extended to 150 minutes. In contrast to a fixed infusion duration of 30 minutes, the 150-minute infusion produces a higher level of dFdCTP within peripheral blood mononuclear cells, increases the degree of myelosuppression, but has uncertain effects on antitumor activity [24].

The activity of dFdCTP on DNA repair mechanisms may allow for increased cytotoxicity of other chemotherapeutic agents, particularly platinum compounds. Preclinical studies of tumor cell lines show that cisplatin-DNA adducts are enhanced in the presence of gemcitabine, presumably through suppression of nuclear excision repair [25].

FDR infusion of gemcitabine improved survival of patients with pancreatic cancer compared with the standard dose-intense protocol, according to the results of a randomized phase II prospective trial [24]. In this study 92 patients with locally advanced and metastatic pancreatic adenocarcinoma were treated with 2,200 mg/m^2 gemcitabine over 30 minutes (standard arm) or 1,500 mg/m^2 gemcitabine over 150 minutes (FDR arm) on days 1, 8, and 15 of every 4-week cycle. Time to progression and objective response were comparable in both arms of this study, but a modest overall improvement in survival –with an unusually high 1-, 2-, and 3-year survivorship – occurred in the patients of the

FDR arm, along with an advantage in accumulation of gemcitabine triphosphate proved by pharmokinetics studies. Even though this study didn't definitively favor one regimen over the other, the results suggested the FDR administration technique could undergo further evaluation studies, either alone or in combination with other agents.

Milella and other [26] have chosen a FDR infusion of gemcitabine for 100 minutes with the dose of 1000 mg/m2, which is 33% less the dosage raccomended in Phase I Studies, gaining encouraging results in terms of patients survival and toxicity. Especially from a toxicity standpoint, this different regimen resulted in a consistently lower hematologic toxicity. In general this 100 minutes infusion is active and extremely well tolerated and gives encouraging survival and case based reasoning outcomes.

Pharmacotoxicity

Myelosuppression is the principal clinical toxic effect of gemcitabine. In general, the longer is the duration of infusion, the greater is the myelosuppression. Other kinds of toxicities not related with hematologic aspects include a flu-like syndrome, asthenia, and mild elevation in liver transaminases may occur in 40% or more of patients. Severe toxicities are rare, but sometimes interstitial pneumonitis may occur and is responsive to steroids. Another rare but serious side is a slowly progressive hemolytic uremic syndrome in patients treated with gemcitabine for many months and it requires drug discontinuation [27]. Gemcitabine is a very potent radiosensitizer and should not be used with radiotherapy except in closely monitored clinical trials [28].

Aim of the study

The aim of the study was to evaluate if hepatic dysfunction leads to increased toxicity of gemcitabine at fixed dose rate and to characterize the pharmacokinetics of gemcitabine and its major metabolite 2´,2´-difluorodeoxyuridine (dFdU). A hyphenated HPLC-MS/MS method has been developed in order to investigate the pharmacokinetics of the drug and its metabolite in human plasma.

Experimental

1. Materials

Gemcitabine (dFdC) and its major metabolite 2´,2´-difluorodeoxyuridine (dFdU) were provided by Eli Lilly (Lilly Corporate Center, Indianapolis, USA) for analytical and reference standards. HPLC grade acetonitrile was obtained from Carlo Erba (Milan, Italy). Filtered deionized 18Ω HPLC grade water was supplied via a MilliQ water purification system (Millipore, Amsterdam, The Netherlands). Analytical grade solvents such as iso-propanol and ethyl-acetate were supplied by Sigma Aldrich (St Louis, MO, USA), along with ammonium acetate and the internal standard (I.S.) 2'-deoxycytidine (dC). Control human plasma samples, used to prepare daily standard calibration curves and quality control (QC) samples, were obtained from volunteers.

2. Equipment

Chromatography was conducted using an Agilent 1100 Series System (Agilent Technologies, Palo Alto, CA, USA) equipped with a binary pump and an automatic injector, vacuum on- line degasser. The HPLC was interfaced with an ion trap mass spectrometer Agilent 6300 (Agilent Technologies, Palo Alto, CA, USA). The mass spectrometer was equipped with an ESI source. The injection system of the Agilent 1100 was fitted with a 50 μL PEEK loop and all tubing post injection was 0.05 mm PEEK. Software used for data acquisition and integration was Agilent ChemStation.

3. Mass spectrometry optimization

The mass spectrometer was operated in the positive ion mode. The optimized mass spectrometry conditions were the following: capillary voltage -3.5 kV; end plate offset voltage-500 V; capillary exit voltage 110.9 V; nebuliser pressure 70 psi; drying gas flow 12 L min−1; temperature 350°C.
The mass spectrometry conditions for each compound were determined by direct infusion in water/acetonitrile (80/20, v/v) plus 0.5% acetic acid.

The mass spectrometer was operated in full scan and multiple reaction monitoring (MRM) modes performed by ion fragmentation over a range of 100–300 m/z.. Quantitation was developed in positive MRM mode by monitoring determined transitions pairs of m/z 264 (molecular ion)/ 112 (major fragment ion) for gemcitabine, m/z 265 (molecular ion)/ 113 (major fragment ion) for dFdU and m/z 228 (molecular ion)/ 112 (major fragment ion) for the internal standard 2'-deoxycytidine (dC).

4. Chromatographic conditions

The chromatographic separation was carried out on a Symmetry C18 (4.6*250mm I.D, 5µm particle size) protected by a sentry guard column Symmetry C18 (3.9*20mm). Mobile Phase: A, 0.5% acetic acid in water; B, 0.5% acetic acid in acetonitrile. Gradient elution procedure: initial conditions – B 2% for 2 min, step 1 – B 2-50% in 10 min, step 2 – B 50-70% in 1 min, step 3 – B 70% for 4 min, return at the initial conditions – B 2% in 2 minutes and equilibration for B 2% for 10 minutes before the next injection. The injected volume was 20 uL.

5. Sample collection

Blood samples (5 to 10 mL each patient) were drawn via an indwelling peripheral catheter or via peripheral venipuncture, into tubes containing heparin. Tetrahydrouridine (Calbiochem-Novabiochem Corp La Jolla CA, USA), a cytidine deaminase inhibitor, was then added (0.1 ml of a 10 mg/ml solution) to prevent *ex vivo* Gemcitabine deamination. Samples were collected 30 minutes before Gemcitabine infusion, at 30, 60 and 80 minutes during the infusion, at the end of the infusion, and at 5, 30, 90, 180 and 240 minutes after the completion of the infusion.

Blood samples were immediately centrifuged at 1000 rpm at room temperature for 10 minutes. The resulting plasma was frozen and stored at -20°C until analysis.

6. Standards and quality control solutions

For Standards a stock solution in methanol for each analyte was accurately prepared at the concentration of approximately 1 mg/mL. Purity and weight variations were adjusted by diluting approximately 1:10 to give an accurate stock solution of 0.1 mg/mL. All stock solutions were stored at -20°C. Working solutions (A-G) (see Table 1) containing both analytes, to obtain the standard points of the calibration curves and working solutions (L, M and H, see Table 2) to prepare quality control (QC) samples were obtained by combining different amounts of the stock solutions and control human plasma samples obtained from healthy volunteers. The human plasma samples were spiked with each working solutions to obtain dFdC and dFdU at the final concentration reported in Table 1 and Table 2.

Table 1 – Standard samples

Standard	dFdC (ug/mL)	dFdU (ug/mL)	
A	5	5	100 uL stock solution dFdC (100ug/mL) + 100 uL stock solution dFdU (100ug/mL) + 1800 uL plasma
B	2.5	2.5	1000 uL A + 1000 uL plasma
C	1.25	1.25	1000 uL B + 1000 uL plasma
D	0.62_5	0.62_5	1000 uL C + 1000 uL plasma
E	0.31	0.31	1000 uL D + 1000 uL plasma
F	0.15	0.15	1000 uL E + 1000 uL plasma
G	0.08	0.08	1000 uL F + 1000 uL plasma

Table 2 – QC samples

Quality control Standard	dFdC (ug/mL)	dFdU (ug/mL)	
H	3.2	3.2	64 uL stock solution dFdC (100ug/mL) + 64 uL stock solution dFdU (100ug/mL) + 1872 uL plasma
L	0.8	0.8	80 uL H + 240 uL plasma
M	0.2	0.2	80 uL B + 240 uL plasma

The stock solution for the internal standard (IS) was 20 ug/mL. The IS working solution was prepared at 20ug/mL by diluting the stock solution with methanol. 10 uL of the IS working solution has been added to 200 uL of each sample.

7. Plasma samples preparation

Plasma samples (200 uL) were mixed with 200 ug of IS (10 uL of 20 ug/mL) and added with 200 uL of isopropyl alcohol and 400 uL of ethyl acetate in a 1.5 mL Eppendorf tube. After vortexing samples were allowed to stay at room temperature for 5 minutes. Then the mixture was centrifuged at 4°C for 10 minutes at 13000 rpm. The supernatant was collected and transferred to a second Eppendorf tube to be dried under nitrogen. The samples were reconstituted in water plus 0.5% acetic acid and after brief vortexing centrifuged at 4000 rpm for 10 min.

8. Data handling and calculations

Quant Analysis software was used to process the quantitative data. A calibration curve for each analyte was determined using linear square analysis in order to quantify plasma concentrations for Gemcitabine and dFdU. The two analytes concentration were calculated from the ratio of the Gemcitabine and dFdU peaks area to the area of IS using least squares linear regression.

9. Assay validation

The linearity of the calibration curves was validated over three days and calculated by the ratio of the HPLC-MS/MS peaks areas for dFdC/IS and dFdU/IS to the nominal total amount of dFdC and dFdU in the sample. The linearity was determinated by a regression model and by calculating the Pearson's correlation factor R^2 and by a comparison of the true and back-calculated concentrations of the calibration standards. Within-day and between-day variabilities were measured as coefficient of variation. The recovery of the extraction was calculated by comparing the peak areas of each standard concentration against equivalent absolute standard dilutions. Lower limit of quantitation (LLOQ) was for both Gemcitabine and dFdU determined by successive standard solution dilutions calculating the signal to noise ratio, the limit set for detection was a signal/noise ratio of 3.

10. Pharmacokinetics parameters

Pharmacokinetic parameters were estimated by non-compartmental method analysis from plasma concentrations of Gemcitabine and its major metabolite. at different timing before, during and after the FDR infusion.

The analysis of Gemcitabine e dFdU pharmacokinetics focused on:

- *Plasmatic peak concentration* (Cmax, µg), determined graphically from the observed experimental values;
- *Area Under the plasma concentration-time Curve* (*AUC*, µg d/ml) from the first to the last sampling time: calculated according to the trapezoidal rule
- *Total body clearance* (*Cl,* Lh/m2): calculated as ration of dose in µg/AUC (µg h/ml)
- *Half-Time* (t1/2,d): calculated as ln2/Kel (d-1)
- *Rate of Elimination* (Kel, d-1): calculated as the negative slope of the log-linear elimination phase of the plasma concentration–time.

1. Sample Preparation

Precipitation of plasma proteins was the most practical and effective sample preparation procedure: since these nucleosides are polar, after protein precipitation they most likely stay in the supernatant. To optimize the protein precipitation procedure we tried different ratios of the two solvent isopropyl alcohol and ethyl acetate (1:1, 1:2, 1:3). We also tried to add a mixture of the two solvents and comparing the obtained results with the results obtained from consecutive addition experiments inverting the order of the solvents. The addition of isopropyl alcohol and then ethyl acetate in the relative ratio 1:2, followed by 5 minutes of standing of the sample at room temperature and a centrifugation step at 4°C for 10 minutes at 13000 rpm, showed the best results in terms of recovery and reproducibility. After centrifugation we evaluated the presence or absence of a clear supernatant by visual inspection and we proceeded to dry the supernatant under a nitrogen stream. After reconstitution of the sample with an HPLC compatible buffer, we centrifuged again the sample to assure the complete clearness of the sample. This extraction method requires a short time and allowed us to process a quite large number of samples at the same time more cost effectively compared to other method previously reported in literature [29-31]. Samples from the same patient were treated at the same time.

2. Recovery

The recovery of dFdU and dFdC extracted from the human plasma is shown in Table 3. The sample deproteinization leaded to a good percentage of recovery always ≥80% evaluated over three concentrations and in triplicate. The absence of significant variations (<6%) for the areas of both analytes exclude the possibility of any matrix effects of ion suppression or enhancement.

Table 3

Spiked concentration ug/mL	Recovery Ratio (%) ± SD	CV%
dFdC		
0.200	84.3 ± 2.0	2.0
0.500	87.2 ± 2.3	2.9
4.000	82.3 ± 2.3	2.7
dFdU		
0.200	86.7 ± 3.1	5.0
1.000	83.2 ± 2.7	3.6
5.000	80.1 ± 3.1	4.9

3. Mass Spectrometry

Most of the methods reported in the literature are based on UV detection and show a sensitive range between 0.1 and 50 ug/mL [32-34]. Some methods also involve diode array detection [29, 30, 35]. This proved to be insufficient for the detection of gemcitabine as long infusion [30, 33, 35], because of the lack of sensitivity and selectivity of the detection, absolutely necessary for the presence of possible random endogenous peaks visible in the UV detection that can interfere with the quantitative determination of the analytes. Multiple reaction monitoring as acquisition mode guarantees high sensitivity and selectivity.

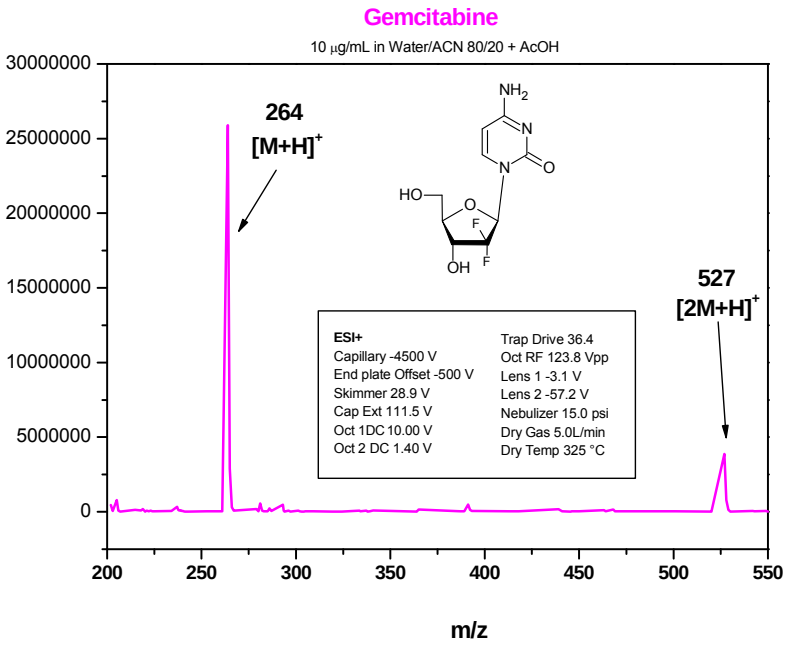
Gemcitabine
10 μg/mL in Water/ACN 80/20 + AcOH
264
[M+H]+
527
[2M+H]+
ESI+
Capillary -4500 V
End plate Offset -500 V
Skimmer 28.9 V
Cap Ext 111.5 V
Oct 1DC 10.00 V
Oct 2 DC 1.40 V
Trap Drive 36.4
Oct RF 123.8 Vpp
Lens 1 -3.1 V
Lens 2 -57.2 V
Nebulizer 15.0 psi
Dry Gas 5.0L/min
Dry Temp 325 °C
m/z

Fig. 5

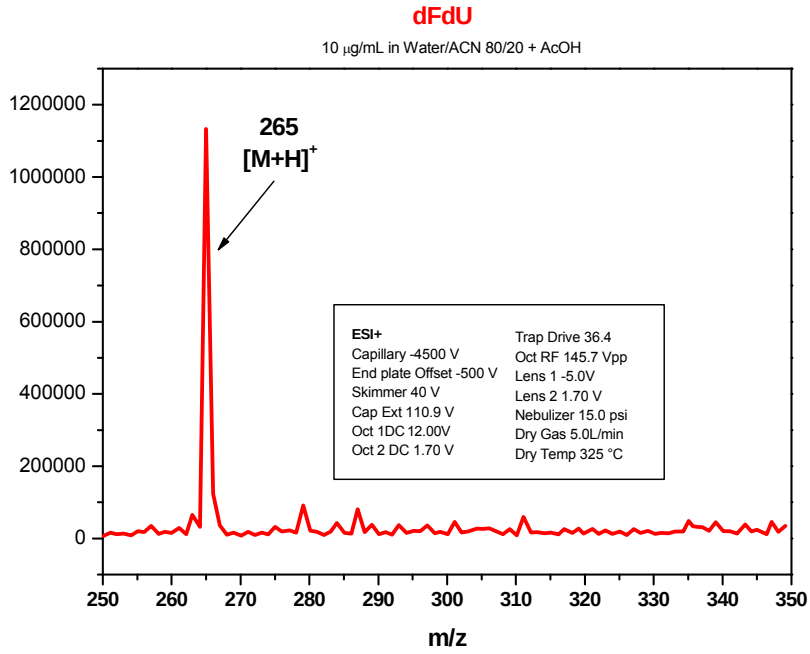
dFdU
10 μg/mL in Water/ACN 80/20 + AcOH
265
[M+H]+
ESI+
Capillary -4500 V
End plate Offset -500 V
Skimmer 40 V
Cap Ext 110.9 V
Oct 1DC 12.00V
Oct 2 DC 1.70 V
Trap Drive 36.4
Oct RF 145.7 Vpp
Lens 1 -5.0V
Lens 2 1.70 V
Nebulizer 15.0 psi
Dry Gas 5.0L/min
Dry Temp 325 °C
m/z

Fig. 6

Figure 4 shows a typical full scan spectrum of dFdC and figure 5 shows the mass spectrum of dFdU. The signal at 264 m/z for dFdC and 265 m/z for its metabolite are clearly the most intense and they both correspond to the molecular ions $[M+H]^+$. No adducts were observed corresponding to $[2M+H]^+$, $[M+Na]^+$ or $[M+K]^+$. The same situation was found in the dC (IS) mass spectrum, in which the molecular ion corresponded to the signal at 228 m/z. In MS isolation and fragmentation experiments of the ions, the primary fragments for each of them resulted to be 112 m/z for dFdC, 113 m/z for dFdU and 112 for dC, due to the loss of the sugar moiety of the nucleoside and the synthetic nucleoside analogs (Fig. 6).

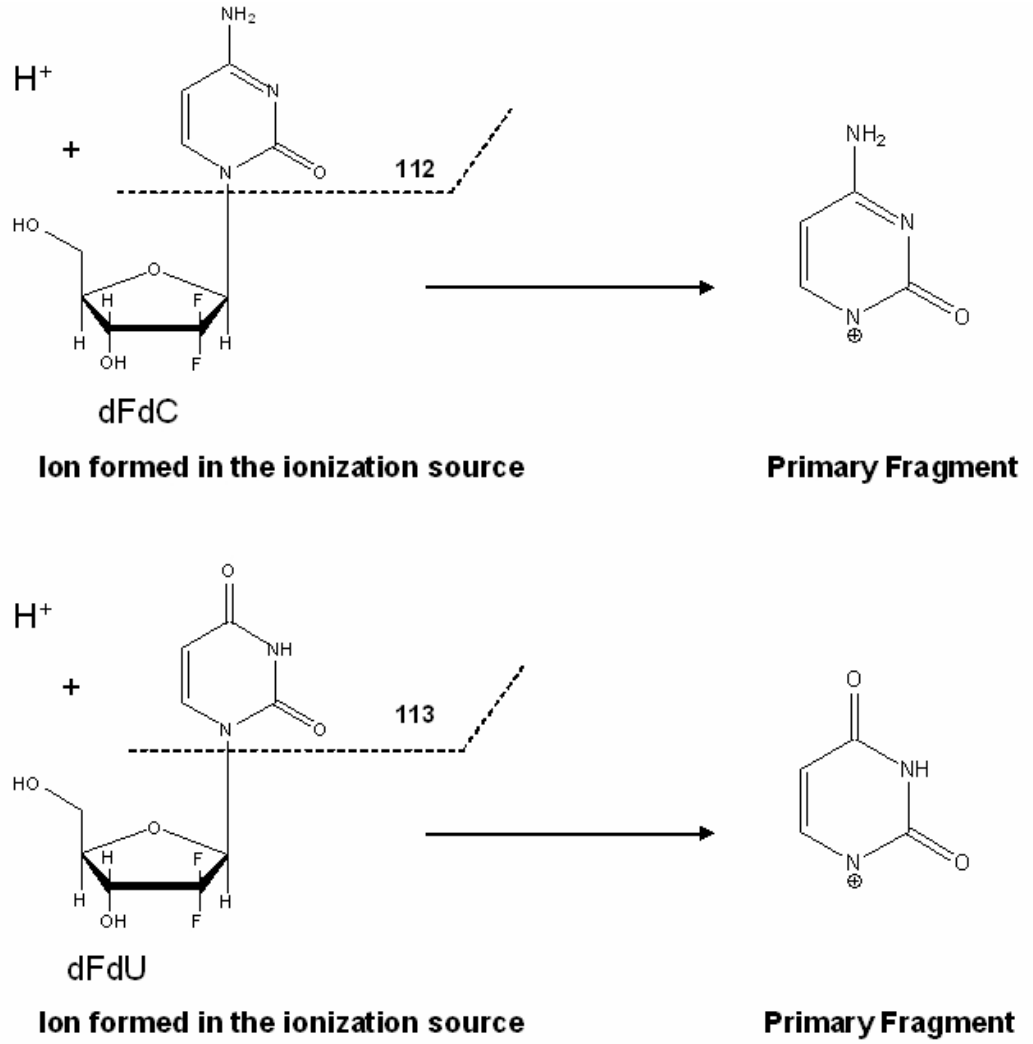

Figure 6

Secondary minor fragments resulting from rearrangement of the primary fragments (loss of oxygen or nitrogen group) were also detected, but their intensity was too low to be considered, therefore the MRM parameters have been optimized on the transitions from the molecular ion to the primary fragment.

Figure 7 reports a typical MRM chromatogram showing the quantifier transition (m/z 264 → 112 for dFdC, m/z 265 → 113 for dFdU) for an extracted human plasma sample containing both dFdC and dFdU.

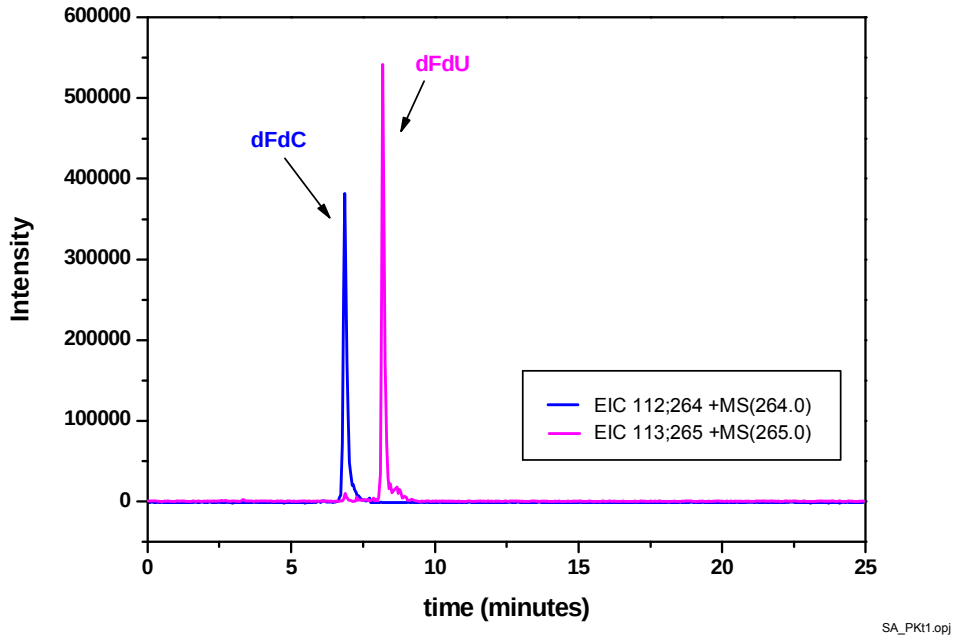

Fig. 7

4. Chromatography

Since dFdU and dFdC are both highly hydrophilic, their separation could result a challenge, if a selective and relatively fast chromatographic method is required like in pharmacokinetics studies. We worked under reversed-phase (RP) mode with 0.5% acetic acid added, since volatile additives should be used in MS instead of non-volatiles which can cause signal suppression. Mobile phase A (water, 0.5% acetic acid) and mobile phase B (acetonitrile, 0.5% acetic acid) were pumped at 1ml/min with gradient elution at the initial

conditions of A/B 98/2 for 2 minutes. The percentage of mobile phase B was linearly increased from 2 to 50% in 10 min and the analytes were eluted in this step as expected. In order to remove all plasma contaminants, mobile phase A was further decreased to 30 % and this ratio between the two mobile phases was kept for 4 min. Under these analytical conditions retention times for dC, dFdC, and dFdU were 2.3, 3.8 and 6.5 min, respectively. As judged by the chromatographic parameters (Table 4) obtained for gemcitabine and its metabolite, investigated peaks were well resolved under the chromatographic conditions described, and they all exhibit a notable symmetrical shape, thus making their electronic integration easy and precise which is necessary for a correct quantification of the analytes in the human plasma in pharmacokinetics studies.

Table 4

	T_R	K'	Asymmetry factor	Tailing Factor
dFdC	6.91	4.16	1.27	1.25
dFdU	8.19	5.82	0.73	1.45

5. Calibration curves

Figure 8 shows the calibration curves for dFdC and dFdC for each day of the validation study and Table 4 reports the accuracy and precision for each standard. The peak area ratios of analytes/IS to the concentrations were plotted and a least squares linear regression weighted by the reciprocal of the concentrations was applied to generate calibrations curves.

Table 5

Calibration curves parameters	dFdC	dFdU
R	0,99822	0,99847
X-coefficient	635,95908 ± 16,9	631,1 ± 17,5
Y-intercept	237608,97 ± 115835,6	298006,5 ± 128592,3

The calibration curves (Figure 5) were prepared on three different days and showed good linearity and acceptable data over a wide range of concentrations (0.050 ug/mL to 16 ug/mL for both dFdU and dFdC), with Pearson's coefficient of correlation R^2 equal or greater than 0.993. Mean accuracy was always close to 100% (range 90.0%–104.3%)

6. Clinical samples

Patients characteristics

The patients (n = 8) were divided into two cohorts depending on their hepatic condition, defined on the basis of their serum bilirubin and AST (Aspartate aminotransferase) levels. Three patients had normal serum bilirubin level and AST level less than two times the upper limit of normal (ULN) (Cohort I); four patients had bilirubin level from 1.6 to 7.0 mg/dL and normal AST level, one patient had serum bilirubin level less than 1.6 mg/dL and AST level greater than two times the ULN (Cohort II). The PK parameters measured were plasmatic peak concentration *Cmax*, area under the plasma concentration-time curve (*AUC*), total plasma clearance (*CL*) and half life ($t_{1/2}$) and they are all represented in Table 5.

Patients characteristics were: median age 62 yrs (range 28-75), male/female 4/4, median cycle cohort I: 6 cycles (3-6), median cycle cohort II: 3 cycle (1-5), median follow-up: 30 weeks (range 3-79) and median weeks of treatment: 14 (1-25).The rate of dose reduction was the same in the two cohorts, as the rate of omitted administration. Patients with liver dysfunction tolerated gemcitabine

without increased toxicity and neither AST nor bilirubin elevation was observed after drug administration. Pharmacokinetics parameters were calculated at the first and at the second cycle and the results are presented in Table 6.

All patients were evaluated for toxicity. All toxicities were reversible, no hospitalization due to severe adverse events was required, and no treatment-related deaths occurred. Results from all patients are summarized in Table 7. The pharmacokinetics of gemcitabine at fixed dose rate in patients with impaired liver function seems similar to control; no difference in terms of toxicity and dose reduction was required for this subset of patients.

Table 6:

	# Pts	*C max (µg/ml)*		*AUC exp (µg h/ml)*		*t 1/2 (h)*		*Cl p (L h/m2)*	
Cohort		**dFdC**	**dFdU**	**dFdC**	**dFdU**	**dFdC**	**dFdU**	**dFdC**	**dFdU**
I									
Mean cy 1	3	6.18	63.00	8.09	138.48	0.15	4.24	124.38	7.29
Mean cy 2	3	5.81	49.90	5.60	107.46	0.05	3.00	181.73	10.62
II									
Mean cy 1	5	6.74	52.47	7.81	117.65	0.11	3.14	179.05	8.59
Mean cy 2	3	5.88	100.53	5.86	205.54	0.21	1.74	175.32	7.92
Mean CV%		2.09	-17.34	198.38	47.80	29.94	2.83	-33.78	20.82

CV = coefficient of variability; cy = cycle; Cl p = plasmatic clearance

Table 7

Cohort I			C max (µg/ml)		AUC exp (µg h/ml)		AUC inf (µg h/ml)		t ½ (h)		Cl p (L h/m2)	
Patient	**Dose (mg)**	**DAY**	**dFdC**	**dFdU**	**dFdC**	**dFdU**	**dFdC**	**dFdU**	**dFdC**	**dFdU**	**dFdC**	**dFdU**
SA	1000	1	5.49	64.90	7.65	155.91	8.16	494.08	0.10	5.62	130.779	6.41
PR	1000	1	5.90	72.02	7.62	135.39	8.52	433.04	0.18	5.35	131.299	7.39
DAR	1000	1	7.14	52.09	9.00	124.14	9.83	194.91	0.17	1.76	111.052	8.06
Mean			***6.18***	***63.00***	***8.09***	***138.48***	***8.84***	***374.01***	***0.15***	***4.24***	***124.38***	***7.29***
SD			***0.86***	***10.10***	***0.79***	***16.11***	***0.88***	***158.08***	***0.04***	***2.16***	***11.54***	***0.83***
S.A	1000	2	4.03	44.29	4.63	76.32	4.82	346.19	0.05	5.76	216.157	13.10
P.R	1000	2	7.23	53.31	6.22	167.97	6.54	238.51	0.05	2.33	160.717	5.95
D.A.R	1000	2	6.16	52.09	5.94	78.10	6.15	114.75	0.06	0.91	168.325	12.80
Mean			***5.81***	***49.90***	***5.60***	***107.46***	***5.84***	***233.15***	***0.05***	***3.00***	***181.73***	***10.62***
SD			***1.63***	***4.89***	***0.85***	***52.41***	***0.90***	***115.81***	***0.01***	***2.50***	***30.05***	***4.04***

Cohort II			C max (µg/ml)		AUC exp (µg h/ml)		AUC inf (µg h/ml)		t 1/2 (h)		Cl p (L h/m2)	
Patient	**Dose (mg)**	**DAY**	**dFdC**	**dFdU**	**dFdC**	**dFdU**	**dFdC**	**dFdU**	**dFdC**	**dFdU**	**dFdC**	**dFdU**
PM	1000	1	12.61	68.70	14.54	125.48	14.61	242.08	0.02	2.72	68.796	7.97
SE	1000	1	7.14	52.09	8.38	117.87	9.24	188.47	0.18	1.75	119.334	8.48
CP	1000	1	2.72	30.87	2.57	117.20	3.38	266.58	0.11	5.08	388.541	8.53
ER	1000	1	3.58	40.76	4.95	97.29	5.62	221.90	0.11	4.30	202.206	10.28
MT	1000	1	7.65	69.95	8.59	130.43	9.35	314.94	0.16	1.83	116.369	7.67
Mean			***6.74***	***52.47***	***7.81***	***117.65***	***8.44***	***246.79***	***0.11***	***3.14***	***179.05***	***8.59***
SD			***3.92***	***17.12***	***4.52***	***12.64***	***4.28***	***47.64***	***0.06***	***1.49***	***126.56***	***1.01***
PM	1000	2	5.01	207.92	5.15	420.96	6.24	639.46	0.25	1.71	194.159	2.38
SE	1000	2	7.60	52.09	7.27	118.43	8.47	191.11	0.25	1.80	137.642	8.44
CP	1000	2	5.01	41.58	5.15	77.24	5.52	179.72	0.12	1.71	194.159	12.95
Mean			***5.88***	***100.53***	***5.86***	***205.54***	***6.74***	***336.77***	***0.21***	***1.74***	***175.32***	***7.92***
SD			***1.50***	***93.15***	***1.22***	***187.69***	***1.54***	***262.21***	***0.07***	***0.06***	***32.63***	***5.30***

References

1. Yeo, C.J., et al., *Cancer: Principles & Practice of Oncology*. 7th Edition ed. Vol. Part 3 - Practice of Oncology > Chapter 29 - Cancers of the Gastrointestinal Tract > SECTION 3: Cancer of the Pancreas > TREATMENT OF METASTATIC AND RECURRENT DISEASE > NEW DRUGS IN PANCREATIC CANCER. 2005, 530 Walnut Street, Philadelphia, PA 19106 USA: DeVita, Vincent T.; Hellman, Samuel; Rosenberg, Steven A. 945-986.
2. Jemal, A., et al., *Cancer statistics, 2007.* CA Cancer J Clin, 2007. **57**(1): p. 43-66.
3. Yeo, T.P., et al., *Pancreatic cancer.* Curr Probl Cancer, 2002. **26**(4): p. 176-275.
4. Lowenfels, A.B. and P. Maisonneuve, *Environmental factors and risk of pancreatic cancer.* Pancreatology, 2003. **3**(1): p. 1-7.
5. Mulder, I., et al., *The impact of smoking on future pancreatic cancer: a computer simulation.* Ann Oncol, 1999. **10 Suppl 4**: p. 74-8.
6. Ojajarvi, I.A., et al., *Occupational exposures and pancreatic cancer: a meta-analysis.* Occup Environ Med, 2000. **57**(5): p. 316-24.
7. Hoppin, J.A., et al., *Pancreatic cancer and serum organochlorine levels.* Cancer Epidemiol Biomarkers Prev, 2000. **9**(2): p. 199-205.
8. Hruban, R.H., et al., *Genetics of pancreatic cancer. From genes to families.* Surg Oncol Clin N Am, 1998. **7**(1): p. 1-23.
9. Tersmette, A.C., et al., *Increased risk of incident pancreatic cancer among first-degree relatives of patients with familial pancreatic cancer.* Clin Cancer Res, 2001. **7**(3): p. 738-44.
10. Solcia E, C.C., Klöppel G., *AFIP Atlas of Tumor Pathology*. 3rd edition ed. Tumors of the pancreas. Vol. Volume 20. 1997, Washington, DC: Armed Forces Institute of Pathology.
11. Chevlen, E.M., *Principles & Practice of Palliative Care & Supportive Oncology*. 3rd Edition ed, ed. A.M.S. Berger, John L.; Von Roenn, Jamie H. Vol. Chapter 50 Palliative Chemotherapy. 2007, 530 Walnut Street, Philadelphia, PA 19106 USA: Lippincott Williams & Wilkins.
12. Cullinan, S.A., et al., *A comparison of three chemotherapeutic regimens in the treatment of advanced pancreatic and gastric carcinoma. Fluorouracil vs fluorouracil and doxorubicin vs fluorouracil, doxorubicin, and mitomycin.* Jama, 1985. **253**(14): p. 2061-7.
13. M.L., M.S.G.B.H.A.R., *Gemcitabine is effective as palliative therapy for 5FU-refractory pancreas cancer patients.* European Journal of Cancer, 1995. **Volume 31**(Supplement 6): p. 117-117.
14. Burris, H.A., 3rd, et al., *Improvements in survival and clinical benefit with gemcitabine as first-line therapy for patients with advanced pancreas cancer: a randomized trial.* J Clin Oncol, 1997. **15**(6): p. 2403-13.
15. Mackey, J.R., et al., *Functional nucleoside transporters are required for gemcitabine influx and manifestation of toxicity in cancer cell lines.* Cancer Res, 1998. **58**(19): p. 4349-57.
16. Grunewald, R., et al., *Saturation of 2',2'-difluorodeoxycytidine 5'-triphosphate accumulation by mononuclear cells during a phase I trial of gemcitabine.* Cancer Chemother Pharmacol, 1991. **27**(4): p. 258-62.
17. Huang, P. and W. Plunkett, *Induction of apoptosis by gemcitabine.* Semin Oncol, 1995. **22**(4 Suppl 11): p. 19-25.
18. Heinemann, V., et al., *Comparison of the cellular pharmacokinetics and toxicity of 2',2'-difluorodeoxycytidine and 1-beta-D-arabinofuranosylcytosine.* Cancer Res, 1988. **48**(14): p. 4024-31.
19. Huang, P. and W. Plunkett, *Fludarabine- and gemcitabine-induced apoptosis: incorporation of analogs into DNA is a critical event.* Cancer Chemother Pharmacol, 1995. **36**(3): p. 181-8.
20. Plunkett, W., et al., *Gemcitabine: metabolism, mechanisms of action, and self-potentiation.* Semin Oncol, 1995. **22**(4 Suppl 11): p. 3-10.

21. Abbruzzese, J.L., et al., *A phase I clinical, plasma, and cellular pharmacology study of gemcitabine.* J Clin Oncol, 1991. **9**(3): p. 491-8.
22. Ruiz van Haperen, V.W., et al., *2',2'-Difluoro-deoxycytidine (gemcitabine) incorporation into RNA and DNA of tumour cell lines.* Biochem Pharmacol, 1993. **46**(4): p. 762-6.
23. Grunewald, R., et al., *Gemcitabine in leukemia: a phase I clinical, plasma, and cellular pharmacology study.* J Clin Oncol, 1992. **10**(3): p. 406-13.
24. Tempero, M., et al., *Randomized phase II comparison of dose-intense gemcitabine: thirty-minute infusion and fixed dose rate infusion in patients with pancreatic adenocarcinoma.* J Clin Oncol, 2003. **21**(18): p. 3402-8.
25. van Moorsel, C.J., et al., *Mechanisms of synergism between cisplatin and gemcitabine in ovarian and non-small-cell lung cancer cell lines.* Br J Cancer, 1999. **80**(7): p. 981-90.
26. Gelibter, A., et al., *Fixed dose-rate gemcitabine infusion as first-line treatment for advanced-stage carcinoma of the pancreas and biliary tree.* Cancer, 2005. **104**(6): p. 1237-45.
27. Humphreys, B.D., et al., *Gemcitabine-associated thrombotic microangiopathy.* Cancer, 2004. **100**(12): p. 2664-70.
28. Lawrence, T.S., et al., *Radiosensitization by gemcitabine.* Oncology (Williston Park), 1999. **13**(10 Suppl 5): p. 55-60.
29. Yilmaz, B., Y.Y. Kadioglu, and Y. Aksoy, *Simultaneous determination of gemcitabine and its metabolite in human plasma by high-performance liquid chromatography.* J Chromatogr B Analyt Technol Biomed Life Sci, 2003. **791**(1-2): p. 103-9.
30. Lin, N.M., et al., *Determination of gemcitabine and its metabolite in human plasma using high-pressure liquid chromatography coupled with a diode array detector.* Acta Pharmacol Sin, 2004. **25**(12): p. 1584-9.
31. Sottani, C., et al., *Validated procedure for simultaneous trace level determination of the anti-cancer agent gemcitabine and its metabolite in human urine by high-performance liquid chromatography with tandem mass spectrometry.* Rapid Commun Mass Spectrom, 2004. **18**(10): p. 1017-23.
32. van Moorsel, C.J., et al., *Pharmacokinetic schedule finding study of the combination of gemcitabine and cisplatin in patients with solid tumors.* Ann Oncol, 1999. **10**(4): p. 441-8.
33. Veerman, G., et al., *Antitumor activity of prolonged as compared with bolus administration of 2',2'-difluorodeoxycytidine in vivo against murine colon tumors.* Cancer Chemother Pharmacol, 1996. **38**(4): p. 335-42.
34. Wang, L.Z., et al., *An expedient assay for determination of gemcitabine and its metabolite in human plasma using isocratic ion-pair reversed-phase high-performance liquid chromatography.* Ther Drug Monit, 2003. **25**(5): p. 552-7.
35. Xu, Y., B. Keith, and J.L. Grem, *Measurement of the anticancer agent gemcitabine and its deaminated metabolite at low concentrations in human plasma by liquid chromatography-mass spectrometry.* J Chromatogr B Analyt Technol Biomed Life Sci, 2004. **802**(2): p. 263-70.
36. Honeywell, R., et al., *The determination of gemcitabine and 2'-deoxycytidine in human plasma and tissue by APCI tandem mass spectrometry.* J Chromatogr B Analyt Technol Biomed Life Sci, 2007. **847**(2): p. 142-52.
37. Sottani, C., et al., *Simultaneous determination of gemcitabine, taxol, cyclophosphamide and ifosfamide in wipe samples by high-performance liquid chromatography/tandem mass spectrometry: protocol of validation and uncertainty of measurement.* Rapid Commun Mass Spectrom, 2007. **21**(7): p. 1289-96.
38. Vainchtein, L.D., et al., *Validated assay for the simultaneous determination of the anti-cancer agent gemcitabine and its metabolite 2',2'-difluorodeoxyuridine in human plasma by high-performance liquid chromatography with tandem mass spectrometry.* Rapid Commun Mass Spectrom, 2007. **21**(14): p. 2312-22.
39. Marangon, E., et al., *Simultaneous determination of gemcitabine and its main metabolite, dFdU, in plasma of patients with advanced non-small-cell lung cancer by*

high-performance liquid chromatography-tandem mass spectrometry. J Mass Spectrom, 2008. **43**(2): p. 216-23.

Chapter II

DISCOVERY OF OVARIAN CANCER BIOMARKERS

Discovery of Ovarian Cancer Biomarkers

Introduction

1. Biomarkers and Ovarian Cancer

In the last few decades a consistent amount of funds have been invested in the research of biomarkers for cancer early detection. The increased number of early diagnosis of malignancies or in some cases even premalignant lesions can be ascribed to mere and more efficient screening procedure and a different clinical practice. The final diagnosis is still possible only after biopsy of the tissue, which involves a quite invasive procedure that would be avoided for a large number of patients if one or more specific biomarker were available for each cancer diseases. The ideal tumor biomarkers should be a protein or a fragment of a protein easy to identify in biological specimens – e.g. urine or serum – and should show a different expression among healthy individuals and cancer patients.

In 1965, Joseph Gold and his group presented the first test recognized for a known type of cancer [1]: he found that the same protein in colon cancer patients was normally expressed in the fetal tissues and he named it carcinoembryonic antigen (CEA). By the end of the ‘70s, several potential serum tests had been developed for a series of different tumors [2].Further biomarkers have been identified during the ‘80s such as CA 19-9 [3] for colorectal and pancreatic carcinoma, CA 15-3 for breast cancer [4] and CA-125 for ovarian cancer [5]. Unfortunately these biomarkers are present also in normal patients and they increase significantly only when the tumor mass is already extremely relevant. In addition these molecules are not specific for a particular cancer; in fact some women can show particularly high levels of CEA or CA-125 due to different and not oncological gynecological conditions [6, 7].

PSA (prostate-specific antigen) is the most well known biomarkers and it has been and it still is used for early detection of prostate cancer. The use of the PSA test in the clinical practice in the last few years leaded to a tremendous increase of the early diagnosis of the disease [8]. The maximum limit for PSA

was established as 4 ng/mL, but in the 33% of the cases in which the PSA level was within 4 and 10 ng/mL, the cancer spreads in other organs, therefore the chemio-therapy and radio-therapy result inefficient. Even though the presence of PSA brings a suspect of the malignancy, only the biopsy can give an accurate diagnosis; each individual with levels of PSA in the range 4-10 ng/mL should undergo the clinical procedure of histological analysis of a collected tissue and the lower limit for PSA have been reduced to 2.5 ng/mL [9]. A higher level of PSA is also correlated with the condition of benign prostatic hyperplasia, so the presence of PSA not necessarily indicates the presence of cancer. The lack of specificity of the PSA for values less than 4 ng/mL is about 25% and as a consequence many men undergo to an unnecessary biopsy [10].

Despite the success of the PSA as tumor biomarker, there is not a specific biomarker that predicts the presence of cancer for the most of the tumoral forms. The PSA itself has his major application in the detection of recidivism. A perfect biomarkers should have 100% sensitivity and 100% specificity and the PSA is very specific, but not that sensitive.

The future of the cancer treatment seems to be extremely dependent on the use of biomarkers that should lead the clinicians in each stages of the disease, from the early detection to the prognosis, through the prediction of a recidivant disease. The biomarkers would be able to direct the pharmaceutical treatment towards one drug or another, basing the choice on the prediction of the outcome of the response to the therapy or the instauration of resistance. Probably the most important aspect of the biomarkers is the early detection, so that could be possible to intervene in the very initial stages of the cancer, when the cure rates are higher than in the later stages.

In despite the fact that just few biomarkers are now used in the clinical practice, technologic improvements in genomics and proteomics have produced a series of potential markers. Calcitonin is one of them and its level in the serum is higher in patients with malignancy in medullary thyroid carcinoma. Calcitonin is a hormone secreted from the thyroid parafollicular C cells and it’s envolved in the regulation of the blood levels of calcium.

Medullary thyroid carcinoma is often an hereditary disease, therefore in patients with family history of this cancer, an elevated amount of the hormone in the blood could indicate the presence of a very early stage of the disease [11]. Secretion of calcitonin has been observed also in lung cancer, but the hormone is not used to monitor this cancer [12].

Several biomarkers have been reported to be not very sensitive and so they cannot be useful as a general screening tool, on the other hand they can be used to monitor patients that present the particular type of cancer that seems to over-express the biomarker itself. One of these biomarkers is CA-125 for the ovarian cancer present in a subtype of ovarian cancers [13-17]. CA-125 is elevated also in other benign gynecological conditions, such as endometriosis, and it allows only the detection of 50% of first stages of diseases and it cannot be used to generically screen for ovarian cancer, but in those patients that show a CA-125 positive tumor, the use of CA -25 reflects the recurrence in the population [18].

The interest in the biomarkers field is not over and in the next years we should see still huge effort in the intent of finding molecules able to help in the diagnosis, prognosis and prediction especially for those diseases that show their symptoms when the cancer is already difficult to treat, both surgically and pharmaceutically.

Ovarian cancer is one example of these insidious diseases and it is often called the "silent killer" because the lack of visible symptoms until the disease has progressed to an advanced stage that makes very difficult its diagnosis in the first and more responsive to treatment stages.

Ovarian cancer affects about 200,000 women every year and kills more than 120,000 in accordance with the International Agency for Research on Cancer (http://www-dep.iarc.fr/). Ovarian cancer is the fifth leading cause of death connected to gynecological diseases and is the second most diagnosed malignancy among women. Unfortunately the diagnosis is often at advanced stages, when the disease is not confined to the ovary, therefore the cure rates decreases dramatically to 20-30%. On the other side patients with cancer that hasn't invaded other organs can be successfully treated in the 70-90% of the

cases [19], even because many effective new therapeutics have been developed and have come into the clinical use.

2. Serum Proteomics in Biomarkers Research

The results that research in the biomarkers field has achieved until today are not completely satisfactory, but in the few years proteomics profiling techniques proved to be able to delivery consistent and interesting results in the identification of proteins correlated with early stages of cancer [20-22].
The fraction of serum proteome defined as Low Molecular Weight (LMW, approximately up to 6000 Da) is awakening some interest since it seems quite plausible that this region of the proteome contains fragments of proteins resulting from pathological or physiological events that take place in every perfused tissue[23]. Proteinase generates fragments from characteristic proteins of the pathological stage released into the tissue micro-environment by particular kind of cell, for example by tumoral cell or by immuno-cell as a response to the presence of the tumor. The biomarkers fragments are released into the circulation by passive diffusion and they are protected from the renal clearance thank to the interaction with bigger proteins (e.g. albumin). In all probability proteins are attacked by circulating enzymes and also in this case the result is the generation of protein fragments with the tendency to associate with big proteins.
One of the mot suitable techniques to investigate the protein fraction in tissues is mass spectrometry and has been used to analyze serum from patients with ovarian cancer [24] and in other cancer and not cancer diseases [21, 22]. Preliminary studies showed a high abundance of information in the LMW fraction of the proteome due to the presence of specific proteins or peptides characteristic for a given patholologgy. Mass spectrometry studies of the LMW fraction of the serum leaded to the identification of unknown proteins that could be potential new biomarkers proving the importance of this fraction of the serum.
Assuming that the LMW fraction of the serum contains important diagnostic information, the research of biomarkers with low molecular weight involved the previous elimination of the proteins with high molecular weight (e.g.

albumin, thyreoglobulins and immunoglobulins) in order to obtain an enrichment of the LMW fraction [25-27].

The LMW molecules free in the circulation are rapidly metabolized by the renal system a that could bring a dramatic decrease of their concentration and they could even become undetectable, but the most of these LMW molecules associate with larger proteins that act as efficient carriers not metabolized by the renal clearance. The association with protein carriers extends the half-life, because it becomes the same half-life of the carrier protein which is higher of several orders of magnitude. The circulating proteins become though a reservoir for the enrichment and the amplification of biomarkers (fig. 1).

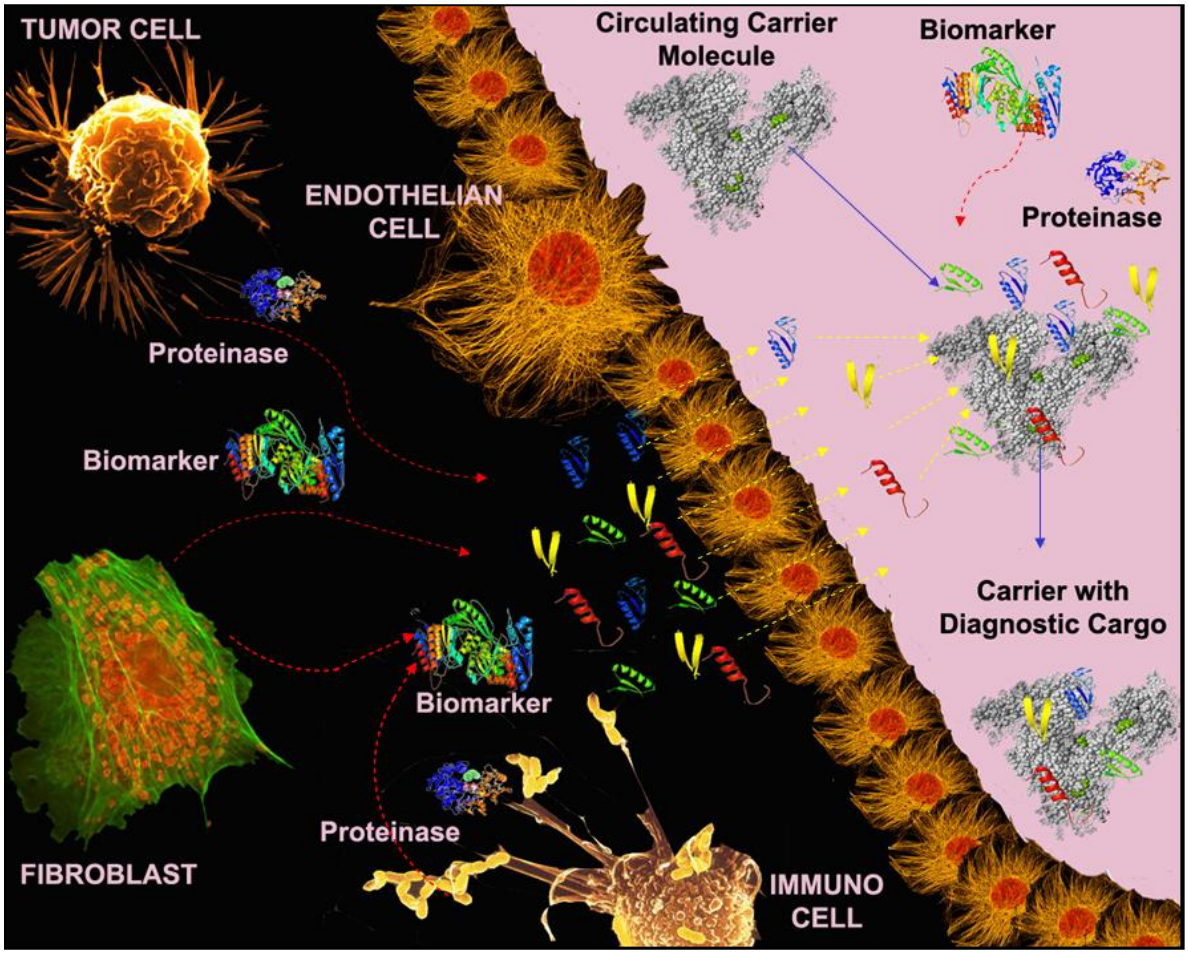

Fig. 1

Considering the binding reaction between the biomarker (b) and the carrier protein (C):

$$b + C \underset{k_R}{\overset{k_F}{\rightleftharpoons}} bC_1$$

The binding reaction is regulated by constant of velocity k_F and the reverse reaction (dissociation) by the constant of velocity k_R.

The mass action kinetics is proper to describe the interaction between carrier and biomarker, because the carrier protein in normal conditions does not bind more than one biomarker, since the carrier exists in a so great relative abundance. So it is possible to assume that the kinetics of the formation of the complex bC_1 is proportional to the product of the concentration [b] of the biomarker and the constant of velocity k_F. The constant of dissociation is proportional to the concentration [bC] of the complex for the constant k_R.

Therefore the equations for the binding reaction and the reverse reaction are the following

$R_F = k_F [b][C]$

$R_R = k_R [bC]$

Considering the extremely large access of the carrier protein ([C]>>[b]), it is correct to affirm that just a small part of it will be involved in the binding reaction, therefore the concentration of the carrier protein [C] can be considered as constant. The concentration of the free carrier can be included in the constant of velocity of the binding reaction:

$R_F = k_F^* [b]$

where $k_F^* = k_F [C]$.

The reaction reaches an equilibrium when

$R_F = R_R$ or

$k_F^* [b] = k_R [bC]$.

The absolute great abundance of the carrier protein enhances k_F^* of the binding reaction and makes it greater of several orders of magnitude than k_R of the reverse reaction. The equilibrium is strongly shifted towards the formation of the complex bC and the equilibrium ratio will be:

$$\rho_{eq} = \frac{[bC]}{[b]} = \frac{k^*_F}{k_R}$$

This equilibrium ratio underlines that the biomarker tends to exit bound to the carrier protein, even when the binding capacity is not great.

3. Mass Spectrometry based approach in Proteomics

Different approaches exit in proteomics. The gel approach provides a method that is both qualitative and quantitative resolving a complex protein mixture to single and discrete spots [28, 29]. While the lack of reproducibility and the strong limitations in the application of the mono-dimensional technique for protein expressed at low levels reduce its use in clinical samples, new improved bi-dimensional techniques seem to have better reproducibility and the possibility of an higher throughput [29, 30].

The most important advances in proteomics in the last few years have been recorded instead in the gel-free methods, such as mass spectrometry that shows better sensitivity and high throughput; mass spectrometry can give information on the molecular weight of the isolated protein which is a peculiar characteristic of the molecule itself and reflects the gene sequence and possible post-translational modifications. Mass spectrometry offers a wide range of possible solutions to identify different categories of proteins possibly related to particular pathological condition, for example identifying post translational modifications (PTMs) that with all probability play in important role in the disease development.

Proteomics mass spectrometry techniques can be divided in four principal categories: (i) LC-MS [30], (ii) LC-FTICR-MS [31, 32], (iii) SELDI-TOF-MS [33], (iv) MALDI-TOF-MS [34].

The research in this field is evolving in two principal directions: the first of them consists in protein profiling studies in order to find diagnostic pattern [35], instead the second one provides characterization information obtained by LC-MS and MALDI-TOF platforms [36]. Other two fields recently are recalling the general attention: immuno-technology based MS assay [37] with the study of interaction of specific antigen-antibody interaction on opportunely modified surface and metabolomics which has already been applied in an ovarian cancer studies [38].

The identification and the validation of biomarkers often includes MS-based technologies, in particular two ionization techniques are the most used and they are MALDI (MATRIX-ASSISTED LASER DESORPTION/IONIZATION) and ESI (ELECTROSPRAY IIONISATION). The MALDI technique has the important advantage of being able to screen quite quickly a large number of samples estimating the molecular weight of peptides and proteins with a TOF (TIME OF FLIGHT) analyzer. The recent developments in the design of new MALDI-TOF instruments assure higher sensitivity and higher accuracy in the determination of the molecular weight. In MALDI-TOF the one protonated peptide is observed in the most of the time, while with the ESI multiple charged molecules can be observed on the spectrum. ESI usually shows resolution and sensitivity with a previous enzymatic digestion (e.g. trypsin), and is often associated with LC (LIQUID CHROMATOGRAPHY). Some examples of the utilization of capillary LC-FTICR-MS (LIQUID CHROMATOGRAPHY-FOURIER TRANSFORM ION CYCLOTRON RESONANCE MASS SPECTROMETRY) in association with sophisticated bioinformatics analysis have been described [39] in the last few years.

SELDI-TOF MS (SURFACE-ENHANCED LASER DESORPTION/IONIZATION), first developed by Hutchens and Yip [40] in 1993, allows the analysis of samples applied directly on differential binding surface without removing salts or detergents, because just what remains attached to the surface of activated

surface will be analyzed. Petricoin et al. demonstrated the utility of this technique in the discovery of differentially expressed proteins and peptides [21] part of a proteomic pattern identified by an algorithm able to classify correctly cancer samples and non-cancer samples.
A new exiting field that is capturing interest in the scientific community is the direct MS imaging [41]. This technique is an alternative to the microdissetion lysate MS and it permits to avoid the microdissetion and the solubilization of the tissue. The tissue slice dries on a MALDI plate, then coated with the most suitable energy-absorbing ionization matrix and finally analyzed with a laser in a vacuum chamber. MALDI imaging has already been used in lung cancer studies [41] and in human tumor tissue sections [42].
All the cited techniques can be used as high-throughput technologies that need bioinformatic analysis in order to accelerate the discovery of new biomarkers and their validation as well. Bioinformatics find classifying patterns and algorithms able to discriminate completely cancer and non-cancer samples based on the change in the proteomic profile as a result of physiological and biochemical conditions due to presence or absence of the tumor itself. Proteomic patterns in serum have showed to be a powerful tool to discriminate confirmed ovarian cancer samples and samples from women with high risk of being affected by the disease [21, 43-45].

In conclusion, since oncology practice in the next few years will be mostly controlled by factors of economic nature, biomarkers should have crucial importance in the management of all the cancer diseases, potentially they will help in the choice of a therapeutic treatment over another or in the identification of earlier and earlier stages of cancer. More likely there will be not just a single biomarker for each disease, but a panel of 6 to 10 molecules able to give an accurate description of the state of the disease and a prediction of the possible metastatic spreading.

Aim of the study

The aim of the study was to identify and characterize potential biomarkers for ovarian cancer. In order to obtain valuable results a number of serum samples from both ovarian cancer patients and women indicated as high risk subject were analyzed with mass spectrometry and the data obtained were objects of bioinformatics investigation to indicate a classifying pattern of potential biomarkers. Finally the selected molecules were characterized.

Experimental

1. Materials

The ovarian cancer study sample set consisted of 352 from Northwestern University (Illinois, USA) under IRB (INSTITUTIONAL REVIEW BOARD) approval, using standard protocols developed by the institution. An addition sample set of 63 specimens were obtained from the Division of Gynecologic Oncology, University of Brescia (Brescia, Italy). The set was constituted of 205 biopsy confirmed ovarian cancer and 190 high risk samples (women with a first degree relative with ovarian cancer, women who had other cancers or women who had pelvic masses). High performance liquid chromatography grade solvents (Water and Acetonitrile) were purchased from EMD (Madison, WI USA). Sinapic Acid was from Sigma-Aldrich (St. Luois, MO, USA), the detergent beta -octyl glucoside (BOG) and SuperBlock were from Pierce. Phosphate-Buffered Saline (PBS) 7.4 (10X) liquid came from Invitrogen Corp., while Trifluoroacetic acid (TFA) was purchased from Pierce. IgG Thyroid Simulating Hormone (TSH) and anti-TSH were purchased from Seradyn Inc. Indianapolis, IN, USA.

Reagents

High performance liquid chromatography grade solvents (Water and Acetonitrile) were purchased from EMD (Madison, WI USA. Alpha-Cyano-4-hydroxycinnamic acid and standard peptides were from Sigma-Aldrich (St. Luois, MO, USA), the detergent beta -octyl glucoside (BOG) was from Pierce as Trifluoroacetic acid (TFA). Magnetic beads were DynaBead-RPC18 (Invitrogen Corp., Campbell, CA, USA).

Serum sample were fractionated on BondElute LCR C18 (Varian Inc., Palo Alto, CA, USA) and 218TP C18, 2.1*250mm I.D, 5µm particle size (Vydac, Deerfield, IL, USA).

2. Equipment

The sample processing has been completely performed on the Halmiton Star Robot (Hamilton Company, Reno, NV, USA) and a Dynal magnetic patirticles concentrator (Invitrogen) has been used to facilitate the removal, washing and elution steps. MALDI-MS experiments were performed in positive ion mode using a PrOTOF (PerkinElmer, Boston, MA, USA). Sample were lyophilized on Freezemobile 12XL – The Virtis Company, New York, USA). Two chromatography systems have been used: UltiMate System (Dionex, Sunnyvale, California, USA), consisting of dual gradient pump, a degasser, a flow manager, a UV detector, a well-plate autosampler Famos and an automatic fractions collector Probot and Agilent 1200 Series (Agilent Technologies, Palo Alto, CA, USA).

3. Methods

3.1 Proteomic Profiling Study

3.1.1 MALDI-TOF analysis

Specimen processing – Sample processing was performed on the Hamilton Star liquid handling workstation, equipped with multiple pipetting, labware gripping devices, shaker device and magnet. All workstation functions and integrated third-party devices are controlled by the Venus software (Hamilton Robotics, Reno, Nevada, USA). The serum samples have been diluted 1: 5 with running buffer (aqueous solution 0.1% Trifluoroacetic acid (TFA)/β-octyl glucoside 500μM) into a 96-well microtiter plate. The C18 magnetic beads (Dynabeads RPC 18, Invitrogen) were washed three times with 200 μL of running buffer, before samples (100 μL) were added to each well of the microtiter plate. The plate was washed an additional three times, before elution from the beads in a new 96-well plate using the energy absorbing matrix solution (5 mg/mL α-cyano-4-hydroxyciunamic acid, CHCA, in 50% acetonitrile/water with 0.1% TFA). The eluted fraction were spotted on the MALDI target and air dried. Each sample was analyzed in duplicate.

High resolution MALDI-TOF analysis – The prOTOF 2000 MALDI O-TOF Mass Spectrometer (PerkinElmer) was used to obtain serum proteomic profiles of th**e** samples with the following settings:

Laser Shot: 80
Laser Energy: 65%
Laser rate: 100.0 Hz
Declustering: 30,0 V
Cooling flow: 190 mL/min
Mass Range: 720-6000 Da
Expected high mass: 6000 Da
Focusing flow: 212.0 mL/min
Acceleration Voltage: 16 kV (+) ion
Detector: 2300 V
Laser pattern: 2 mm, rings 02 + 04, 32 spots
A 2-points external calibration will be performed using angiotensin and ACTH fragment 18-39.

3.1 Proteomic Pattern Analysis

Spectral Preprocessing – Due to the high resolution of the prOTOF, there was no drift effect, therefore no peak alignment was required. The intensities of each spectrum were scaled with adjust coefficient so that the total ion current (TIC, that can vary across different spectra) of the scaled spectrum was equal to the average TIC of all the spectra. The cut-off limit for spectra was established as the value 3 and all the spectra with TIC or adjust coefficient <3 were consider as outliers and excluded from further analysis. The spectra were binned with a linear growing window size and the data points were reduced to about 10,000 for each spectrum.

Pattern Analysis – Preprocessed data were randomly divided in training set (70%) and testing set (30%), so that the duplicate spectra of each sample was assigned to the same group. The classification of the samples was performed using a proteomic biomarker discovery system developed by the Clinical Proteomics Reference Laboratory (NCI-SAIC Frederick Inc., Frederick, Maryland, USA), which consists in the combination of three different and

independently trained machine learning tools: Partial Least Square regression (SAS Institute, Inc., Cary, North Carolina, USA), Support Vector Machine (Chih-Chung Chang and Chih-Jen Lin, LIBSVM: A library for support vector machines, 2001) and C5 decision tree from RuleQuest (St Ives, NSW, Australia). The classification result for a sample was determined using the major vote of the six classification results from those three algorithms on the duplicate spectra of the sample. In presence of a tie, the classification was declared unknown.

3.2 Identification Study

3.2.1 Peptides Isolation

Sample Processing – The serum samples were fractionated using BondElute LCR C18 (Varian, Inc.) solid-phase extraction cartridges. The C18 cartridges were preconditionated with acetonitrile (2 mL, two times) and washed with 0.1% TFA (2 mL, four times). The sample diluted 1:2 in 0.1% TFA was loaded onto the column (500 μL of serum to a final volume of 1 mL). The column was washed three times withTFA 0.1% (2 mL each wash) and the peptides were eluted with 50% acetonitrile, 0.1% TFA (2 mL, two times). The eluted samples were frozen for 2 hours at -80°C and then lyophilized (Freezemobile 12XL – The Virtis Company, New York, USA) over night and then reconstituted with 30 μL of water 0.1% formic acid. 0.5 μL of the obtained sample solution was diluted 1:10 and spotted on a MALDI target in order to analyze the sample on the prOTOF to confirm the presence of the investigated peptides before proceeding to further investigation.

HPLC fractionation – The chromatographic separation was carried out on a Vydac 218TP C18 (2.1*250mm I.D, 5μm particle size) on a UltiMate System (Dionex, Sunnyvale, California, USA), consisting of dual gradient pump, a degasser, a flow manager, a UV detector, a well-plate autosampler Famos and an automatic fractions collector Probot. The flow was of 200 μL/min. Mobile Phase: A, 0.1% formic acid; B, acetonitrile, 0.1% formic acid. Gradient elute procedure: initial conditions – B 0% for 15 min; step 1 – B 0-80% in 80 min; step 2 – B 80-100% in 5 min; step 3 – B 100% for 5 min; return at the initial conditions – B 0% in 2 minutes and equilibration for B 2% for 8 minutes

before the next injection. The injected volume was 30 μL and the wavelength used to monitor the elution was 206 nm, which is within the range of wavelengths 180-230 nm for the peptide bond. From each diluted serum aliquot a total of 96 fractions (1 minute fraction, 200 μL each) were collected into a microtiter plate and later checked with the PrOTOF to identify the fraction containing the investigated peaks. The peptides of interested were eluted in presence of about 12-14% organic modifier, therefore the corresponding peak presented a T_R around 12-14 min. this fractionation procedure was repeated a total of X times in order to collect a discrete amount of the potential biomarker peptides for the following procedure; finally a total amount of 2 mL of serum were fractionated.

3.2.2 CapLC-ESI MS analysis

CapLC conditions **–** The capLC separation was performed on Agilent 1200 Series System, that consisted in a binary pump, a degasser and a autosampler. Mobile Phase: A, 0.1% formic acid; B, acetonitrile 0.1% formic acid. The flow rate was 3 μL/min and the injection volume was 2 μL. The HPLC fraction from the previous experiment has been lyophilized and reconstituted with the 0.1% formic acid for the direct CapLC-MS/MS analysis. Before the CapLC fractionation a small aliquot of the 0.5% formic acid peptides solution was spotted on a MALDI target along with CHCA matrix solution to verify the presence of the investigated peaks.

The purified peptide fractions of interest were applied on the Phenomenex Jupiter (4u, 90A) Proteo Micro-HPLC Column, 150 x 0.30 mm (Phenomenex, Sydney, Australia) and separated using gradient elution. The column was connected to a LCQ mass spectrometer (ThermoQuest, San Jose, CA) equipped with an electrospray ion source and operated in the positive ion mode. The instrument was tuned by direct infusion (FIA) of standard peptides (ACTH 18-39 2465.198 Da; Angiotensin I, 2465.198 Da) in 0.1% formic acid, 2 pmol/μL.Source corrent was 80 μA. Source voltage was held at 5 kV, tube lens offset was -4.25 V. The heated capillary was kept at 250°C with a voltage of 23 V. The LCQ was set to acquire a full MS scan between 200 and 3000 *m*/*z* followed by full MS/MS scans of the top three ions from the preceding full

MS scan. Activation time for CID was 30 ms and the relative collision energy was set to 42%. Dynamic exclusion was enabled with one repeat count, repeat duration of 30 s and 30 sec exclusion duration window. Spectra were searched with the Bioworks software against selected database.

Results and Discussion

The first part of this study involved a proteomic profiling investigation of 415 samples from patients affected by biopsy confirmed ovarian cancer and a population of high risk subjects; the number for each group was equally distributed. The proteomic profiles of the samples were obtained with a high resolution MALDI-TOF experiment in which the low molecular weight fraction was isolated using reverse phase magnetic beads chromatography (FIG).

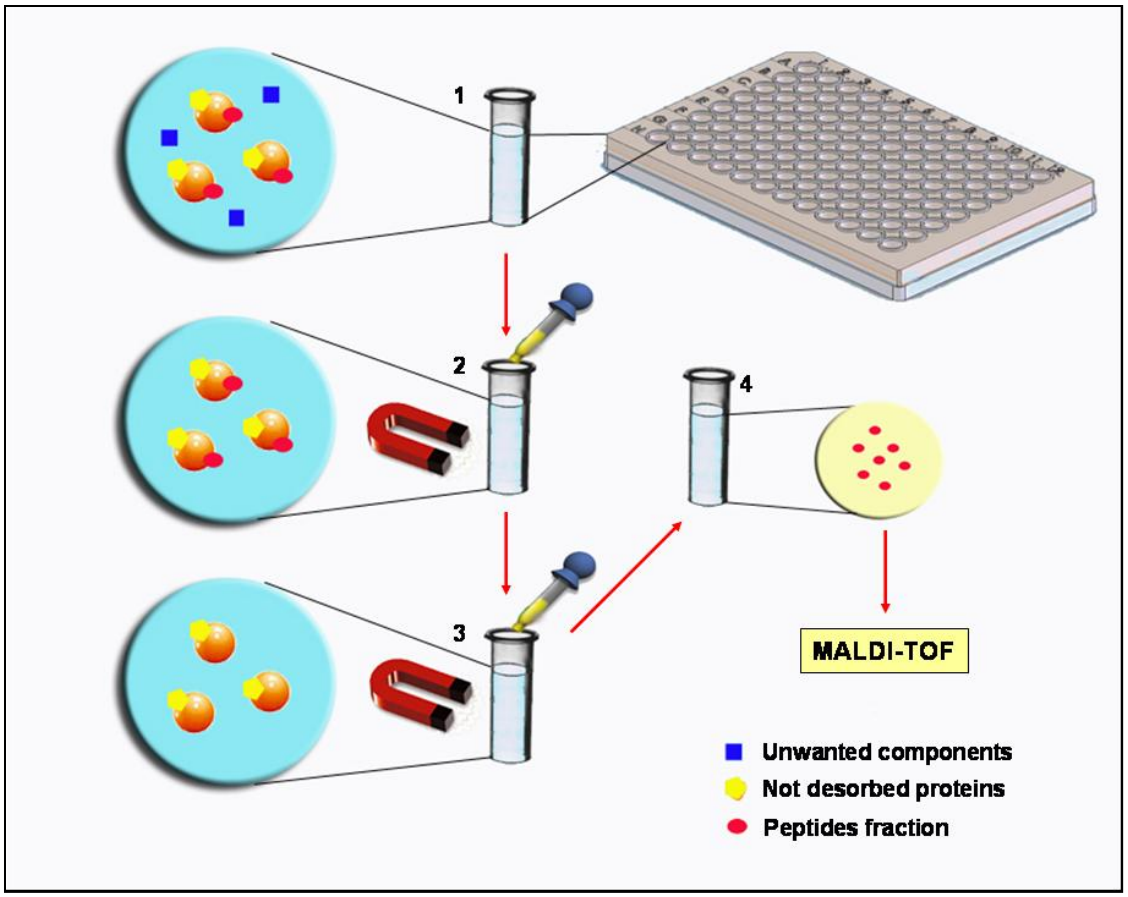

FIG. 2

1 – Wash and remove unwanted components; 2 – desorbtion followed by magnetic separation; 3 – Possible further fractionation; 4 – Peptides fraction.

The samples diluted with the acidic buffer (running buffer) were added directly to the pre-washed beads. A mixture of proteins and peptides in the serum adsorbed to beads and then the complex beads-protein/peptides was easily washed with the same acidic buffer, eliminating unwanted components such as salts and other not adsorbed substances. Peptides and small proteins were desorbed in one single step using a small volume matrix solution that contained 50% acetonitrile in order to reduce a potential loss of low molecular weight components of the serum and to reduce the time of analysis; this expedient helped also in the concentration of the analytes before the MALDI analysis and improved the high throughput of the technique, compare to other precedent experience [46]. Figure 3 shows a typical spectrum obtained from human serum with this technique.

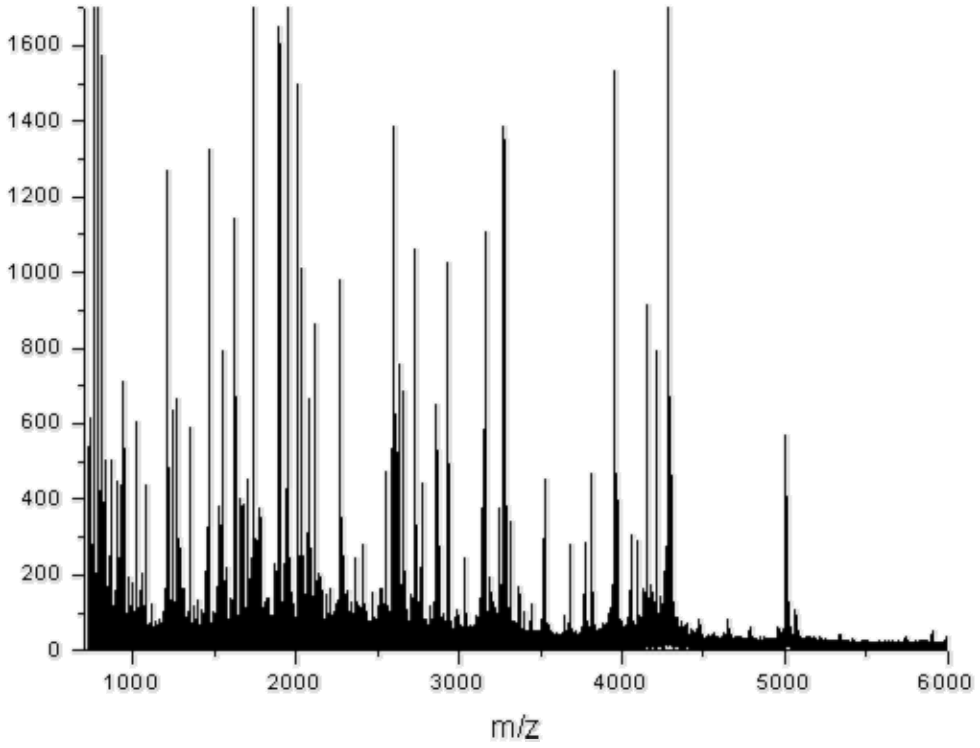

FIG. 3

We analyzed the samples on the high resolution PrOTOF mass spectrometer (FIG). The PrOTOF combines orthogonal injections (A) to introduce sample ions from the MALDI source to the TOF with a reflectror TOF (B), providing high resolution in a wide range. Differently from conventional axial MALDI-TOF systems, in the PrOTOF the MALDI source is decoupled from the TOF, increasing the instrument's accuracy, resolution and sensibility. Ions entering the mass analyzer have reduced energy distribution for collitional cooling focusing (C). Lower energy distribution improves sensitivity of the system.

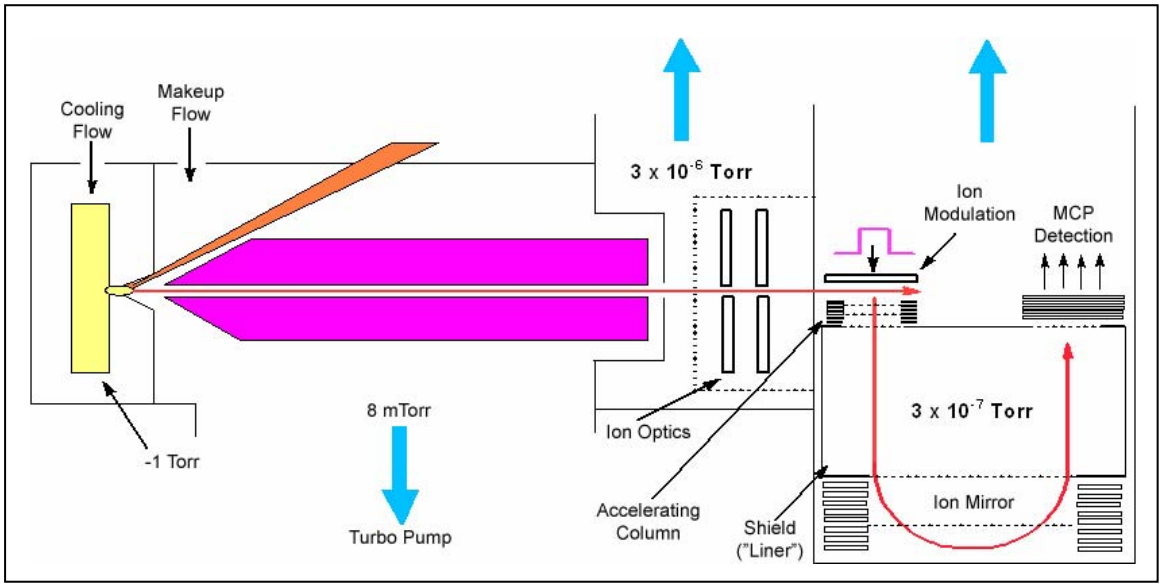

FIG. 4

Proteomic modelling successfully distinguished ovarian cancer patients' samples from high risk samples (TAB) and used the top 100 up-regulated and the top 100 down-regulated peaks with the lowest p-value to build the classifiers, with sensitivity of 82.1% and Specificity of 86.2%.

Table 1

	Predicted as *Unknown*	**Predicted as *High Risk***	**Predicted as *Cancer***
High Risk	**5**	**44**	**7**
Cancer	**3**	**10**	**46**

The bioinformatics indicated a list of top and down-regulated peaks and the ones that showed higher reproducibility underwent further investigation in order to identify their amino acid sequence. Four of them were particularly interesting both for the quite constant presence and also because apparently somehow correlated. The peaks in question showed respectively *m/z* 3191, 3207, 3262 and 3278. The difference between the first and the second peak was of 16 Da, which can be correlated to an oxidation, and the same difference was found between the third and fourth peak. Not less interesting was the difference between the first and the third peak – corresponding to the not oxidized peaks – that was of 71 Da, that could be due to the delation of one amino acid, in particular of the alanine, therefore the same 71 Da difference was found between the second and the fourth peak. The resolution and the accuracy of the instrument was determinant for the confidence in the results. Another down-regulated peak was 2769.

In order to identify the peaks it has been necessary to concentrate and to isolate as much as possible the investigated peptides. The first step in this process was to separate the LMW fraction of the serum again with a reverse phase method. The C18 solid-phase extraction method was found to be the most efficient and the less expensive to up-scale and the elute from the cartridges was easy to concentrate by lyophilization. With this quick and reproducible method it was possible to eliminate the salts and the large proteins naturally present in the serum and that can interfere with the detection on mass spectrometry. The dried samples were reconstituted in a buffer suitable for the HPLC fractionation and fractions from the outlet of the column were collected after UV detection into a 96 well plate. The robot collection of the samples assured a complete recovery of the whole elute. The fig 5 shows a typical chromatogram obtained fractionating the extracted LMW proteins and peptides. The peptides of interest were eluted in presence of 12-18% of organic modifier (12-18 minutes).

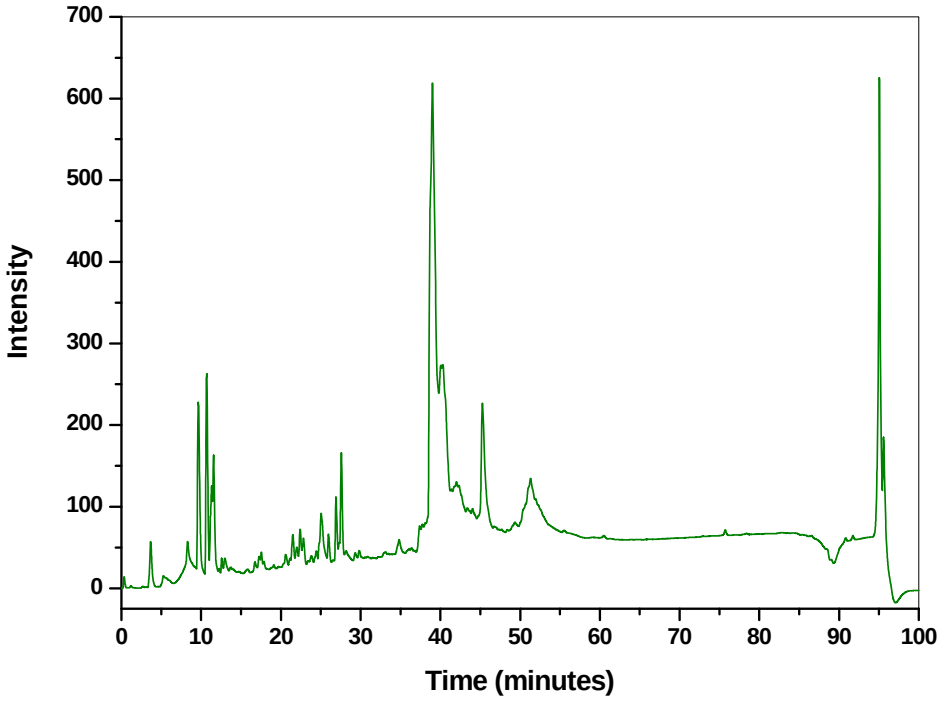
Intensity
700
600
500
400
300
200
100
0
0
10
20
30
40
50
60
70
80
90
100
Time (minutes)

FIG. 5

All the collected fractions were checked on the mass spectrometer and the ones containing the peaks were controlled and they showed a dramatic increase of the signal definitively reflecting an increase in the concentration of the peptides. The figures 6 and 7 show the spectrum relative to an isolated fraction containing the four peaks of interest isolated by HPLC from human serum.

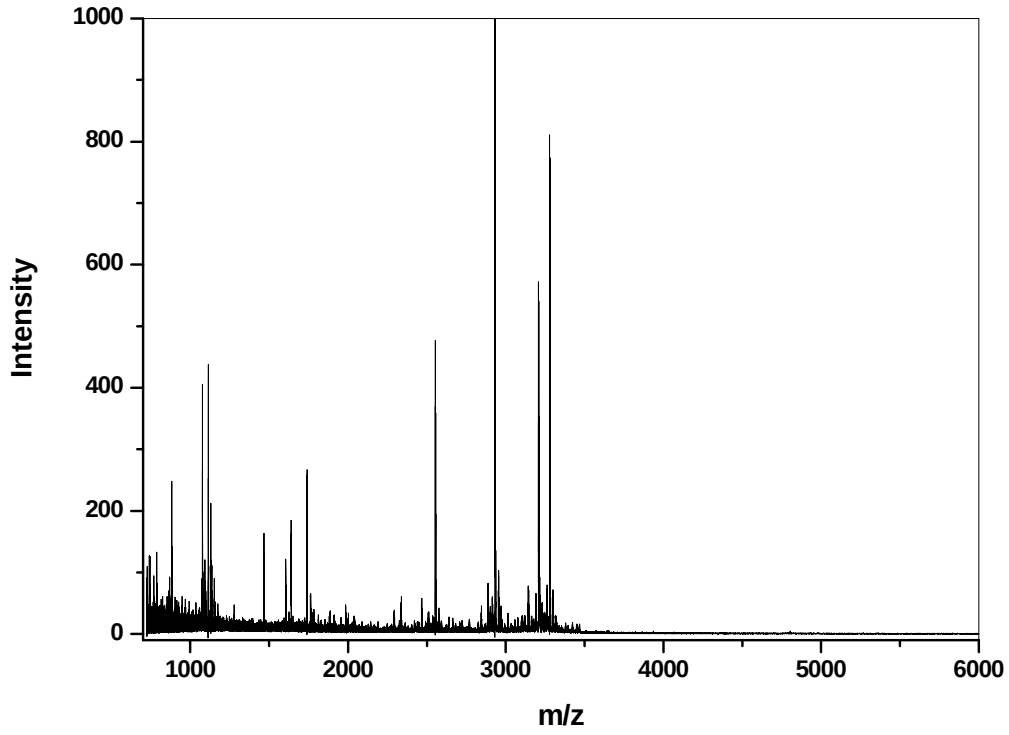

FIG. 6

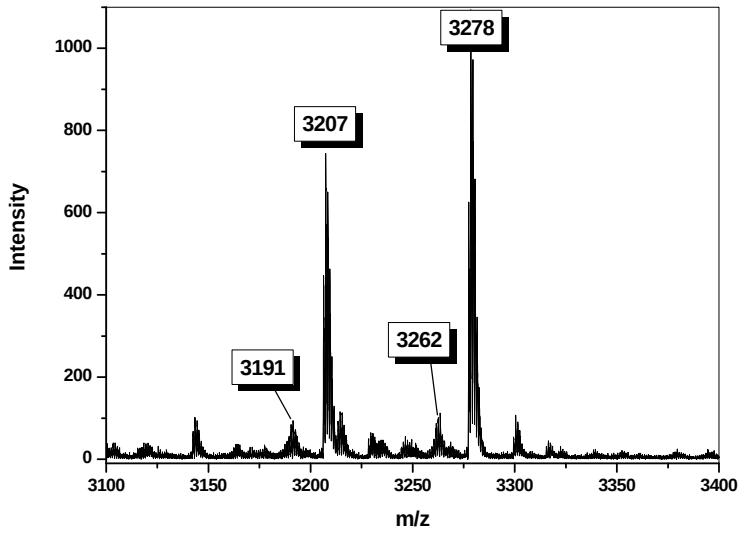

FIG. 7

We tried to identify the peaks of interest using LC-MS/MS and the technique was successful for the identification of the peptide with m/z 2770. Data-dependent MS/MS was generated using a 0.5-sec MS survey scan and 2.5-sec MS/MS scans on the three most abundant peaks found in the survey scan. The collision-induced dissociation (CID) energy was between 25 and 65 eV depending on the mass and charge state of the precursor ion. Dynamic exclusion was applied in the data depending acquisition to prevent that the most abundant ion was constantly subject to tandem mass spectrometry (MS/MS), so if the peptide was selected for the MS/MS scan, it wasn't selected again for a certain time, so that other less intense ion could have been analyzed. Peptides fragment in a predictable way in the collision-induced dissociation that occurs in tandem mass spectrometry. This peculiar aspect allows the use of algorithms able to correlate the experimental fragmentation pattern with the theoretical pattern in order to identify the protein. For this purpose the software Bioworks 3.3.1 (Thermo Scientific, Waltham, Massachusetts, USA) has been used. First of all, Bioworks matches amino acids sequence in the database and the measure mass of the peptide

and then calculate a cross-correlation value to give an estimate of the quality of the match between the experimental data and the database. For the peak 2770 a list of B and Y ions (Tab. 2, fig. 8) has been identified and the list has been correlated with a sequence of 25 amino acids (Ions 12/48, P (pep) = 2.09E-3). The sequence is a fragment of fibrinogen alpha chain, which has been associated with ovarian cancer by many scientists [46-49].

Table 2

AA	B	Y
S	8.803.930.485	-
S	1.750.713.333	2.681.196.159
S	2.621.033.617	259.416.413
Y	4.251.666.902	2.507.132.102
S	**5.121.987.186**	2.344.068.773
K	6.402.936.816	2.257.036.745
Q	7.683.522.591	2.128.941.782
F	**915.420.673**	2.000.883.205
T	**1.016.468.351**	**1.853.814.791**
S	110.350.038	**1.752.767.112**
S	**1.190.532.408**	1.665.735.084
T	1.291.580.087	**1.578.703.055**
S	1.378.612.115	**1.477.655.377**
Y	1.541.675.444	1.390.623.348
N	1.655.718.371	122.756.002
R	**1.811.819.482**	1.113.517.093
G	1.868.840.946	9.574.159.815
D	1.983.867.889	**9.003.945.178**
S	2.070.899.917	**7.853.675.748**
T	2.171.947.596	6.983.355.464
F	231.901.601	5.972.878.679
E	2.448.058.603	450.219.454
S	2.535.090.631	3.211.768.609
K	2.663.185.594	2.341.448.325
S	-	1.060.498.695

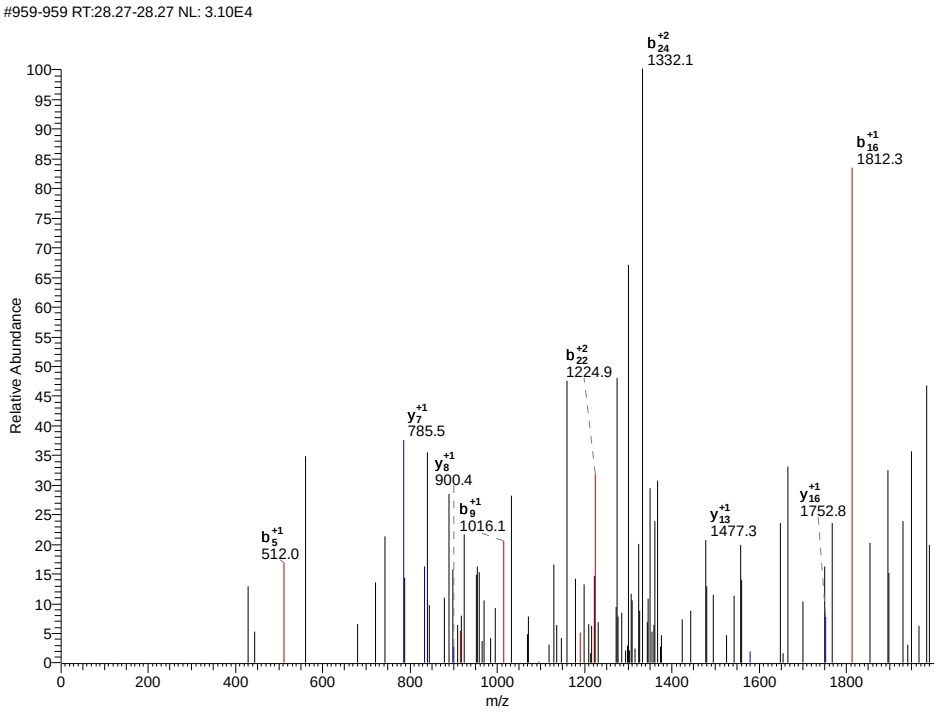

Fig. 8

The interesting four peaks (3191, 3207, 3262 and 3278, Fig. 7) showed an absolutely not satisfactory ionization in electro-spray, therefore further analysis will be performed on these analytes in order to determinate their amino acidic sequence. The most suitable technique seems to be MALDI-TOF/TOF mass spectrometry, since the peptides already showed a good degree of ionization in MALDI.

References

1. Gold, P. and S.O. Freedman, *Specific carcinoembryonic antigens of the human digestive system.* J Exp Med, 1965. **122**(3): p. 467-81.
2. Chatterjee, S.K. and B.R. Zetter, *Cancer biomarkers: knowing the present and predicting the future.* Future Oncol, 2005. **1**(1): p. 37-50.
3. DelVillano, B.C. and V.R. Zurawski, Jr., *The carbohydrate antigenic determinant 19-9 (CA 19-9): a monoclonal antibody defined tumor marker.* Lab Res Methods Biol Med, 1983. **8**: p. 269-82.
4. Neville, A.M., et al., *Monoclonal antibodies as probes of human breast disorders.* Ann N Y Acad Sci, 1983. **417**: p. 251-61.
5. Bast, R.C., Jr., et al., *A radioimmunoassay using a monoclonal antibody to monitor the course of epithelial ovarian cancer.* N Engl J Med, 1983. **309**(15): p. 883-7.
6. Yalta, K., et al., *Evaluation of tumor markers CA-125 and CEA in acute myocardial infarction.* Adv Ther, 2006. **23**(6): p. 1052-9.
7. Yilmaz, A., et al., *The value of Ca 125 in the evaluation of tuberculosis activity.* Respir Med, 2001. **95**(8): p. 666-9.
8. Meigs, J.B., et al., *Risk factors for clinical benign prostatic hyperplasia in a community-based population of healthy aging men.* J Clin Epidemiol, 2001. **54**(9): p. 935-44.
9. Potter, S.R. and A.W. Partin, *Prostate biopsy schemes and the detection of prostate cancer.* Rev Urol, 1999. **1**(4): p. 207-8.
10. Harris, R. and K.N. Lohr, *Screening for prostate cancer: an update of the evidence for the U.S. Preventive Services Task Force.* Ann Intern Med, 2002. **137**(11): p. 917-29.
11. Cox, C.E., et al., *Carcinoembryonic antigen and calcitonin as markers of malignancy in medullary thyroid carcinoma.* Surg Forum, 1979. **30**: p. 120-1.
12. Yesner, R., *Spectrum of lung cancer and ectopic hormones.* Pathol Annu, 1978. **13 Pt 1**: p. 207-40.
13. Jacobs, I. and D. Oram, *Screening for ovarian cancer.* Biomed Pharmacother, 1988. **42**(9): p. 589-96.
14. Pulay, T. and S. Csomor, *[Significance of CA-125 antigen in the monitoring of therapy and clinical course of ovarian cancer].* Orv Hetil, 1987. **128**(50): p. 2615-9.
15. Szymendera, J.J., *Clinical usefulness of three monoclonal antibody-defined tumor markers: CA 19-9, CA 50, and CA 125.* Tumour Biol, 1986. **7**(5-6): p. 333-42.
16. Visentin, M.C., et al., *[CA-125 serum levels in the diagnostic and clinical approach to ovarian cancer].* Minerva Ginecol, 1990. **42**(4): p. 109-16.
17. Ruibal, A., *[CA 125, a marker of ovarian epithelial tumors].* Med Clin (Barc), 1988. **91**(2): p. 54-7.
18. Rose, P.G., et al., *Serial serum CA 125 measurements for evaluation of recurrence in patients with endometrial carcinoma.* Obstet Gynecol, 1994. **84**(1): p. 12-6.
19. Ozols RF, e.a., *Principle and Practice of Gynecological Oncology*. 5th Edition ed. Epitelian ovarian cancer, ed. P.C. Hoskins WJ, Young R, Barakat R, et al. 2005, Philadelphia: Lippncott Williams & Wilkins. 895-987.
20. Lopez, M.F., et al., *High-resolution serum proteomic profiling of Alzheimer disease samples reveals disease-specific, carrier-protein-bound mass signatures.* Clin Chem, 2005. **51**(10): p. 1946-54.
21. Petricoin, E.F., et al., *Use of proteomic patterns in serum to identify ovarian cancer.* Lancet, 2002. **359**(9306): p. 572-7.
22. Li, J., et al., *Independent validation of candidate breast cancer serum biomarkers identified by mass spectrometry.* Clin Chem, 2005. **51**(12): p. 2229-35.
23. Geho, D.H., et al., *The amplified peptidome: the new treasure chest of candidate biomarkers.* Curr Opin Chem Biol, 2006. **10**(1): p. 50-5.
24. Villanueva, J., et al., *Differential exoprotease activities confer tumor-specific serum peptidome patterns.* J Clin Invest, 2006. **116**(1): p. 271-84.
25. Pieper, R., et al., *The human serum proteome: display of nearly 3700 chromatographically separated protein spots on two-dimensional electrophoresis gels and identification of 325 distinct proteins.* Proteomics, 2003. **3**(7): p. 1345-64.

26. Pieper, R., et al., *Multi-component immunoaffinity subtraction chromatography: an innovative step towards a comprehensive survey of the human plasma proteome.* Proteomics, 2003. **3**(4): p. 422-32.
27. Wang, Y.Y., P. Cheng, and D.W. Chan, *A simple affinity spin tube filter method for removing high-abundant common proteins or enriching low-abundant biomarkers for serum proteomic analysis.* Proteomics, 2003. **3**(3): p. 243-8.
28. Rai, A.J. and D.W. Chan, *Cancer proteomics: Serum diagnostics for tumor marker discovery.* Ann N Y Acad Sci, 2004. **1022**: p. 286-94.
29. Van den Bergh, G. and L. Arckens, *Recent advances in 2D electrophoresis: an array of possibilities.* Expert Rev Proteomics, 2005. **2**(2): p. 243-52.
30. Wall, D.B., et al., *Isoelectric focusing nonporous silica reversed-phase high-performance liquid chromatography/electrospray ionization time-of-flight mass spectrometry: a three-dimensional liquid-phase protein separation method as applied to the human erythroleukemia cell-line.* Rapid Commun Mass Spectrom, 2001. **15**(18): p. 1649-61.
31. Umar, A., et al., *NanoLC-FT-ICR MS improves proteome coverage attainable for approximately 3000 laser-microdissected breast carcinoma cells.* Proteomics, 2007. **7**(2): p. 323-9.
32. Conrads, T.P., et al., *Utility of accurate mass tags for proteome-wide protein identification.* Anal Chem, 2000. **72**(14): p. 3349-54.
33. Tang, N., P. Tornatore, and S.R. Weinberger, *Current developments in SELDI affinity technology.* Mass Spectrom Rev, 2004. **23**(1): p. 34-44.
34. Reyzer, M.L. and R.M. Caprioli, *MALDI mass spectrometry for direct tissue analysis: a new tool for biomarker discovery.* J Proteome Res, 2005. **4**(4): p. 1138-42.
35. Bons, J.A., W.K. Wodzig, and M.P. van Dieijen-Visser, *Protein profiling as a diagnostic tool in clinical chemistry: a review.* Clin Chem Lab Med, 2005. **43**(12): p. 1281-90.
36. Radulovic, D., et al., *Informatics platform for global proteomic profiling and biomarker discovery using liquid chromatography-tandem mass spectrometry.* Mol Cell Proteomics, 2004. **3**(10): p. 984-97.
37. Nelson, R.W., et al., *Mass spectrometric immunoassay.* Anal Chem, 1995. **67**(7): p. 1153-8.
38. Denkert, C., et al., *Mass spectrometry-based metabolic profiling reveals different metabolite patterns in invasive ovarian carcinomas and ovarian borderline tumors.* Cancer Res, 2006. **66**(22): p. 10795-804.
39. Ekegren, T., J. Hanrieder, and J. Bergquist, *Clinical perspectives of high-resolution mass spectrometry-based proteomics in neuroscience: exemplified in amyotrophic lateral sclerosis biomarker discovery research.* J Mass Spectrom, 2008. **43**(5): p. 559-71.
40. Hutchens TW, Y.T., *New desorption strategies for the mass spectrometric analysis of macromolecules.* Rapid Commun Mass Spectrom. , 1993. **7**(7): p. 576 - 580.
41. Chaurand, P., S.A. Schwartz, and R.M. Caprioli, *Assessing protein patterns in disease using imaging mass spectrometry.* J Proteome Res, 2004. **3**(2): p. 245-52.
42. Schwartz, S.A., et al., *Protein profiling in brain tumors using mass spectrometry: feasibility of a new technique for the analysis of protein expression.* Clin Cancer Res, 2004. **10**(3): p. 981-7.
43. Alexe, G., et al., *Ovarian cancer detection by logical analysis of proteomic data.* Proteomics, 2004. **4**(3): p. 766-83.
44. Daly, M.B. and R.F. Ozols, *The search for predictive patterns in ovarian cancer: proteomics meets bioinformatics.* Cancer Cell, 2002. **1**(2): p. 111-2.
45. Sorace, J.M. and M. Zhan, *A data review and re-assessment of ovarian cancer serum proteomic profiling.* BMC Bioinformatics, 2003. **4**: p. 24.
46. Koh, S.C., et al., *The association between fibrinogen, von Willebrand Factor, antithrombin III, and D-dimer levels and survival outcome by 36 months from ovarian cancer.* Clin Appl Thromb Hemost, 2006. **12**(1): p. 3-8.

47. Ma, Y., Y. Qian, and W. Lv, *The correlation between plasma fibrinogen levels and the clinical features of patients with ovarian carcinoma.* J Int Med Res, 2007. **35**(5): p. 678-84.
48. Ogata, Y., et al., *Elevated levels of phosphorylated fibrinogen-alpha-isoforms and differential expression of other post-translationally modified proteins in the plasma of ovarian cancer patients.* J Proteome Res, 2006. **5**(12): p. 3318-25.
49. Wang, X., et al., *Ovarian cancer, the coagulation pathway, and inflammation.* J Transl Med, 2005. **3**: p. 25.

Chapter III

MALDI MASS SPECTROMETRY AUTOMATED IMMUNO PRECIPITATION TEST OF MONOCLONAL ANTIBODY SPECIFICITY

MALDI Mass Spectrometry Automated Immuno Precipitation test of Monoclonal Antibody specificity

Introduction

1. Origin and Application of the Monoclonal Antibodies

In 1890 Emil von Behring and Shibasaburo Kitasato discovered that resistance to diphtheria could be transferred from one animal to another by taking blood serum from an immunized guinea-pig and injecting it into another animal [1]. They concluded that the immune serum contained a substance able to deactivate the diphtheria toxin and they called it *anti-toxin*. Later the *anti-toxin* was defined *antibody* and in 1901, the first Nobel Prize for Physiology and Medicine was awarded to Emil von Behring for "his work on serum therapy against diphtheria". For many years animal sera were considered the treatment of excellence for microbical infectious disease and for neutralization of toxins in man [2]. In more recent times the serum therapy has been replaced with rodent monoclonal antibodies. In the 1970s the B-cell cancer multiple myeloma was known, and it was understood that these cancerous B-cells all produce a single type of antibody (a paraprotein). This was used to study the structure of antibodies, but the first real production of monoclonal antibodies to a specific antigen was described by Schwaber and Cohen in 1973 [3]. They observed that even though hybrids between two distinct differentiated cell types keep on producing enzymes necessary for the metabolism of the cell, the specific proteins production is suppressed. They were able to isolate a myeloma X lymphoma cell lines that showed to continue the secretion of immunoglobulin. The isolated hybrid clone resulted from the fusion of a mouse myeloma cells secreting known specific immunoglobulin and human peripheral blood lymphocytes not secreting detectable immunoglobulin. The hybrid cells did not just secreted the mouse immunoglobulin but also the human immunoglobulin. Schwaber is widely cited as the inventor of the technique, but there are some controversies about the priority of the invention [4] and Georges Köhler, César Milstein, and Niels Kaj

Jerne shared the Nobel Prize in Physiology and Medicine in 1984 for the discovery. Köhler and Milsten described the manufacture of predefined specific antibodies from hybrid cell – fusion of mouse myeloma cell and mouse spleen cell from an immunized donor – secreting anti-sheep red blood cell [5].

The most important trait that makes of the monoclonal antibodies (MoAb) such a valuable tool in biochemistry and in medicine is their specificity. This distinguishing feature renders MoAbs absolutely helpful in several fields, for example in the therapy and in the diagnosis of many different diseases, detecting the presence of abnormal substances in the body.

The use of MoAbs in therapy has been possible only after improvement of the manufacture technology in order to overcome the limitation of the use of mouse antibodies due to the induced immunity by the foreign substances in the treated patients; the achievement of humanization and chimerization of mouse Abs brought to the improvement in 1995 of the first antibody for the treatment of cancer: that was Edrecolomab [6] and today there are 20 or so antibodies involved in clinical trials and 10 of them have advanced to Phase III trials or even further [7]. Antibodies can be used in therapy as *naked* antibodies – without any drug or radioactive material attached to them – or as *conjugated* MoAbs – with a drug or any other active substance attached to them. Their *naked* forms have also been used in combination with cytotoxic drugs and it has led to controversial outcomes as in the case of Herceptin that has synergistic antitumor activity with cisplatin and carboplatin [8, 9] and additive benefits in combination with other drugs such as doxorubicin and cyclophosphamide, however the association of this MoAb therapy and the anthracycline drug with cyclophosphamide has been associated with a significant increase in cardiotoxic effects [10].

Several strategies for monoclonal antibodies therapy are now used or under investigation (Fig. 1). One of the mechanisms is the enhancement of the antibody dependent and/or complement dependent cytotoxicity, in which the tumor cell killing is activated by the interaction between the FC region of the

Ab bound to the cell and the FCγ receptor on the immuno effector cell. This mechanism could be very useful in the treatment of minimal residual disease and metastatic disease in the attempt to overcome the lack of accessibility and the limited penetration of solid tumor by antibodies [11, 12]. The probably most explored approach is the direct arming by covalent linkage of active molecules to the antibody that acts as a vehicle for targeted therapy; although this strategy showed in many cases unacceptable high levels of toxicity [13], Gemtuzumab ozogamicin (Mylotarg) has been approved in 2000 for acute myelogenous leukemia [14]. On the other hand also indirect arming is a possible approach, for example attaching liposomes containing active drugs to the MoAb [15] or bispecific antibodies (BsAbs) that are not natural antibodies able to bind both a tumor associated antigen and a trigger antigen on a immuno effector cell, in order to activate the immuno system against a tumor cell that otherwise would have been ignored. BsAbs showed some interesting results in ovarian cancer trials [16]. The pre-targeting approach provides a selective delivery of radionuclides using the high affinity interaction between streptavidin and biotin [17, 18] or of progrugs [19, 20] that should be ideally converted in drug only inside the tumor.

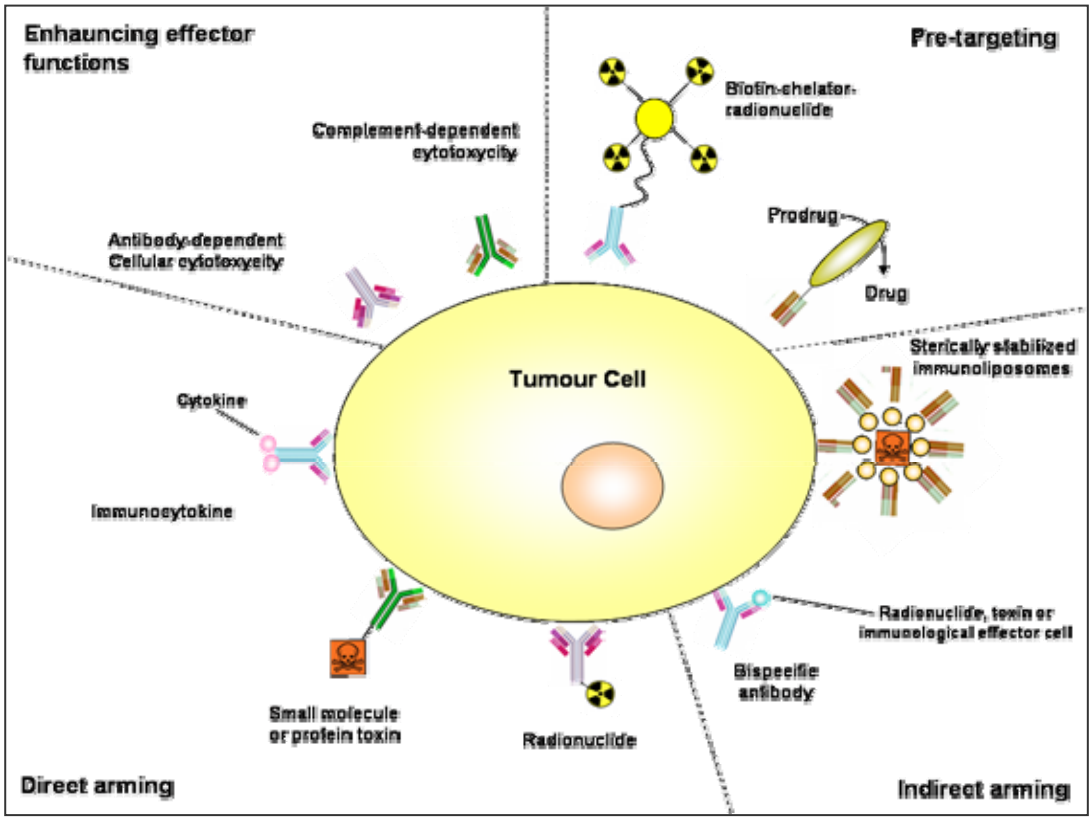

Figure 1

Strategies for monoclonal antibodies therapy

The use of MoAbs in the diagnosis and in the prognosis of diseases does not involve the use of humanized antibodies; simple mouse antibodies that can be easily obtained in large quantities are sufficient to create sensitive and selective tests for potentially any molecule. This peculiar aspect has been utilized for example in the development of tests for cancer biomarkers, e.g. Prostate-specific antigen (PSA) [21]. In March 2000 the Food and Drug Administration approved the first automated PSA test (Hybritech Tandem-R, Beckman Coulter Inc.), based on the use of two monoclonal antibodies for the determination of the free and the total PSA, producing equimolar results with reliable consistency, sensitivity and specificity. The CA-125 test instead is an example of the use of monoclonal antibodies to monitor the course of a particular disease [22-24], in other words of the prognosis of the disease. The Roche test for the antigen CA-125 is an sandwich ELISA *(ENZYME-LINKED*

IMMUNOSORBENT ASSAY) assay in which the secondary antibody is in a detectable form due to the electrochemiluminescence of Ruthenium(II) complexes with tripropylamine (TPA).
Since it is possible to obtain MoAbs virtually for any type of molecule, it is also possible to develop the appropriate ELISA assay for a quantitive determination of the investigated molecule, so it could be an ELISA assay for a potential molecule involved in cancer development [25], or for a particular drug [26], an endogenous factor [27]. Recently some interesting applications of MoAbs in ELISA assays have been described such as sensors of specific proteins in solution [28], for the detection of botulinum neurotoxin type A [29] and for post translational modification of cytosolic proteins [30]. The key in any of the described applications of the MoAbs is the specificity of the antibody itself that could be obtained and tested with different techniques, more or less sophisticated.

2. Monoclonal Antibodies Production

Given such a diversity of uses for the MoAbs, their production in pure quantities has long been the focus of scientific investigation. The conventional method was to inject a laboratory animal with an antigen and then, after antibodies had been formed, collect those antibodies from the blood serum (antibody-containing blood serum is called antiserum). The most widely used MoAbs production technology is the hybridoma technique – first developed by Kohler and Milstein in 1977 [5] – which involves the fusion of myeloma cells and spleen cells from most typically a rodent – commonly mouse, sometimes rat – or lately also a rabbit, in either cases the animals have been previously immunized with the desired antigen. Myeloma is a tumour of the bone marrow that can be adapted to grow permanently in cell culture. The fusion is usually mediated by the presence of polyethylen glycol [31], but the success rate is very low, so the selection of the fused cells is necessary. The growth of spleen cells will eventually stop because of their limited life span; instead for the myeloma cell the loss of ability to synthesize hypoxanthine-guanine-

phosphoribosyl transferase (HGPRT) will be exploited to select the hybrid cells. HGPRT is the enzyme that allows the synthesis of purines using an extracellular source of hypoxanthine as a precursor; in normal conditions the absence of the enzyme can be overcome by the activation of an alternative biochemical pathway, but if the cells are exposed to the folic acid analogue aminopterin, the alternative pathway is locked and in this way the myeloma cells survival is completely denied. The selective culture medium is called HAT medium because it contains Hypoxanthine, Aminopterin, and Thymidine. However, hybridoma cells are able to grow indefinitely because the spleen cell partner supplies HGPRT and the myeloma partner is immortal because it is a cancer cell. In this way immortal hybridomas have been obtained and they will continually produce antibodies. These antibodies are called monoclonal because they derivate from the preparation containing only one kind of clone – the hybridoma – instead the polyclonal antibodies come from preparation with many kinds of cells, therefore the monoclonal antibodies are potentially more pure than the polyclonal antibodies obtained with conventional techniques, perhaps more specific. In the monoclonal antibodies production, the hybrid clones are diluted and clones are grown from single parent cells. Antibodies produced by each different clones are tested and only the selected clone are use in the next step that is the propagation of the antibody, that could be performed *in vitro* or *in vivo* injecting the hybridoma cells in mice – in the peritoneal cavity – where they produce tumours containing an antibody-rich fluid called produce large ascites fluid.

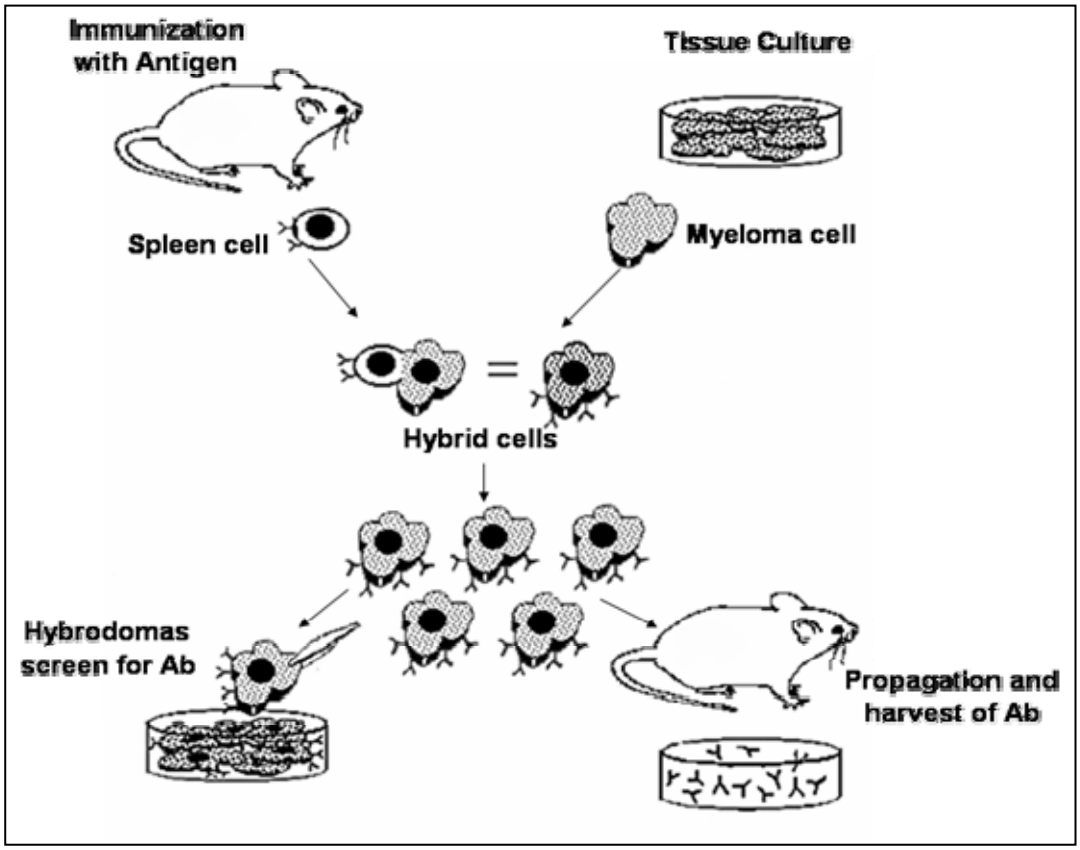

Figure 2

Over a quarter century ago the development of murine hybridoma technology, with its capacity to produce large quantities of well-characterized monoclonal antibodies, revolutionized diagnostic and therapeutic medicine. For many applications in transfusion medicine, however, the production of serological reagents in mice has certain biological limitations relating to the induction of anti-mouse immune responses. Human hybridoma formation presented several technical difficulties that have led to novel molecular approaches that do not require cell fusion, immortalization or even immunization of individuals. These technologies, referred to as 'repertoire cloning' or 'Fab/phage display', are a relative new combination of molecular techniques for the display of proteins and they have been introduced by Smith in 1985 [32]. In this technique the genetic material encoding the antigen is inserted into a filamentous phage that will be hosted by *Escherichia Coli* [33]. *E.Coli* is an expression and display system. The only one prerequisite for this technique is

that the immunoglobulin gene of the species has to be sufficiently sequenced in details so the PCR amplification is possible. In the phage approach the lymphocyte cells are isolated from the spleen – just like for the hybridoma technique – but from the bone marrow as well; the immortalization concerns just the DNA region encoding the immunoglobulin of interest and not the whole cell. RNA is prepared from the lymphocytes and by reverse transcriptase it is transcripted into cDNA of the variable regions of immunoglobulins that can be amplified by PCR. Combining phage libraries prepared from various immunized animals can provide very large antibody libraries. Many techniques can be used to enrich the population of *E.Coli* and also binding affinity of phage antibodies can be enhanced by optional *in vitro* affinity maturation. When the specifically binding phage is identified, the Ab can be expressed in soluble form in *E.Coli* without phage and in large quantities.

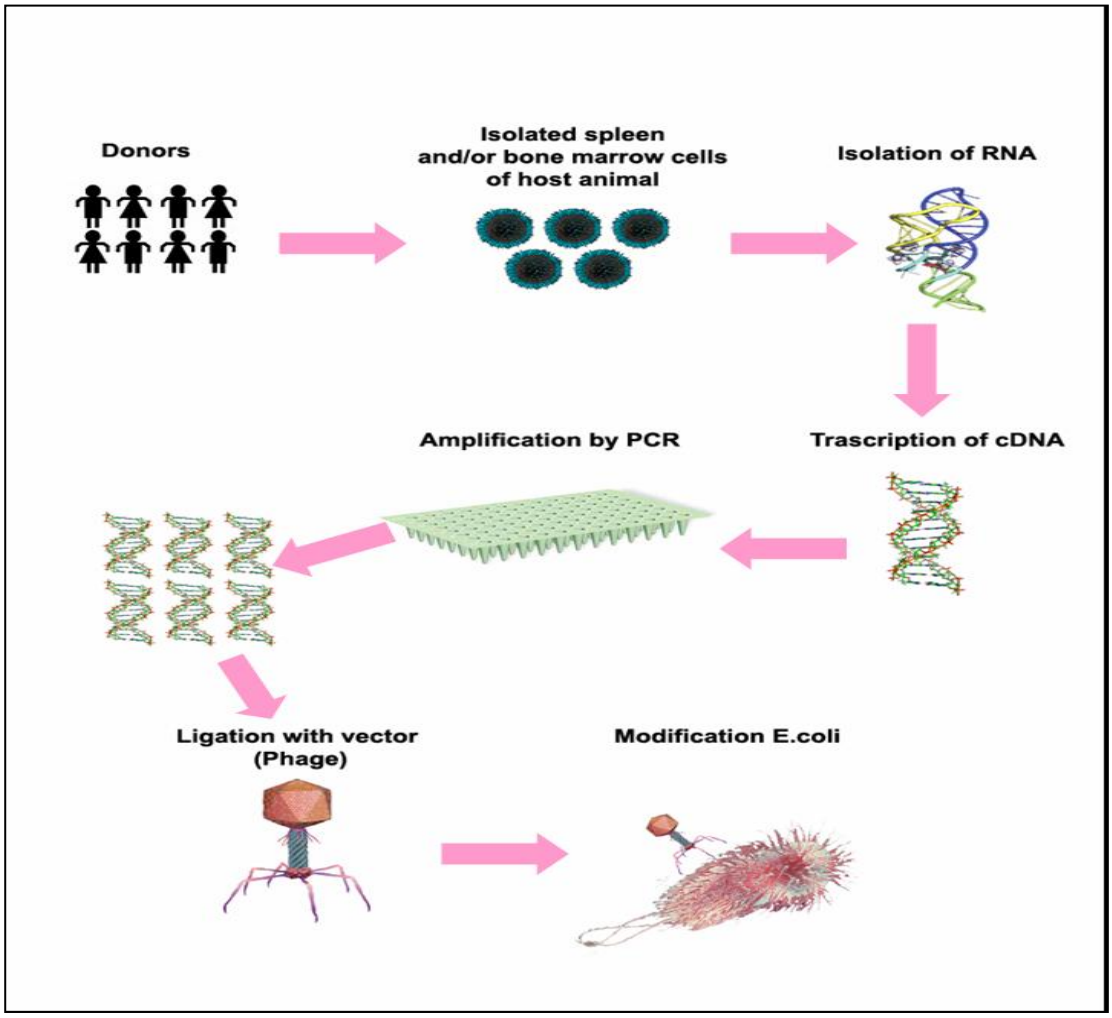

Figure 2

The evaluation of antibody binding is generally performed by ELISA or Western Blotting, but other techniques such as Surface Plasmon Resonance (SPR) [34-36] or Immuno Precipitation Mass Spectrometry could be extremely useful to determinate of the presence of interaction between antigen and antibody.

Aim of the Study

This study is part of the five-year National Cancer Institute (NCI) Clinical Proteomic Technologies for Cancer (CPTC) Initiative initiative to build a foundation of technologies, data, reagents, reference materials, analysis systems, and infrastructure needed to systematically advance protein biology for the diagnosis, treatment and prevention of cancer. As part of the CPTC initiative, that involves several structures in North America and Europe, monoclonal antibodies have been raised to potential protein biomarkers to provide a series of renewable and highly characterized affinity binding reagents to the research community.

The goal is to determine an analytical assay that provides information about the specificity of the IgG mouse monoclonal antibodies using mass spectrometry. The assay has to be automated to allow the analysis of many antigen/antibody pairs in the same assay with the lowest possibility of error. The Immuno Precipitation Mass Spectrometry approach has been selected in order to integrate other analytical techniques involved in the choice of the best monoclonal antibody for the specific antigen, in particular Western Blot and Surface Plasmon Resonance. The selected monoclonal antibodies will be involved in the development of ELISA assays for the screening of clinical samples, in order to clinically validate the potential biomarker and obtain easy and accessible diagnostic tools, for a rapid, specific and selective kit that should be available in the clinics.

Experimental

1. Material

Magnetic beads

Three different types of beads were tested: MagnaBind Protein A Beads and MagnaBind Goat Anti-Mouse IgG Beads (Pierce, Rockford, IL, USA) and Dynabeads Pan Mouse (Invitrogen Corp., Campbell, CA, USA).

Reagents

High performance liquid chromatography grade solvents (Water and Acetonitrile) were purchased from EMD (Madison, WI USA). Sinapic Acid was from Sigma-Aldrich (St. Luois, MO, USA), the detergent beta -octyl glucoside (BOG) and SuperBlock were from Pierce. Phosphate-Buffered Saline (PBS) 7.4 (10X) liquid came from Invitrogen Corp., while Trifluoroacetic acid (TFA) was purchased from Pierce. IgG Thyroid Simulating Hormone (TSH) and anti-TSH were purchased from Seradyn Inc. Indianapolis, IN, USA.

2. Equipment

The sample processing has been completely performed on the Halmiton Star Robot (Hamilton Company, Reno, NV, USA) and a Dynal magnetic patirticles concentrator (Invitrogen) has been used to facilitate the removal, washing and elution steps. MALDI-MS experiments were performed in positive ion mode using a Voyager DE-PRO (Applied Biosystems, Framingham, MA, USA).

3. Methods

Automated Immunoaffinity test of Antibody specificity – A complete automated run allows the analysis of 48 Antigen/Antibody pairs in duplicate in the same experiment. The robotic method was performed on the Hamilton Robot. Both antigen and antibody solution of each duplicate analysis came from the same vial in order to reduce variability due to the preparation of the solution.
Different types of beads have been tested to define the more convenient from the standpoint of efficacy, reproducibility and economic suitability.
The assay was performed placing a dilution of beads suspension in PBS 1x/BOG 500 μM (running buffer), for a final volume of 250 μL and a concentration of 1mg/mL. The beads were washed two times with PBS

1x/BOG 500 μM (200 μL each). The robot provided also a distribution of the MoAbs from 500 μL tubes to a different 96 well plate, picking 120 μL of solution and dividing it into two equal aliquots of 60 μL in two contiguous wells on the plate. The positive control MoAbs was anti-TSH, in a dilution 1:20 of the stock solution 4.75 mg/mL in running buffer. In the next step the robot added 50 μL of the MoAbs solution to the washed beads, the plate was covered with a lid and mixed for 40 minute at room temperature. At this point the MoAbs should have been capture by the beads surface (Protein A, GAM or PAN Mouse) and further three washes with PBS 1x/BOG 500 μM (200 μL each) were executed. In the blocking experiments, after attachment of the antibodies on the surface of the beads, the beads are treated with SuperBlock (3 times, 200 μL each) and washed again with running buffer. The robot distributed also the antigen from the 500 μL tubes into a new 96 well plate, following the same procedure used for the antibodies distributions, so it was possible to add a volume of 50 μL of antigen into the beads plate. The following incubation involved the only manual step of the procedure: the plate was cover with a lid and manually transfer into a cold room (4°T) for slow tilt agitation for 1 hour. At the end of the incubation the plate was again manually transferred to the robot and three washes were executed with PBS 1x/BOG 500 μM (200 μL each), followed by three more washes with water to eliminate the salt and the detergent that could affect the mass spectrometry determination. The elution of the antigens and of the antibodies from the beads was performed automatically and directly adding 35 μL of a matrix solution to the beads (Sinapic Acid 10 mg/mL, 0.1% TFA/Acetonitrile, 60/40) and then from the plate the elute solutions were spotted directly onto the surface of the MALDI target (2 μL each spot). The plate was left to dry at room temperature and when completely dry it was introduced into the MALDI-MS analyzer to determine the molecular weight of the eluted antigen.

MALDI-MS conditions – Mass spectra were acquired with a Voyager-DE™ PRO Biospectrometry Workstation. This instrument was equipped with a nitrogen laser (337 nm), and data were obtained by using the linear acquisition mode under delayed extraction conditions. The laser spot size on target was approximately circular, with a diameter of 25 lm. Instrument settings were an accelerating voltage of 25 kV, 91.5% grid voltage, 0.15% guidewire voltage, delay time of 600 nsec, and bin size of 4 nsec. 50 shots per spectrum were collected with m/z range 5,000-100,000.

Results and Discussions

We tested three kinds of beads with different properties and from different companies. The aim of these screening was to select the most suitable beads for the purpose of the study. In table one the beads' properties are summarized.

Tab 1

Company	*Name*	*Coating Molecule*	*Specificity*	*Composition*	*Magnetization type*	*Beads size*	*Concentration*
Pierce	MagnaBind Protein A Beads	Protein A	Fc-part of IgG_1, IgG_2 and IgG_4	Silanized iron oxide	Superparamagnetic	1-4 □m	5 mg/mL
Pierce	MagnaBind Goat Anti-mouse IgG beads	GAM Goat Anti-mouse IgG (GAM)	Both heavy and light chains to IgG	Silanized iron oxide	Superparamagnetic	1-4 □m	1 mg/mL
Invitrogen	Dynabeads Pan Mouse IgG	Monoclonal human Anti-mouse IgG	Mouse IgG subclasses, Fc specific	Polystyrene	Superparamagnetic	Uniform 4.5 □m	10 mg/mL

The differences between the three kinds of beads are basically due to their sizes, which affects the amount of available area for the binding with the monoclonal antibodies with indirect proportion with the beads diameter, and to the molecule coating the surface of the beads. Pan Mouse IgG and the Protein A [41] beads are specific for IgG subclasses and Fc specific, while Pierce GAM antibodies cannot guarantee the correct orientation of the secondary antibody – in this case the monoclonal antibody to be tested – but they have been tested anyway because of their extremely reduced cost, that calculated on a complete single assay results at least twenty-five time less that the other beads (Fig. 4). In the washing and incubating steps of the assay it was introduced the use of a small amount of detergent BOG which showed to lead to a greater intensity of the signal due to the antigen in the MALDI MS spectra, probably due to the increment of the solubility of the species involved

in the binding reaction, therefore the improvement of the efficacy of the washes.

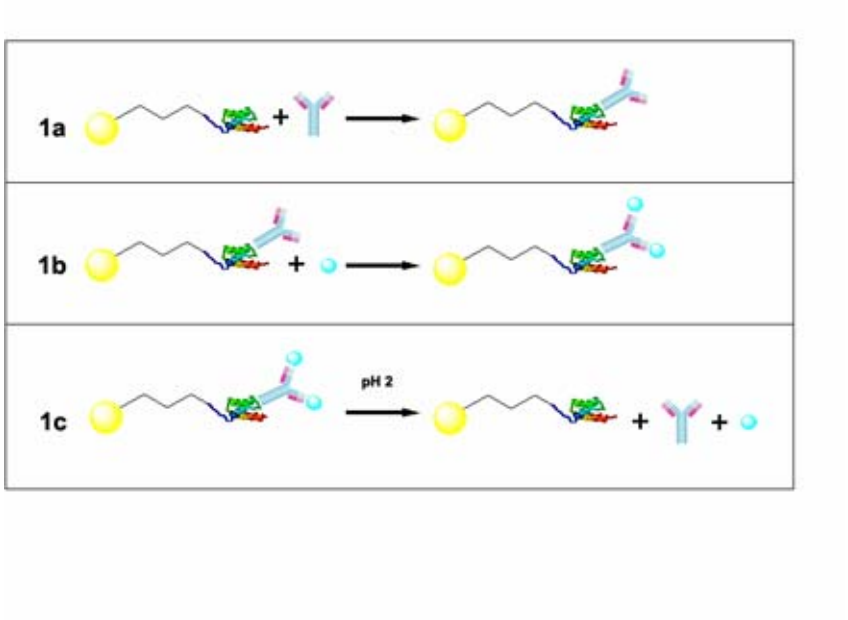

Fig. 4a – Protein A beads

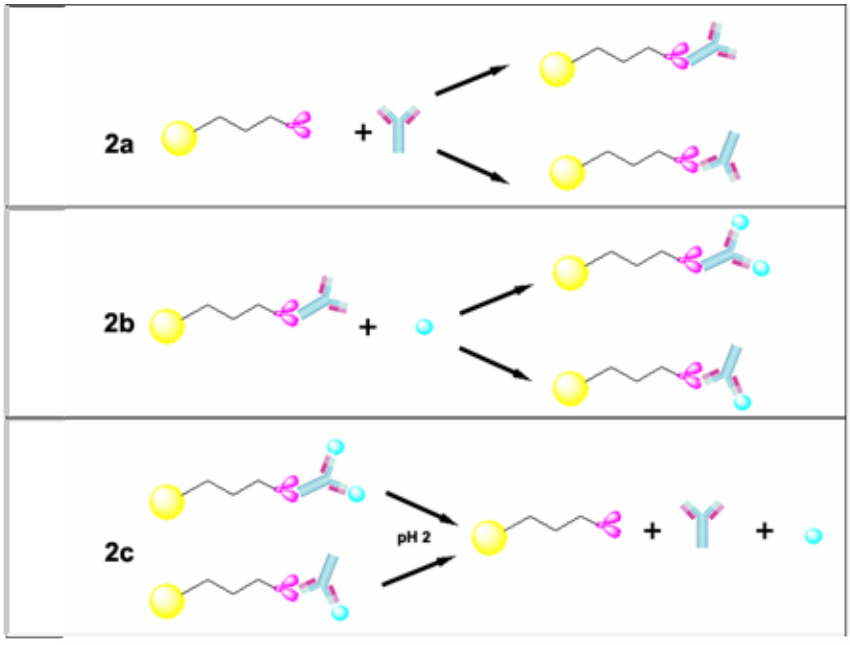

Fig 4b – GAM beads

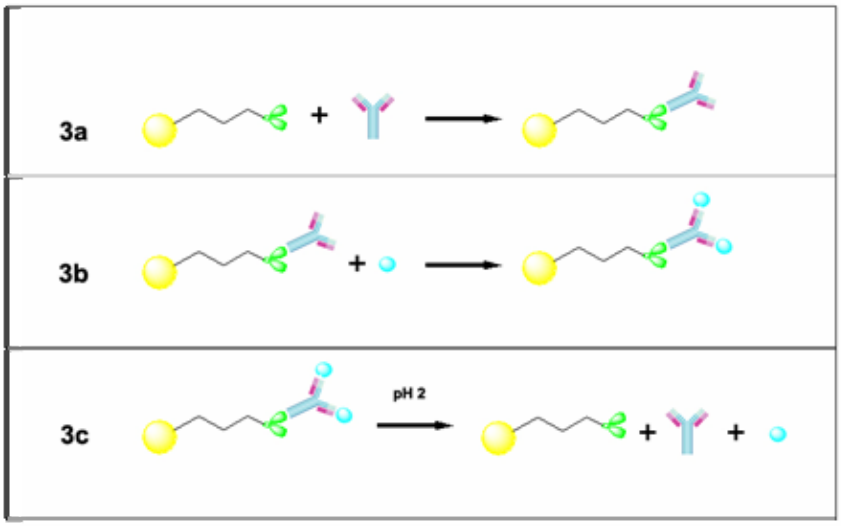

Fig 4c – PAN Mouse Beads

The three types of beads have been compared using a commercial monoclonal antibody anti-TSH and the correspondent antigen TSH and the results are showed in figure 5.

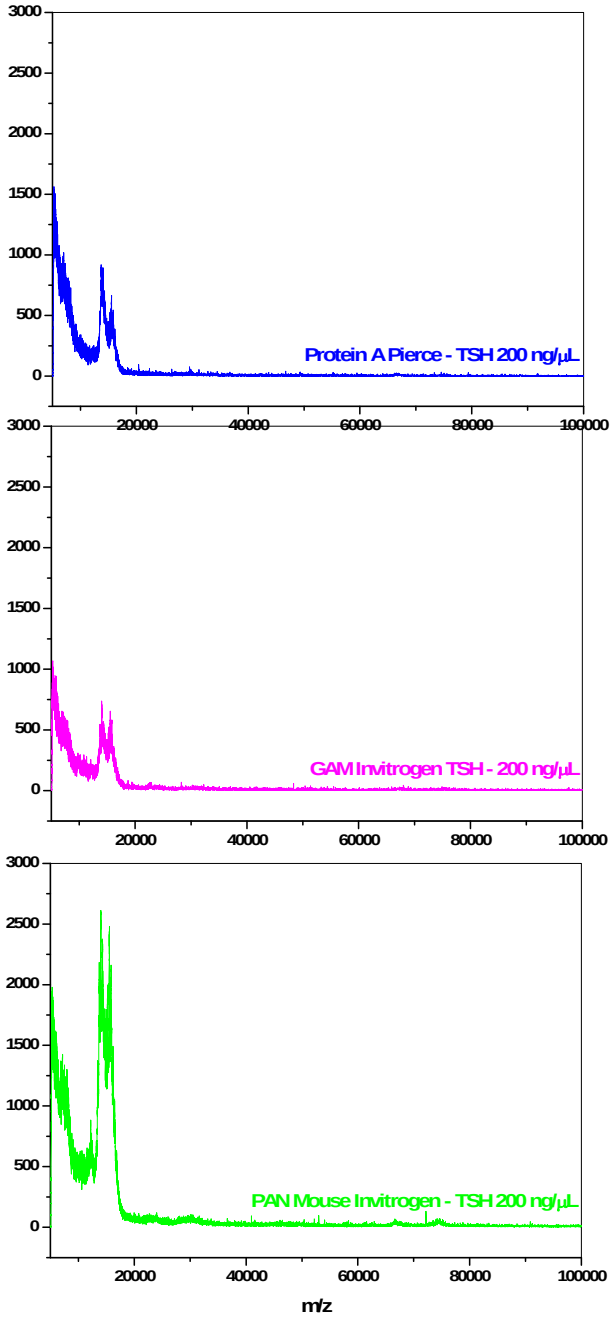
Protein A Pierce - TSH 200 ng/µL
GAM Invitrogen TSH - 200 ng/µL
PAN Mouse Invitrogen - TSH 200 ng/µL
m/z

Figure 5

The results in figure 1 showed that the best outcomes were obtained with Pierce Protein A beads and Invitrogen Pan Mouse IgG. We were expecting better results for the Protein A beads instead of the PAN Mouse due to the fact that the surface of Protein A beads is higher in average (1-4 μm diameter) than the surface of the Pan Mouse IgG (4.5 μm diameter), providing more available area for the binding between the primary and the secondary antibody. A higher surface leads to higher possibility of specific binding between the monoclonal antibody and the antigen, therefore a higher concentration of the antigen in the elute from the beads, but in this study the beads with lower surface – PAN mouse – showed better results, probably due to the nature of the coating molecule and its strong interaction with the IgG (MoAbs) to be capture. The beads were eluted directly with the matrix solution which is acidic enough (pH ≤ 2) to dissolve the non covalent interaction between primary antibody, secondary antibody and antigen. Direct elution also avoids a further dilution of the antigen and also time delay. The matrix solution of choice is sinapic acid, indicated for large molecular weight protein, in a concentration of 10 mg/mL in 0.1% TFA/ACN 60/40 that allows a good crystallization without spreading of the material over the edges of the spot on the MALDI target in the automated spotting procedure (2 μL for each spot).
In order to narrow the selection to just one bead type, the two candidate kinds of beads – Pierce GAM beads and Invitrogen Pan Mouse IgG – have been tested for non specific binding and cross-reaction with the control couple anti-TSH and TSH and two series of testing monoclonal antibodies for two specific antigens. The two antigens were Metastasin 100 calcium-binding protein A4 (Calvasculin) and Ras-related C3 botulinum toxin substrate 1 (rho family small GTP binding protein Rac1) and they were indicated respectively as Ag 10337 and Ag 10295.
Ras-related C3 [42] belongs to the Rac family of small GTPases, known to be responsible for the regulation of actin cytoskeletal structures and the influence on the cellular processes of integrin-mediated adhesion and migration. RAC3 as a factor associated with adhesion and migration signaling pathways has

been indicated by Baugher at al. as involved in human breast cancer along with RAC1, correlating high endogenous Rac activity with the progression of the disease. On the other hand Calvasculin or S100A4 [43, 44] belongs to the family of EF-hand calcium-binding proteins and it shows to be expressed in cancer cells and to contribute to tumor cell motility and metastatic progression as well, even though the exact underlying mechanisms remain elusive. The two antigens are part of a group of proteins considered to have a high potential as putative biomarkers and they represent just examples on how the IPMS assay can be conducted. The importance of the use of authentic material to develop the IPMS methods is due to the fact that these two antigens with the corresponding monoclonal antibodies are the prototype of what a regular sample would be delivered and ready for IPMS testing from the standpoint of concentration and buffer used for dilution after purification.
The test for the non specific binding has been performed incubating the antigen directly with the beads, with or without the use of a blocking step. Again the PAN beads showed a better signal and visible non specific binding effect due to the not monoclonal antibody conjugated surface of the beads (fig. 6). The effect has been completely eliminated in the PAN Mouse beads blocking the surface of the beads that had not reacted with the antibodies with BSA or similar mixture, we decided to use a commercial solution commonly used in ELISA, the SuperBlock by Pierce. The blocking step involves another variable and a higher degree of complexity which is not always the most desirable approach, but in this case it was necessary because the aim of the test was to evaluate only the specific interaction between MoAb and the correspondent antigen. The not specific binding effect shown by Protein A beads was higher and the blocking expedient did not provide an acceptable elimination or attenuation of the not specific binding (fig .7).

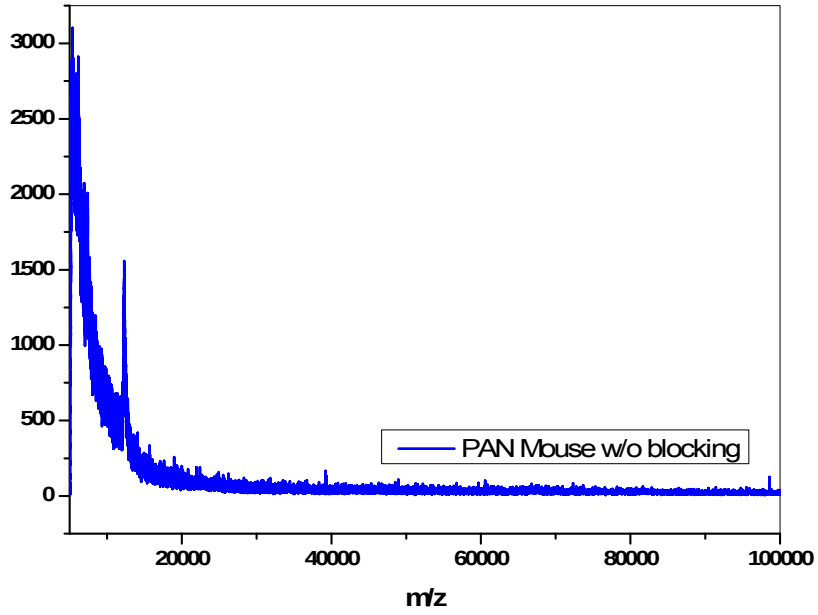

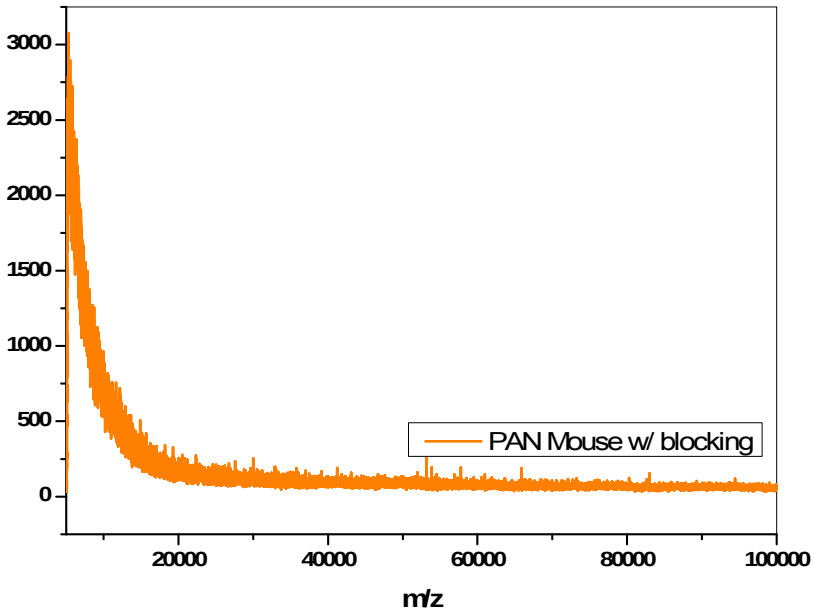

Fig. 6

Non specific binding of antigen 10337 in PAN Mouse beads

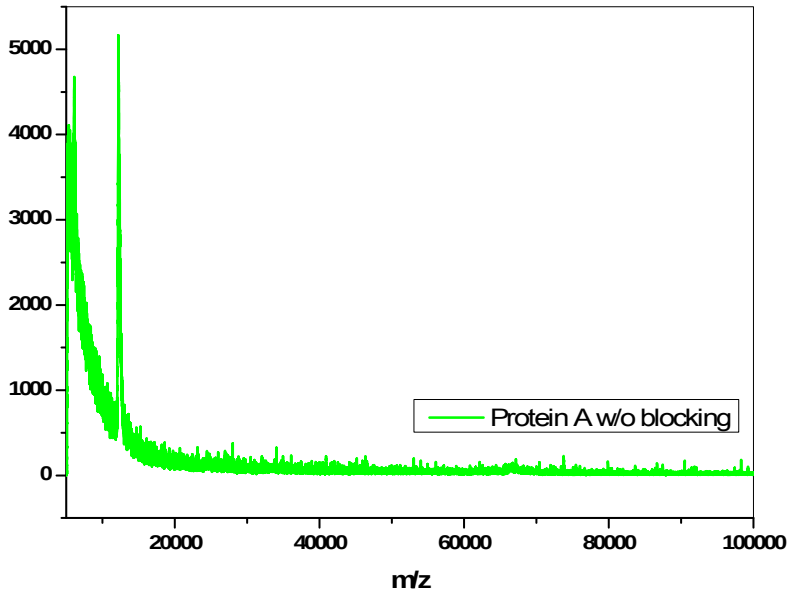

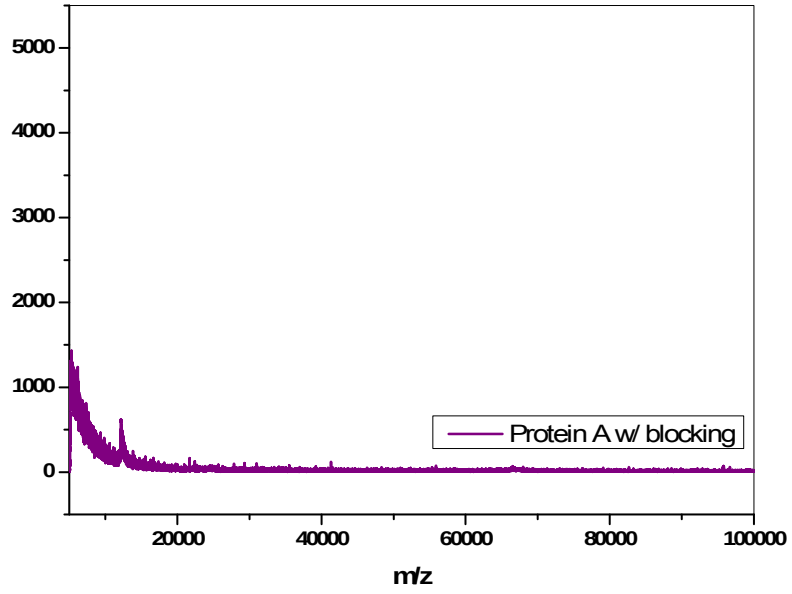

Fig. 7

Non specific binding of antigen 10337 in Protein A beads

The next set of experiments was a titration of the monoclonal antibodies in order to test the appropriate amount of antibody needed on the surface of the selected beads, Pan Mouse IgG. The starting amount was 12.5 μg in 50 μL of solution (0.25 μg/μL) which is an extremely high excess to assure a complete capture of the secondary antibody, but it also means an unnecessary waste of material. The titration (fig. 3) was from the starting amount of antibody (amount 12.5 μg) to 0.002 μg/μL (amount 0.1 μg), a concentration that supposedly should not have showed enough binding coverage, while the concentration of the antigen was kept constant (200 ng/μL). The selected concentration of the MoAb to be conjugated to the surface of the beads was 0.020 μg/μL (amount 1 μg), concentration that guarantees the necessary saturation of the beads surface without wasting of materials.
The same antigens have been used to test the cross-reactivity: beads conjugated with one MoAb have been incubated with the not correspondent antigen and none of the MoAbs showed any cross-reactivity effects as shown in figure 4 for Antigen 10295 with MoAbs specific for the Antigen 10337.

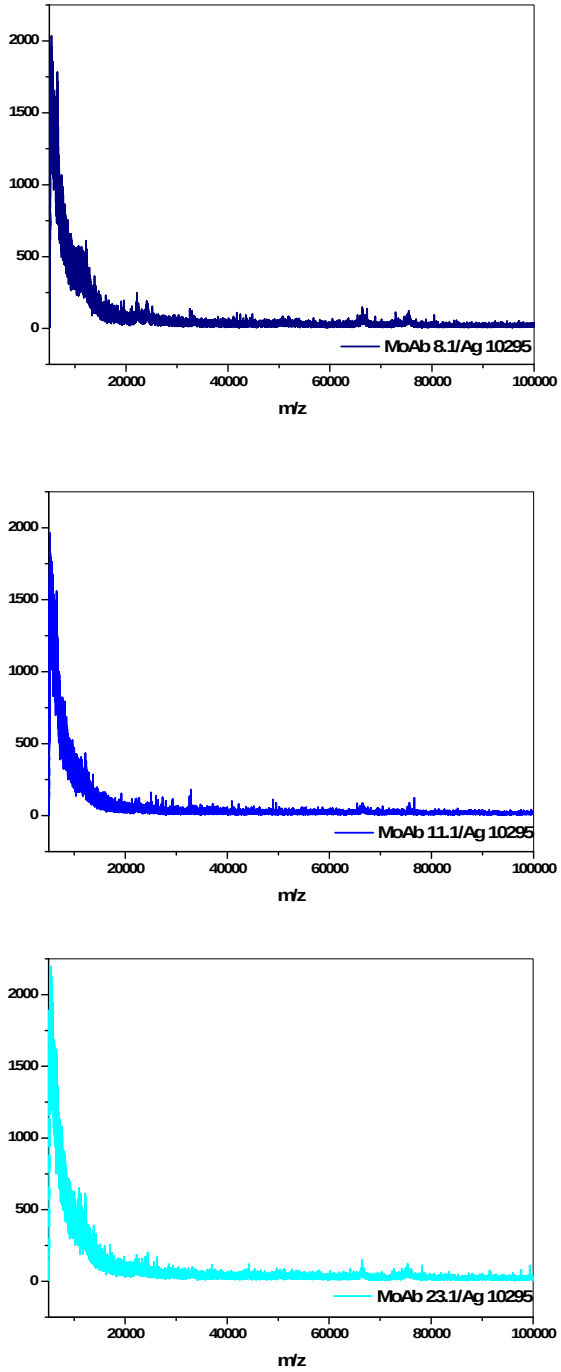

Fig. 8

Cross-reactivity on PAN Mouse beads
Antigen 10295 with MoAbs specific for Antigen 10337

The optimized test has been used to evaluate the specificity of the MoAbs for Metastasin 100 calcium-binding protein A4 (Calvasculin) and Ras-related C3 botulinum toxin substrate 1. Figure 9 shows how Immuno Precipitation Mass Spectrometry (IPMS) can provide information about the specificity of the monoclonal antibodies and the peculiar aspect of this technique is the possibility to obtain information about the structure of the antigen captured by the monoclonal antibody: in this case the three selected MoAbs for the antigen 10337 are able to capture not only the antigen in its monomeric form (12 KDa), but also in its dimeric conformation (24 KDa).

This study proved IPMS has a high potential as a complementary tool of crucial importance in the selection of the monoclonal antibody, in association with other techniques such as Surface Plasmon Resonance (SPR), Western Blotting and Enzyme-Linked ImmunoSorbent Assay (ELISA). The monoclonal antibodies selected with the combination of the mentioned techniques will be used in the development of ELISA based assay to be applied in the screening of a consistent number of human specimens for the clinical validation of proteins indicated in literature as potential biomarkers. If the biomarker will be estimated sensitive and specific, it will be a powerful tool in clinics in the diagnosis as well as in the prognosis and in the prediction of different diseases.

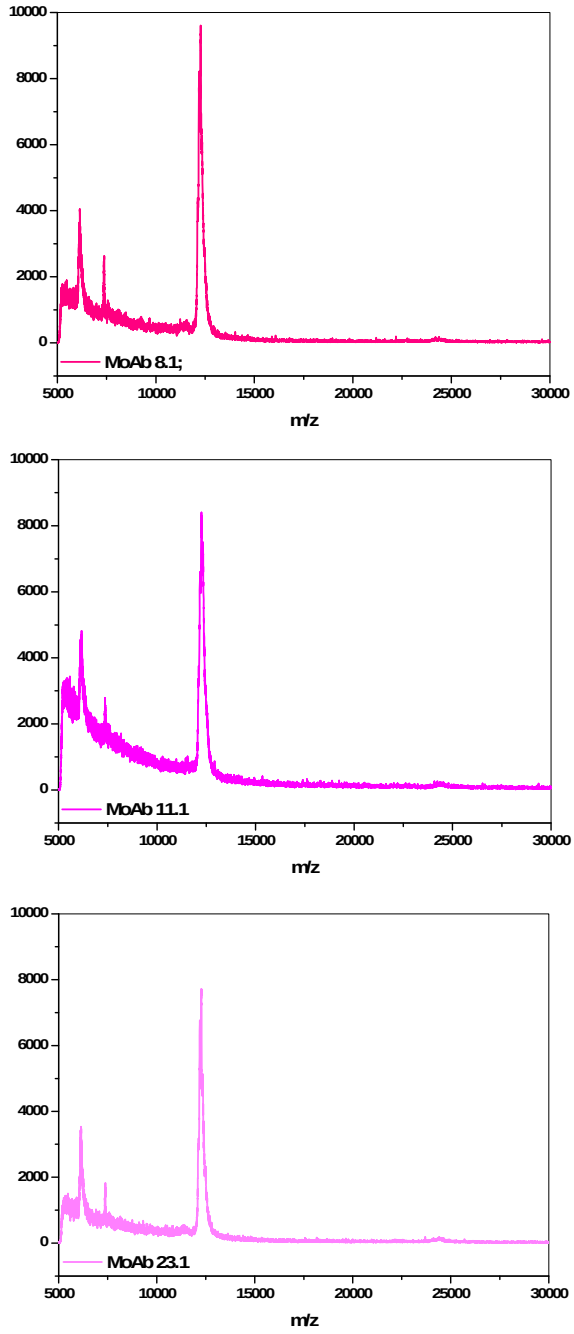
10000
8000
6000
4000
2000
0
MoAb 8.1;
5000
10000
15000
20000
25000
30000
m/z
10000
8000
6000
4000
2000
0
MoAb 11.1
5000
10000
15000
20000
25000
30000
m/z
10000
8000
6000
4000
2000
0
MoAb 23.1
5000
10000
15000
20000
25000
30000
m/z

Fig. 9

References

1. Behring and Kitasato, *[On the development of immunity to diphtheria and tetanus in animals].* Dtsch Med Wochenschr, 1965. **90**(49): p. 2183.
2. Ratner, B., *Allergy, Anaphylaxis and Immunotherapy*, ed. W.a. Wilkins. 1943, Baltimore.
3. Schwaber, J. and E.P. Cohen, *Human x mouse somatic cell hybrid clone secreting immunoglobulins of both parental types.* Nature, 1973. **244**(5416): p. 444-7.
4. Cambrosio, A. and P. Keating, *Between fact and technique: the beginnings of hybridoma technology.* J Hist Biol, 1992. **25**(2): p. 175-230.
5. Kohler, G. and C. Milstein, *Continuous cultures of fused cells secreting antibody of predefined specificity.* Nature, 1975. **256**(5517): p. 495-7.
6. Punt, C.J., *New drugs in the treatment of colorectal carcinoma.* Cancer, 1998. **83**(4): p. 679-89.
7. Carter, P., *Improving the efficacy of antibody-based cancer therapies.* Nat Rev Cancer, 2001. **1**(2): p. 118-29.
8. Pietras, R.J., et al., *Antibody to HER-2/neu receptor blocks DNA repair after cisplatin in human breast and ovarian cancer cells.* Oncogene, 1994. **9**(7): p. 1829-38.
9. Pietras, R.J., et al., *Remission of human breast cancer xenografts on therapy with humanized monoclonal antibody to HER-2 receptor and DNA-reactive drugs.* Oncogene, 1998. **17**(17): p. 2235-49.
10. Slamon, D.J., et al., *Use of chemotherapy plus a monoclonal antibody against HER2 for metastatic breast cancer that overexpresses HER2.* N Engl J Med, 2001. **344**(11): p. 783-92.
11. Riethmuller, G., et al., *Randomised trial of monoclonal antibody for adjuvant therapy of resected Dukes' C colorectal carcinoma. German Cancer Aid 17-1A Study Group.* Lancet, 1994. **343**(8907): p. 1177-83.
12. Riethmuller, G., et al., *Monoclonal antibody therapy for resected Dukes' C colorectal cancer: seven-year outcome of a multicenter randomized trial.* J Clin Oncol, 1998. **16**(5): p. 1788-94.
13. Farah, R.A., et al., *The development of monoclonal antibodies for the therapy of cancer.* Crit Rev Eukaryot Gene Expr, 1998. **8**(3-4): p. 321-56.
14. Miller, C.B., *New research and treatment options for acute myeloid leukemia.* Am J Manag Care, 2000. **6**(18 Suppl): p. S973-4.
15. Lasic, D.D. and D. Papahadjopoulos, *Liposomes revisited.* Science, 1995. **267**(5202): p. 1275-6.
16. Lamers, C.H., et al., *Local but no systemic immunomodulation by intraperitoneal treatment of advanced ovarian cancer with autologous T lymphocytes re-targeted by a bi-specific monoclonal antibody.* Int J Cancer, 1997. **73**(2): p. 211-9.
17. Stoldt, H.S., et al., *Pretargeting strategies for radio-immunoguided tumour localisation and therapy.* Eur J Cancer, 1997. **33**(2): p. 186-92.
18. Wu, A.M., *Tools for pretargeted radioimmunotherapy.* Cancer Biother Radiopharm, 2001. **16**(2): p. 103-8.
19. Niculescu-Duvaz, I., et al., *Prodrugs for antibody- and gene-directed enzyme prodrug therapies (ADEPT and GDEPT).* Anticancer Drug Des, 1999. **14**(6): p. 517-38.
20. Syrigos, K.N. and A.A. Epenetos, *Antibody directed enzyme prodrug therapy (ADEPT): a review of the experimental and clinical considerations.* Anticancer Res, 1999. **19**(1A): p. 605-13.
21. Roth, H.J., S.C. Stewart, and M.K. Brawer, *A comparison of three free and total PSA assays.* Prostate Cancer Prostatic Dis, 1998. **1**(6): p. 326-331.
22. Yalta, K., et al., *Evaluation of tumor markers CA-125 and CEA in acute myocardial infarction.* Adv Ther, 2006. **23**(6): p. 1052-9.
23. Hogdall, E., *Cancer antigen 125 and prognosis.* Curr Opin Obstet Gynecol, 2008. **20**(1): p. 4-8.
24. Bast, R.C., Jr., et al., *A radioimmunoassay using a monoclonal antibody to monitor the course of epithelial ovarian cancer.* N Engl J Med, 1983. **309**(15): p. 883-7.

25. Ye, J., et al., *A monoclonal-antibody-based ELISA for the detection of human FADD (Fas-associated death domain).* Biotechnol Appl Biochem, 2008. **50**(Pt 3): p. 143-6.
26. Mercader, J.V., et al., *Hapten synthesis and monoclonal antibody-based immunoassay development for detection of the fungicide trifloxystrobin.* J Agric Food Chem, 2008. **56**(8): p. 2581-8.
27. Lee, S.H., et al., *Monoclonal antibody-based screening assay for factor inhibiting hypoxia-inducible factor inhibitors.* J Biomol Screen, 2008. **13**(6): p. 494-503.
28. Heyduk, E., et al., *Molecular pincers: antibody-based homogeneous protein sensors.* Anal Chem, 2008. **80**(13): p. 5152-9.
29. Chiao, D.J., J.J. Wey, and S.S. Tang, *Monoclonal antibody-based enzyme immunoassay for detection of botulinum neurotoxin type A.* Hybridoma (Larchmt), 2008. **27**(1): p. 43-7.
30. Ahrend, M., et al., *Immunochemical methods for the rapid screening of the o-glycosidically linked N-acetylglucosamine modification of proteins.* Methods Mol Biol, 2008. **446**: p. 267-80.
31. Davidson, R.L. and P.S. Gerald, *Induction of mammalian somatic cell hybridization by polyethylene glycol.* Methods Cell Biol, 1977. **15**: p. 325-38.
32. Smith, G.P., *Filamentous fusion phage: novel expression vectors that display cloned antigens on the virion surface.* Science, 1985. **228**(4705): p. 1315-7.
33. Schmitz, U., et al., *Phage display: a molecular tool for the generation of antibodies--a review.* Placenta, 2000. **21 Suppl A**: p. S106-12.
34. Fivash, M., E.M. Towler, and R.J. Fisher, *BIAcore for macromolecular interaction.* Curr Opin Biotechnol, 1998. **9**(1): p. 97-101.
35. Fujiwara, S., et al., *Monoclonal antibodies specific to human ETS-2 oncoprotein: recognition of epitopes clustered on the B domain.* Hybridoma, 1990. **9**(6): p. 559-71.
36. Safsten, P., et al., *Screening antibody-antigen interactions in parallel using Biacore A100.* Anal Biochem, 2006. **353**(2): p. 181-90.
37. Qingwen Li, G.L.J.F., *Direct Electron Transfer for Heme Proteins Assembled on Nanocrystalline TiO_{<FONT SIZE='-1'>2</FONT>} Film*. 2001. p. 359-363.
38. Collinson, M., E.F. Bowden, and M.J. Tarlov, *Voltammetry of covalently immobilized cytochrome c on self-assembled monolayer electrodes.* Langmuir, 1992. **8**(5): p. 1247-1250.
39. Frey, B.L. and R.M. Corn, *Covalent Attachment and Derivatization of Poly(L-lysine) Monolayers on Gold Surfaces As Characterized by Polarization-Modulation FT-IR Spectroscopy.* Anal. Chem., 1996. **68**(18): p. 3187-3193.
40. Caruso, F., et al., *Quartz Crystal Microbalance Study of DNA Immobilization and Hybridization for Nucleic Acid Sensor Development.* Anal. Chem., 1997. **69**(11): p. 2043-2049.
41. Hober, S., K. Nord, and M. Linhult, *Protein A chromatography for antibody purification.* Journal of Chromatography B, 2007. **848**(1): p. 40.
42. Baugher, P., et al., *Rac1 and Rac3 isoform activation is involved in the invasive and metastatic phenotype of human breast cancer cells.* Breast Cancer Research, 2005. **7**(6): p. R965 - R974.
43. Kaplan, J.H., *A Moving New Role for the Sodium Pump in Epithelial Cells and Carcinomas.* Sci. STKE, 2005. **2005**(289): p. pe31-.
44. Tarabykina, S., et al., *Metastasis-associated protein S100A4: spotlight on its role in cell migration.* Curr Cancer Drug Targets, 2007. **7**(3): p. 217-28.

APPENDIX A

Publications

in vivo *20*: 735-738 (2006)

Liposomal Doxorubicin with and without TNFα in the Perfusional Treatment of Advanced Soft Tissue Limb Sarcoma: Preliminary Results

FRANCO DI FILIPPO, MICHELE ANZÀ, ROSA GARINEI, FRANCESCO CAVALIERE, PASQUALE PERRI, CLAUDIO BOTTI, PIERA DI ANGELO, SIMONA DI FILIPPO, CARLO LUDOVICO MAINI, ROSSELLA PASQUALONI, SUSANNA DI SEGNI, SIMONA COLANTONIO, PIETRO BRUNO, LOREDANA PIARULLI and FRANCESCA PRINCIPI

Department of Surgery, Regina Elena National Cancer Institute, Rome, Italy

Abstract. *Background: A combination of doxorubicin and tumor necrosis factor alpha (TNFα) has been proven to be very effective in the perfusional treatment of advanced soft tissue limb sarcoma both in terms of tumor necrosis and limb conservative surgery rate. Unfortunately, in some patients a grade IV limb reaction has been recorded. The key solution might be the use of liposomal doxorubicin (Caelyx®) because the carrier seems to release the drug preferentially in the tumor rather than in the healthy tissue. Patients and Methods: Twenty patients were treated with Caelyx: 14 with Caelyx alone and 6 in combination with a low TNFα dose (1 mg). In the first series of 14 patients a dose escalation study was carried out starting from a dose of 10 mg/L of limb volume. Six patients were treated with Caelyx (16 mg) and TNFα (1 mg). Results: The maximum tolerated dose (MTD) was 16 mg/L as in two patients treated with 18 mg/L a grade IV limb reaction was observed. Tumor response was satisfactory and conservative surgery was carried out in 13 patients. In 6 patients treated with Caelyx and TNFα, only a grade I limb reaction was recorded, thus, confirming that TNFα did not increase toxicity, at least at a dose of 1 mg. The Caelyx-TNFα combination did increase treatment efficacy. Tumor necrosis ≥70% was observed in 4 out of 6 patients, one with 100% necrosis (pathological complete response). All the patients underwent conservative surgery. Conclusion: The Caelyx-TNFα combination was proven to increase the efficacy of Caelyx alone, with a very low toxicity. These preliminary results have to be tested in a larger patient population.*

Correspondence to: Franco Di Filippo, MD, Department of Surgery, Regina Elena National Cancer Institute, Via Elio Chianesi, 53, 00144 Rome, Italy. Tel: +390 652662720, Fax: +390 652666907, e-mail: difilippo@ifo.it

Key Words: Soft tissue sarcoma, Caelyx®, perfusion.

In order improve the therapeutic effectiveness of hyperthermic isolation limb perfusion (HILP), a combination of tumor necrosis factor alpha (TNFα), doxorubicin and true hyperthermia (41°C) was employed in the treatment of limb threatening soft tissue sarcoma.

The results of a phase I-II study conducted in 58 patients affected with limb threatening soft tissue sarcoma employing 1 mg TNFα were very satisfactory (1, 2).

The pathological at complete, partial and objective response rates were 34%, 48% and 82%, respectively; the limb salvage surgery rate (LSS) was 84%. Finally, the 5-year locoregional recurrence, disease-free and overall survival rates were 22%, 42.4% and 72.4%, respectively.

Unfortunately, a grade IV limb was recorded in 5 patients, all treated with a TNFα dose >1 mg and a temperature level ≥41.5°C.

Recently, liposomes containing doxorubicin have been successfully employed in the *i.v.* treatment of many cancers, including soft tissue sarcoma, with less systemic toxicity. In fact, the liposomes pass many times through the blood vessels feeding growing tumors, extravasate and enter the tissue compartment, lodging in the tumor interstitium near the vessels.

Drug molecules are released from liposomes preferentially in hypoxic (tumor) rather than euoxic (healthy) tissue (3).

The biological characteristics of liposomal doxorubicin (Caelyx®) make this drug particularly suitable for isolation limb perfusion because it decreases the previously described limb toxicity. Moreover, the combination of doxorubicin, TNFα and hyperthermia results synergistically (4-6).

The aim of this paper was to report the results of a phase I-II study carried out employing Caelyx with/without TNFα in the perfusional treatment of advanced soft tissue sarcoma.

0258-851X/2006 $2.00+.40

Patients and Methods

Patients characteristics. Twenty patients with soft tissue limb sarcomas were treated with HILP. Eight patients were male and 12 female, between the ages of 30 and 71 years (median: 50 years). The majority of the patients had lower limb tumors and only two patients had a tumor of the upper limb. All patients had grade 2-3 tumors: the tumor size ranged between 10 and 20 cm (average 15 cm). The tumor histology was: malignant fibrous histiocytoma (10 patients), liposarcoma (5), synovialsarcoma (2), angiosarcoma (1), alveolar soft part sarcoma (1) and leiomyosarcoma (1).

The eligibility criteria were described in detail in previous papers (1, 2, 7).

Caelyx® (liposomal doxorubicin, supplied by Schering Plough S.p.A., Milan, Italy) was administered at a starting dose of 10 mg/L of limb volume; the dose was escalated at a rate of 2 mg for each triplet of patients. The maximum tolerated dose (MTD) was the amount causing a grade IV limb reaction in at least two out of three patients; the temperature level was the same for all treatments (41.5°C). The limb toxicity was recorded according to the Wieberdink classification (8).

In patients treated with both Caelyx and TNFα, the drug dosages were 16 mg/L and 1 mg, respectively.

HILP technique. The technique of HILP has been described previously (9). Only a few details that are strictly related to the treatment will, therefore, be reported. The axillary and iliac vessels were cannulated for tumor of upper and lower limbs, respectively. As soon as tumor temperature reached 41.5°C, Caelyx was injected in the extracorporal circuit at the pre-established dose. In patients treated with the combination of drugs, TNFα (1 mg) was first administered followed by Caelyx (16 mg/L) after 30 minutes. During regional perfusion, leakage was accurately monitored with technetium 99 labelled albumin (0.5 Bg/kg). (10)

At the end of perfusion, the extracorporeal circuit was washed with saline solution and low molecular dextran to remove any residual drug.

Pharmacokinetics. In six patients treated with Caelyx and TNFα, liposomal doxorubicin pharmacokinetics was carried out. Blood samples of both perfusional and systemic circulation were taken at 0, 10, 20, 30, 50 and 60 minutes from commencement of perfusion. At the end of perfusion, tumor and muscle samples were taken in order to measure the healthy and tumor tissue doxorubicin concentration.

A modified reversed-phase high performance liquid chromatography method reported previously, was used to quantify Doxorubicin in plasma samples (11).

(i) Plasma sample extraction: 0.2 ml of plasma were prepared for the analysis by adding 200 μl of a $CHCl_3$:MeOH (1:2) solution and 4 μl of Triton X-100. After 5 min at room temperature, the mixture was vortexed and centrifuged for 5 min at 8000 rpm. An aliquot of the supernatant solution (150 μl) was decanted and evaporated to dryness under a nitrogen stream. The concentrated samples were reconstituted in 200 μl of mobile phase (ammonium acetate buffer pH 4: acetonitrile 98:2 v/v) and 20 μl were injected for the analysis. Samples from circuit were diluted before treatment 1:4 with PBS 1x.

(ii) Tissue extraction: homogenized tissue (0.5 g of tumor or muscle tissue) was added to 0.5 ml of double-distilled water (DDW) and after one night at room temperature the mixture was vortexed for 5 min at 8000 rpm. The total doxorubicin was then separated from contaminating materials using a solid-phase extraction procedure (C18 Sep-Pak cartridges; Waters, Milford, MA, USA). The C18 cartridges (100 mg) were preconditioned with methanol and washed with 10 mM phosphate-buffered saline (pH 7.4) before applying 0.2 ml of sample. After washing the cartridge with buffer, the doxorubicin was eluted from the cartridge with chloroform : methanol (2:1). The eluant was evaporated to dryness under nitrogen, reconstituted with a mixture of ammonium acetate buffer (pH 4) : acetonitrile (98:2 v/v) and analyzed using HPLC.

Pharmacokinctics of plasma samples was determined according to standard non-compartmental equations. The area under the concentration time-curve (AUC) was calculated using the linear trapezoidal rule from time zero to the time corresponding to the last sampling point (C last). C_{max}=maximum plasma concentration (observed). AUC=area under the plasma concentration time-curve. Doxorubicin tissue concentration was calculated as the ratio of AU (absorbance units) of the doxorubicin peaks and AU of the doxorubicin peaks generated with known amounts of the drug by HPLC chromatography. The doxorubicin into the tissue samples was referred as mg of drug per mg of proteins from the tissue homogenates.

Table I. *HILP with liposomal doxorubicin and TNFα pharmacokinetic results.*

Patients	Perfusional circuit		Systemic circulation	
	AUC 0-last (μg min/ml)	C_{max} (μg/ml)	AUC 0-last (μg min/ml)	C_{max} (μg/ml)
CL	48.00	1.30	7.30	0.15
NV	1056.90	24.20	66.62	1.31
RF	489.48	13.90	39.41	1.03
PM	11713.00	286.04	162.30	9.50
LM	32816.10	783.20	233.50	7.84
CP	1287.60	45.90	268.52	7.98

Results

Toxicity. In patients treated only with Caelyx, the grade of limb reaction was always mild (I-II) up to a dosage of 18 mg/L. At this dosage, two grade IV limb reactions were observed, therefore, the MTD is 16 mg/L. The combination of Caelyx (16 mg/L) and TNFα (1 mg) did not result in increased toxicity; in all six patients only a grade I limb reaction was recorded.

Pharmacokinetics. The results of Caelyx pharmacokinetics in terms of AUC and C_{max} related to perfusional and systemic circulation are reported in Table I.

It is apparent that the amount of doxorubicin is constantly greater in the perfusional circuit than in the systemic circulation. This is the aim of isolation perfusion:

Table II. *HILP with liposomal doxorubicin with or without TNFα in the treatment of advanced soft tissue sarcoma: clinical results.*

	Drug dosage	No. of patients	Grade of limb reaction	Tumor necrosis (%)	Surgery
Doxorubicin	10 mg/L	3	I - I -I	30-40-90	D - C - C
(DX)	12 mg/L	3	I - II - I	40-50-80	C - C - C
	14 mg/L	3	I - I - I	40-50-50	C - C - C
	16 mg/L	3	I - I - I	40-50-90	C - C - C
	18 mg/L	2	IV - IV	40-70	C - C
DX+TNFα	16 mg/L + 1 mg	1	I	70	C
	16 mg/L + 0.5 mg*	1	I	50	C
	16 mg/L + 1 mg	1	I	100	C
	16 mg/L / 1 mg	1	I	90	C
	16 mg/L + 1 mg	1	I	50	C
	16 mg/L + 1 mg	1	I	70	C

*High leakage during regional perfusion. C=conservative; D=demolitive.

to expose the tumor to a high drug concentration, while reducing the systemic side-effects. The doxorubicin tumor concentration ranged from 100 to 1,400 mcgs in relation to the amount of the employed drug, thus, demonstrating that even in a short time (60 min) the liposomes open and release the drug that accumulates in tumor tissue.

Tumor response. In patients treated with Caelyx alone, a tumor necrosis ≥70% was observed in 4 out of 14 patients, in 4 patients the tumor necrosis was equal to 50%, and in 6 patients the tumor necrosis was <50%.

In patients treated with Caelyx and TNFα, a tumor necrosis ≥70% was recorded in 4 of 6 patients, and one with 100% tumor necrosis (pathological complete response), thus, demonstrating that TNFα was able to increase the tumor response when combined with antineoplastic drugs. All six patients were treated with conservative surgery (Table II).

Discussion

The rationale for employing hyperthermia-doxorubicin and TNFα by perfusion is based on the following: doxorubicin has been proven to be one of the most active cytotoxic agents against soft tissue sarcoma, with objective response rates ranging between 15% and 35% (C.R. 6%): a dose-response relationship has been observed in non-randomized studies. *In vivo* studies have demonstrated that simultaneous application of heat and doxorubicin (41.5°C) increases the antitumor effect of doxorubicin (4). Doxorubicin tissue concentrations obtained with hyperthermic perfusion are 5, 25 and 45 times greater than those obtained with normothermic perfusion and with *i.a.* and systemic infusion, respectively.

In vitro studies have demonstrated that the tumoricidal effect of doxorubicin is enhanced more by the association with TNFα (86% enhancement) than with any other drugs (5).

Experimental studies have shown a direct correlation between the antineoplastic effect of TNFα and the temperature level, moreover, the TNFα-hyperthermia association is able to kill TNFα-resistant cells (6).

Finally, phase I-II studies have demonstrated that hyperthermia-doxorubicin-TNFα association, carried out by regional perfusion, is feasible and effective in clinical settings (2). Unfortunately, the trimodality association may result in high local toxicity if high temperature levels (>41.5°C) are reached and maintained during perfusion.

Liposomal doxorubicin may represent the key solution because of its biochemical characteristics.

Our phase I-II study seem to confirm the liposome pharmacodynamic properties: only a mild toxicity has been observed in the perfused limb even though a temperature level >41.5°C and doxorubicin dosages greater than the standard dose (10 ml/L of limb volume) have been employed until the MTD (16 mg). Objective response was obtained from all patients and tumor necrosis >75% was recorded in 4 out of 14 patients. These results are quite similar to those obtained with free doxorubicin (2). Therefore, it is suggested that the association of liposomal doxorubicin-hyperthermia and TNFα might further improve the therapeutic effectiveness of perfusion.

In *in vivo* experimental studies doxorubicin, doxorubicin-TNFα, liposomal doxorubicin and liposomal doxorubicin-TNFα were systemically administered to sarcoma bearing rats. The results clearly demonstrated that, among these combinations, the liposomal doxorubicin associated to low TNFα dose gave the best results (OR 50%) (12). These

results have been confirmed by *in vivo* experiments carried out by Brouckaert *et al.* who demonstrated in B16 BL6 melanoma bearing mice that the association of free-TNF and systemically administered liposomal doxorubicin strongly improve tumor response (13).

The above mentioned studies have been confirmed in our clinical settings. In patients treated with low TNFα (1 mg) and liposomal doxorubicin a tumor necrosis ≥70% was observed in 66% of them with one 100% tumor necrosis (pCR). TNFα is able, not only to induce a hemorrhagic tumor necrosis, but also to increase the drug concentration selectively in tumor tissue, thus, further increase the tumor necrosis (13).

At a median follow-up of 15 months, 1 local and 2 systemic relapses have been recorded in patients treated only with Caelyx.

In conclusion, a combination of Caelyx and TNFα is effective in the treatment of threatening soft tissue limb sarcoma because it reduces limb toxicity and guarantee a high limb-sparing surgery rate. These preliminary results should be tested in a larger patient population.

Acknowledgements

We are grateful to Miss Tiziana Piccolo for typing the manuscript and to the technicians Romano Augeri and Roberto Di Bona for their assistance during extracorporeal circulation. This work was founded by grants from Ministero della Salute and AIRC.

References

1 Di Filippo F, Rossi CR, Vaglini M, Azzarelli A, Anzà M, Santinami M, Lise M, Cavaliere F, Giannarelli D, Quagliuolo V, Vecchiato A, Deraco M, Garinei R, Foletto M, Botti C and Cavaliere R: Hyperthermic antiblastic perfusion with alpha tumor necrosis factor and doxorubicin for the treatment of soft tissue limb sarcoma in candidates for amputation: results of a phase I study. J Immunother *22(5)*: 407-414, 1999.

2 Di Filippo F, Garinei R, Anzà M, Cavaliere F, Giannarelli D, Cagol PP, Rossi CR, Santinami M, Deraco M, Botti C, Perri P, Di Filippo S, Piarulli L and Bruno P: Doxorubicin in isolated limb perfusion in the treatment of advanced limb soft tissue sarcoma. J Exp Clin Cancer Res *22(4)*: 81-87, 2003.

3 Gabizon A, Shmeeda H and Barenholz Y: Pharmacokinetics of pegylated liposomal Doxorubicin: review of animal and human studies. Clin Pharmacokinet *42(5)*: 419-436, 2003.

4 Baba H: Effect of whole body hyperthermia combined with adriamycin on tumor and normal tissue in rats. 37th Annual Meeting of the Radiation Research Society and 9th Annual Meeting of the North American Hyperthermia Group. March 18-22, Seattle, WA, 34, 1989.

5 Alexander RB, Nelson WG and Coffey DS: Synergistic enhancement by tumor necrosis factor of *in vitro* cytotoxicity from chemotherapeutic drugs targeted at DNA topoisomerase II. Cancer Res *47(9)*: 2403-2406, 1987.

6 Niitsu Y, Watanabe N, Umeno H, Sone H, Neda H, Yamauchi N, Maeda M and Urushizaki I: Synergistic effects of recombinant human tumor necrosis factor and hyperthermia on *in vitro* cytotoxicity and artificial metastasis. Cancer Res *48(3)*: 654-657, 1988.

7 Di Filippo F, Cavaliere F, Anzà M, Garinei R, Botti C, Perri P, Di Angelo P, Patrizi V, Di Filippo S and Visca P: Liposomal doxorubicin in the perfusional treatment of advanced soft tissue limb sarcoma. J Chem *16(5)*: 66-69, 2004.

8 Wieberdink J, Benckhuysen C, Braat RP, van Slooten EA and Olthuis GA: Dosimetry in isolated perfusion of the limbs by assessment of perfused tissue volume and grading of toxic tissue reaction. Eur J Cancer Clin Oncol *18(10)*: 905-910, 1982.

9 Di Filippo F, Calabrò AM, Cavallari A, Carlini S, Buttini GL, Moscarelli F, Cavaliere F, Piarulli L and Cavaliere R: The role of hyperthermic perfusion as a first step in the treatment of soft tissue sarcoma of the extremities. World J Surg *12(3)*: 332-338, 1988.

10 Casara D, Rubello D, Pilati PP, Scalerta R, Foletto M and Rossi CR: Optimized procedure of real-time systemic leakage monitoring during isolated limb perfusion using a hand held gamma probe and 99mTc-HAS. Nucl Med Commun *25(1)*: 61-66, 2004.

11 Swenson CE, Bolcsak LE, Batist G, Guthrie TH Jr, Tkaczuk KH, Boxenbaum H, Welles L, Chow SC, Bhamra R and Chaikin P: Pharmacokinetics of doxorubicin administered *i.v.* as Myocet (TLC D-99; liposome-encapsulated doxorubicin citrate) compared with conventional doxorubicin when given in combination with cyclophosphamide in patients with metastatic breast cancer. Anticancer Drugs *14(3)*: 239-246, 2003.

12 Ten Hagen TL, Van der Veen, Seynhaeve AL, van Tiel ST and Eggermont AM: Pegylated liposomal tumor necrosis factor-alpha results in reduced toxicity and synergistic antitumor activity after systemic administration in combination with liposomal doxorubicin (Doxil) in soft tissue sarcoma-bearing rats. Int J Cancer *87(6)*: 829-837, 2000.

13 Brouckaert P, Takahashi N, van Tiel ST, Hostens J, Eggermont AM, Seynhaeve AL, Fiers W and ten Hagen TL: Tumor necrosis factor-alpha augmented tumor response in B16 BL6 melanoma-bearing mice treated with stealth liposomal doxorubicin (Doxil) correlates with altered Doxil Pharmacokinetics. Int J Cancer *109(3)*: 442-448, 2004.

Received July 3, 2006
Revised October 30, 2006
Accepted October 31, 2006

Session 1. Plenary lecture

LMW PROTEIN FRAGMENTS MAY DETECT EARLY STAGE BREAST CANCER

Gordon Whiteley (a), Sally Rucker (a), Chenwei Liu (a), Simona Colantonio (a), Andrea Sacconi (a), Enzo Mammano (b), Giorgia Marconato (b), Cosimo Di Maggio (b), Donato Nitti (b), Mario Lise (b,c), Claudio Belluco (c)
(a) Clinical Proteomics Reference Lab, NCI-Frederick, Gaithersburg, MD, USA
(b) Department of Oncological and Surgical Sciences, University of Padova, Padova, Italy
(c) CRO- IRCCS, National Cancer Institute, Aviano, Italy

Introduction

Breast cancer is the leading cause of cancer mortality in women worldwide. While screening by mammography has been shown to reduce breast cancer mortality, this test is not as useful in early stages of disease where the lesions are smaller or in cases where the breast tissue is denser (1). Detection at early stages also results in a more favorable outcome, especially in women with pT1a tumors. The search for early biomarkers using conventional techniques has been largely unsuccessful. Recently, serum proteomic profiling has emerged as a technology with great potential for early detection of disease with reports of patterns for a variety of cancers and other disease conditions. (2-4). The advances in mass spectrometry, computer bioinformatics, robotics and more powerful computers have made these discoveries possible (5).

The goals of the Clinical Proteomics Reference Lab are to develop and validate proteomics pattern recognition methods to the standards of the FDA. In doing so, we utilize serum sample sets that are well characterized and have valid clinical data for comparison. The serum sets that were obtained first from the University of Padova and then from several additional sites in Italy provided us with such a set that could not only be used for the development of new methods but also help validate some of our earlier findings.

Sample processing and mass spectrometry

There were a total of 369 samples analyzed in this study. The first group were 324 consisting of 154 normal samples and 170 early stage cancer samples. The second group consisted of 15 normal samples and 30 early stage cancer samples received approximately one year after the first study. Samples were thawed and 10 µl aliquots were obtained. These were used immediately for high resolution surface enhanced laser desorption ionization (SELDI) using an IMAC surface which is known to have a high affinity for albumin. Albumin was targeted because of the association of low molecular weight peptides and proteins with carrier proteins and the fact that these may be the source of diagnostic information (6). All steps were carried out on a Tecan Genesis 200 robotic processor to ensure reproducibility. A 5 µl aliquot was applied to the surface and incubated for 30 minutes. After washing with PBS and water, CHCA was applied as the matrix and was dried. The arrays were then read in an ABI Q-Star XL equipped with a Ciphergen P1000 interface. The spectra were extracted into an SQL database for processing. All spectra were examined for quality and spectra showing low total ion current

were eliminated. Spectra were then normalized to total ion current and randomly split into a training set (70% of samples each from the normal and cancer groups) and a testing set (30% of samples).

Pattern bioinformatics

The bioinformatics developed at the CPRL utilize two basic paths as outlined in Figure 1. For the first method, each data point is examined in the groups of training samples and a Wilcoxon test is used to determine if there is any discriminating potential. The top 250 peaks showing the greatest power are selected and they are then used to build three classifiers as outlined below.

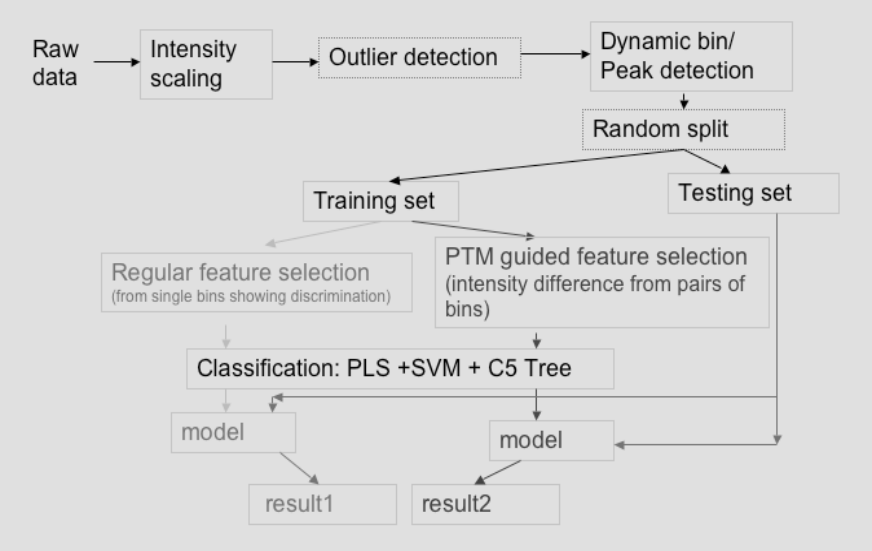

Figure 1. CPRL Classification methods

The second method of peak selection involves the possibility of classification based on post translational modifications (PTM's). This method looks at peak ratios at given distances that would correlate with a PTM: 1 (deamidation), 2 (disulfide bond formation) and 80 (phosphorylation). These three have been shown to be associated with cancer (7-9). The ratios of each peak pair in the normal samples are compared with the peak pair ratios in the cancer group. Those pairs showing a significant difference are then selected to be fed into the bioinformatics classification tools outlined below.

The classifiers consist of three very different methods: C 5.0 decision tree (Clementine), partial least squares (SAS) and the support vector machine (libsys SMV). Each of these classifiers is independently trained on a training set of samples and the best model for each algorithm is selected to classify samples held in an evaluation set of samples. These samples have not been part of the training and are used simply to evaluate sensitivity and specificity. When the samples are classified, each method "votes" on the classification of the unknown samples. Where there is agreement, the samples are classified as cancer or normal; where there is no agreement, the samples are called "unknown".

Results of studies and discussion

The demographics of the breast cancer samples used are outlined in Table 1. The training, testing and masked validation sets all showed similar age ranges with the average age ranging from 55 to 60 years. However, the masked validation set had a larger number of stage T1a samples than the earlier training and testing sets.

Table 1. Demographics of study samples

Group	Number	Average age (range)	Stage of disease (number)
Training set			
Normal	109	55.0 (36-80)	
Cancer	126	59.1 (38-88)	1a (8) 1b (39) 1c (79)
Masked Testing Set			
Normal	45	60.8 (37-75)	
Cancer	44	59.8 (39-79)	1a (3) 1b (13) 1c (28)
Masked Validation Set (14 months later)			
Normal	15	60.5 (47-75)	
Cancer	30	58.6 (36-77)	1a (16) 1b (11) 1c (3)

The predicted performance was calculated for each model based on a 10% cross validation within the training set of samples and the results for each individual method are outlined in Table 2.

Table 2. Predicted performance of each model

Model	Sensitivity	Specificity
C5.0 decision tree	83.61%	91.80%
SVM	78.69%	86.89%
Partial Least Square	83.61%	90.16%
C5.0+SVM +PLS	90.32%	90.32%

The performance was then validated using the 30% of samples that were held and not used as part of training. This showed performance of 83.3% sensitivity and 96.8% specificity based on 61 samples. A blinded set of samples was collected over the next year and was then used to evaluate the algorithm to demonstrate the stability of the system. Although the sample numbers were low (15 normal and 30 cancer), the age distribution was similar to the previously used samples and the sensitivity of 97% and specificity of 80% were very similar to that observed one year earlier (Table 3).

Table 3. Performance of algorithm over 14 months

C5nn+pls+svm	0-normal	1-cancer
Original Results*		
Normal	30	1
Cancer	5	25
Results on new samples 14 months later**		
Normal	12	3
Cancer	1	29

*Sensitivity: 83.3%, specificity: 96.8%.
**Sensitivity:97%, specificity: 80%.

The top peaks used by the C5.0 decision tree are shown in Figure 2. Although there are differences seen between the normal and cancer groups, the differences are not sufficient for any single peak to be used. Only a combination of these peaks could give sensitivity and specificity confirming that a single biomarker for breast cancer probably does not exist.

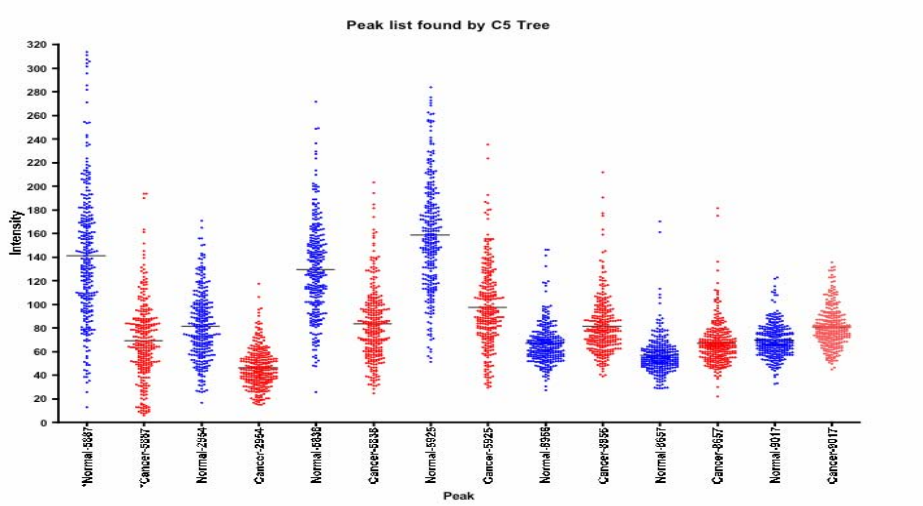

Figure 2. Top peaks used in the C5.0 Decision Tree

The performance of this test was compared with mammography using BI-RADS score demonstrating that many samples that would be missed by mammography were detected by this method (Table 4). This suggests that a blood test would be a valuable adjunct to imaging tests like mammography especially for early stages of the disease where treatment is more successful.

Table 4. Classification of serum cancer samples from masked testing set by proteomic pattern according to BI-RADS mammogram

	Cancer	Normal
BI-RADS 3	3/3	0/3
BI-RADS 4	16/17	1/17
BI-RADS 5	13/14	1/14

Identification of some of the peptides and proteins that are carried on albumin and may be associated with disease was carried out. Albumin was separated from serum samples using cibachrome blue capture, washing and then elution by acetonitrile. The resulting solution was dried, reconstituted, trypsin digested and analyzed by LC MS/MS using nanospray as previously described (10). This revealed many peptide fragments that have not been found in serum before and could be associated with cancer. A list of these is found in Table 5. Since the time of this study, further protein fragments have been identified and it would appear that the patterns seen would be useful as tools to guide identification of those proteins that are associated with disease and could be early markers.

Table 5. Protein fragments found only in early stage breast cancer pool

Parental Protein	Accession ID
Alpha-amylase 2B precursor	P19961
Alpha-amylase, salivary precursor	P04745
Alpha-mannosidase IIx	P49641
Cellular repressor of E1A-stimulated genes	O75629
Cystatin A	P01040
Cystatin SN precursor	P01037
Glucosamine-6-phosphate isomerase	P46926
Kallistatin precursor	P29622
Olfactory receptor 9Q1	Q8NGQ5
Prolactin-inducible protein precursor	P12273
Protein Plunc precursor	Q9NP55
Short palate, lung and nasal epithelium carcinoma associated protein 2 precursor	Q96SN8
Calcium binding protein 1 (calbrain)	Q8N6H5
Solute carrier family 13, member 3	Q8WWT9
Von Ebner's gland protein precursor	P31025
CDK5 regulatory subunit associated protein 2	Q96SN8
Myeloid/lymphoid or mixed-lineage leukemia protein 4	Q9UMN6
Phosphatidylinositol 3-kinase regulatory beta subunit	O00459
Tumor protein p73	O15350

In order to refine this guidance, we utilized a more sophisticated mass spectrometer system than our original profiling study. This system is outlined in Figure 3 and involves the specific targeting of fragments that are associated with albumin.

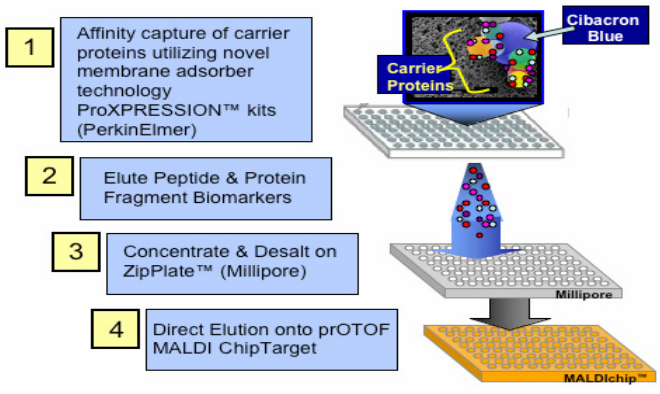

Figure 3. ProXpression™ Methodology

The albumin is first captures on cibachrome blue plates, washed and the load is eluted into solution. The peptides and protein fragments are then recovered and concentrated on a ZipPlate with a C18 base. This is then eluted and directly spotted on a target using a solution of CHCA matrix in acetonitrile and using a 3µl volume. The target is then analyzed in a PerkinELmer prOTOF mass spectrometer. This instrument has an orthoganol design that yields high resolution data that is very tolerant of rough target surfaces. The collisional cooling keeps fragments in tact, something that we utilized in our data analysis (2). Our assumption was that post-translational modifications would also be intact and could be detected by the instrument. We therefore specifically looked for these modifications and looked for peak pair ratios rather than differences between normal and cancer sera that were shown by individual peaks. In looking for peak pair ratios corresponding to phosphorylation, deamidation and disulfide bond formation, we had demonstrated that a low number of peak pairs could be identified that differentiated ovarian cancer and cutaneous t-cell lymphoma samples from normal samples. We therefore analyzed the breast cancer samples to see if this was also the case. Our findings showed that a sensitivity of 93.5% and a specificity of 91.69% could be attained using 24 peak pairs (48 peaks total). This information can now be used to specifically target these peak pairs for identification from the long list of potential peptides and protein fragments that have been randomly identified in these samples as well as the long list of peaks that were used in our first analysis.

Conclusions

The use of profiling in early diagnosis is still a long way from being practical in the routine clinical lab setting. It requires specialized equipment, laboratories and a highly trained and diverse staff to be successful. However, we have demonstrated that it is feasible both on the basis of long-term algorithm stability and the use of algorithms that are simple and utilize knowledge of the disease mechanism. The results of the PTM study target very specific proteins and peptides for identification and hopefully panels of tests can be developed that will have routine clinical lab application and practicality.

Acknowledgements

The entire CPRL staff is a dedicated and focused group that have worked on developing and validating profiling technology. Without their work, these studies would not have been possible or completed. The invaluable collaboration with our colleagues in Italy have provided the crucial materials – the patient samples and information that are the foundation of this work.

References

1. Elmore JG, Armstrong K, Lehman CD, Fletcher SW. Screening for breast cancer. *JAMA* 2005;293:1245-56.
2. Lopez MF, Mikulskis A, Kuzdzal S, Bennett DA, Kelly J, Golenko E, DiCesare J, Denoyer E, Patton WF, Ediger R, Sapp L, Ziegert T, Lynch C, Kramer S, Whiteley GR, Wall MR, Mannion DP, Della Cioppa G, Rakitan JS, Wolfe GM. High-resolution serum proteomic profiling of Alzheimer disease samples reveals disease-specific, carrier-protein-bound mass signatures. *Clin Chem* 2005;51:1946-54.

3. Petricoin EF, Ardekani AM, Hitt BA, Levine PJ, Fusaro VA, Steinberg SM, Mills GB, Simone C, Fishman DA, Kohn EC, Liotta LA. Use of proteomic patterns in serum to identify ovarian cancer. *Lancet* 2002;359:572-7.
4. Li J, Orlandi R, White CN, Rosenzweig J, Zhao J, Seregni E, Morelli D, Yu Y, Meng XY, Zhang Z, Davidson NE, Fung ET, Chan DW. Independent validation of candidate breast cancer serum biomarkers identified by mass spectrometry. *Clin Chem* 2005;51:2229-35.
5. Whiteley GR. Proteomic patterns for cancer diagnosis-promise and challenges. *Mol Biosyst* 2006;2:358-63.
6. Mehta AI, Ross S, Lowenthal MS, Fusaro V, Fishman DA, Petricoin EF 3rd, Liotta LA. Biomarker amplification by serum carrier protein binding. *Dis Markers* 2003;19:1-10.
7. Mann M, Jensen ON. Proteomic analysis of post-translational modifications. *Nat Biotechnol* 2003;21:255-61.
8. Li C, Thompson CB. Cancer. DNA damage, deamidation, and death. *Science* 2002;298:1346-7.
9. Bae SC, Lee YH. Phosphorylation, acetylation and ubiquitination: the molecular basis of RUNX regulation. *Gene* 2006;366:58-66.
10. Lowenthal MS, Mehta AI, Frogale K, Bandle RW, Araujo RP, Hood BL, Veenstra TD, Conrads TP, Goldsmith P, Fishman D, Petricoin EF 3rd, Liotta LA. Analysis of albumin-associated peptides and proteins from ovarian cancer patients. *Clin Chem* 2005;51:1933-45.

PHARMACOKINETICS OF GEMCITABINE AT FIXED DOSE RATE INFUSION IN PATIENTS WITH NORMAL AND IMPAIRED HEPATIC FUNCTION

Clinical Pharmacokinetics. In press.

Felici A. [1,2], Di Segni S. [1], Milella M. [2], Colantonio S. [1], Sperduti I. [3], Nuvoli B. [1], Contestabile M.[1], Sacconi A[1], Zaratti M. [1], Citro G. [1], Cognetti F [2].

[1] *Laboratory of Pharmacokinetic, Regina Elena Cancer Institute, Rome, Italy;*
[2] *Division of Medical Oncology A, Regina Elena Cancer Institute, Rome, Italy;*
[3] *Division of Biostatistics, Regina Elena Cancer Institute, Rome, Italy.*

Key words: pharmacokinetics, gemcitabine, fixed dose rate, hepatic dysfunction

Address for correspondence:

Alessandra Felici, M.D.

Division of Medical Oncology A,

Regina Elena Cancer Institute

Via Elio Chianesi, 53

00144, Rome, Italy

Tel: +39 06 5266 6919

Fax: + 39 06 5266 5637

e-mail: alefelici@yahoo.it

ABSTRACT

Background: Gemcitabine (dFdC) can be administered at standard 30 minutes infusion or at fixed dose rate (FDR) infusion to maximize the rate of triphosphate accumulation, its major intracellular metabolite. The standard 30 minutes infusion requires dose adjustment in patients with organ dysfunction, especially in patients with baseline elevated bilirubin levels. On the other hand, FDR infusion is burdened by increased hematological toxicity.

Materials and Methods: In this prospective study, patients with pancreatic or biliary tract carcinoma and normal or impaired liver function tests were considered eligible. Patients were accrued according to the following criteria: 1) serum bilirubin <1.6 mg/dl, and AST, ALT <2 ULN (cohort I): 2) serum bilirubin >1.6 mg/dl, and/or AST, ALT >2 ULN (cohort II). Gemcitabine 1000 mg/m2 at FDR infusion was administered on days 1,8,15 every 28 days. The pharmacokinetic analysis of gemcitabine and its metabolite difluorodeoxyuridine (*dFdU*) was performed with HPLC assay at cycle 1 and 2.

Results: Thirteen patients were enrolled, four in cohort I and nine in cohort II. All patients were assessable for toxicity and pharmacokinetic analysis. Grade and rate of toxicities were similar in both groups, and patients with elevation of bilirubin and/or transaminases did not require dose reduction of gemcitabine. Pharmacokinetic analysis revealed a reduction of the experimental area under the concentration time curve (AUCexp) for *dFdC* and *dFdU* in patients with hepatic dysfunction when compared with patients with normal liver function. All the other pharmacokinetic parameters results similar in the two cohorts . No statistical difference was demonstrated for all the parameters evaluated between cycle 1 and cycle 2 in the two groups.

Conclusion: Gemcitabine 1000 mg/m2 at fixed dose rate infusion can be administered in patients with altered hepatic function without causing additional toxicity compared with patients with normal liver function.

INTRODUCTION

GEMCITABINE (2,2-difluorodeoxycytidine, *dFdC*) is a fluorinated analog of deoxycytidine , which has shown a broad spectrum of activity against several solid tumors, such as non-small cell lung cancer and pancreatic adenocarcinoma [1, 2].

dFdC is a prodrug that requires intracellular activation: after its uptake, the nucleoside analog is converted by deoxycitidine kinase in its monophosphate form (*dFdCMP*), followed by subsequent phosphorilation steps to diphosphate (*dFdCDP*) and triphosphate forms (*dFdCTP*) [3]. Gemcitabine undergoes also intracellular and extracellular metabolism by cytidine deaminase (CDA), the enzyme that converts the prodrug into its inactive metabolite difluorodeoxyuridine (*dFdU*). The rate-limiting step in the intracellular accumulation of *dFdCDP* e *dFdCTP* is the conversion of *dFdC* in *dFdCMP* by deoxycitidine kinase [4]. It has been demonstrated that deoxycytidine kinase has a saturable kinetic and the optimal plasma *dFdC* concentration to obtain maximal *dFdCTP* formation and accumulation by mononuclear cells is 10-20μM [5].

Several studies have reported that the range from 1000 to 1500 mg/m^2 of gemcitabine is active and well tolerated when given over 30 minutes on a weekly schedule [6,7], although patients receiving doses ranging from 800 to 2600 mg/m^2 as 30 minutes intravenous infusion generate plasma concentrations of dFdC >60μM. Under these conditions, triphosphate accumulation process may be saturated [5,8] and target cells may not use a substantial portion of the drug due to metabolic clearance. Fixed dose rate (FDR) of 10 mg/m^2/min has been proposed to escape this hitch and achieve plasma steady-state concentrations from 10 to 20 μM [4,8], optimizing the intracellular *dFdCTP* accumulation [9-12].

A phase II trial [13], which compared gemcitabine 30 minutes (2200 mg/m^2) with FDR infusion (1500 mg/m^2 over 150 minutes) in patients with pancreatic adenocarcinoma, revealed improvement in survival and clinical benefit in favor of FDR infusion, with an increased incidence of hematological toxicity and grade 3 hypertransaminasemia in the FDR arm. Despite this initial promising result, other studies with gemcitabine alone or in combination with other drugs (cisplatin, carboplatin, paclitaxel) failed to show any clinical benefit in favor of FDR infusion [7].

The FDR gemcitabine infusion implies a linear increase of dFdCTP intracellular concentration and its intracellular area under the concentration-time curve (AUC) is higher following the prolonged infusion compared with the standard 30 min infusion schedule [14].

The pharmacokinetic of gemcitabine, as clearance or metabolic capacity, can be influenced by abnormal hepatic function due to liver metastases from pancreatic/biliary tract carcinoma or other hepatic diseases (cirrhosis, hepatitis). Venook et al. [15] explored the pharmacokinetic disposition of gemcitabine given as 30 minutes standard infusion in patients with liver and renal impairment, suggesting a dose reduction for patients with elevated bilirubin levels, due to elevated risk of hepatic toxicity. Supported by their PK and clinical results, Venook et al. suggested to initially

treat patients showing elevated bilirubin levels, with gemcitabine 800 mg/m2, escalating subsequently the dose, if well tolerated.

Based on the above mentioned hepatic toxicity [13] by gemcitabine at FDR infusion and on the recommendation suggested by Venook in patients with high bilirubin levels, we performed a pharmacological study to evaluate the safety of gemcitabine 1000 mg/m2 at 10 mg/m^2/min infusion on days 1, 8 and 15 every 4 weeks, in patients with normal and impaired hepatic function. The principal aim of this study was to define the pharmacokinetic disposition of *dFdC* and *dFdU* in the two cohorts of patients. Secondary end points were to evaluate the toxicity in both groups, starting from the same dose of gemcitabine, and to confirm the repeatability of the pharmacokinetic parameters analyzed within the same patient in two different cycles.

MATERIALS AND METHODS

Patient Selection

Patients with cytological or histological diagnosis of recurrent or metastatic pancreatic adenocarcinoma or biliary tract carcinoma were included into the study. Eligibility criteria included: age ≥ 18 years; WHO Performance status of 0 to 2; life expectancy of two months or longer; more than 4 weeks since prior systemic chemotherapy, major surgery or radiation therapy; granulocyte >1,500 cells/μL, platelet count >100,000 cells/μL, albumin level >2.0 g/dl, serum creatinine level less than 1.6 mg/dl; compliance of the patients with testing. To limit entry to patients with hepatic dysfunction, other eligibly criteria were: AST/ALT level greater than or equal to two times the upper limit of normal with normal bilirubin levels; total bilirubin levels 1.6 to 7.0 mg/dL with any AST/ALT level. All patients signed an informed consent approved by the Institutional Ethical Committee.

Exclusions criteria included: prior treatment with gemcitabine**;** known untreated brain metastases; uncontrolled or severe cardiac disease; concomitant medication that could affect hepatic function; pregnant or lactating patients; patients with reproductive potential not implementing adequate contraceptives measures; patients who cannot be regularly followed up for psychological, social, familial or geographic reasons.

Patients were enrolled in two different cohorts: control patients with normal liver function in cohort I (serum bilirubin level less than 1,6 mg/dl and aspartate aminotransferase/alanine aminotransferase (AST/ALT) level less than two times the upper limit of normal (ULN)), and patients with impaired liver function in cohort II (serum bilirubin level less than 1.6 mg/dL and AST/ALT level greater than or equal to two times the upper limit of normal; or bilirubin level from 1.6 to 7.0 mg/dL with any AST/ALT/AP level).

Study Design

This single centre study focused on gemcitabine 1000 mg/m2 at FDR infusion administered on days 1,8,15 every 28 days until progressive disease or unacceptable toxicity, in patients with normal and hepatic dysfunctions. Drug toxicity and pharmacokinetics were analyzed in patients with impaired hepatic function and compared with patients with normal liver parameters. The safety dose of gemcitabine and the dose reduction required, were evaluated for a maximum of 6 cycles. Sampling for PK analysis were performed at day 1 of cycle 1 and repeated at day 1 of cycle 2, to calculate the variability of PK parameters in the same patient (each patient being his own control).

No systemic anticancer agent other than the study drug was administered, and a concomitant treatment with corticosteroids was discouraged at least from day -2 to day 2 at cycle 1 and 2. Granulocyte-colony stimulating factors (G-CSF) were not allowed in the first two cycles.

Clinical biochemistry and hematology were assessed within 7 days before starting treatment; in particular, a complete blood and platelet count as well as liver function tests (serum total and fractionated bilirubin, AST/ALT level) were obtained at baseline and weekly during treatment course. A physical examination and a record of concomitant medications were carried out at baseline and before every cycle. An electrocardiogram and chest X-ray were obtained at baseline, at discontinuation off the study treatment, and at any time when clinically indicated during the trial. Patients with measurable disease were assessed for response every three cycles with CT scan or ultrasound of the abdomen (and of other disease sites as appropriate). Responses were documented using RECIST criteria [16]. After the off-treatment visit, patients were followed up monthly with clinical and instrumental evaluation.

Values of white blood cells, platelets, hemoglobin, red blood cells, neuthrophils, PT (protrhombin time), PTT (partial thromboplastin time), bilirubin, AST/ALT, AP (alkaline phosphatase), total protein and albumin were recorded at baseline and every each cycle to evaluate a possible relationship between blood value, drug disposition and toxicity.

Evaluation of toxicity and dose modifications

The starting dose of gemcitabine was 1000 mg/m2 infused at 10 mg/m2/min; dose modifications were applied on the basis of toxicity. Administration of gemcitabine was delayed on day 1, until hematological recovery (ANC ≥1500/μL and/or PLT ≥100,000/μL and/or Hb ≥9 g/dL) up to a maximum of 3 weeks; for day 8 and 15 the dose was reduced as follows: ANC ≥1500/μL and/or PLT ≥100.000/μL: full dose; ANC:1.500-1.000/μL and/or PLT:99.999-75.000/μL: 75% of full dose; ANC:1.000-500/μL and/or PLT: 74.999-50.000/μL: 50% of full dose; ANC ≤500/μL and/or PLT≤50.000/μL: omission. Patients who required a delay of >2 weeks but <3 weeks received dose reduction of 25%. If ANC ≤500/μL, PLT ≤50,000/μL, Hb≤ 7g/dL for a period longer than 5 days, in any case of febrile neutropenia or stomatitis toxicity ≥G3 the doses of gemcitabine was reduced

by 25% in the next cycles. A 25% dose reduction was planned for gastrointestinal grade 3 and 4 toxicities. For liver toxicity, doses of gemcitabine were delayed when bilirubin and AST/ALT levels were >2.5 and >5 from baseline (the starting values of each patients), respectively; doses were reduced by 50% when bilirubin and AST/ALT levels were from 1.5 to 2.5 and from 2.5 to 5 respectively from baseline; doses were reduced by 25% when bilirubin level was from 1.5 to 2.0 from baseline, and AST/ALT levels were from 2.5 to 5 from baseline. Patients who require a delay of >2 weeks but <3 weeks will receive dose reduction of 25%; patients who were not recover after 3 weeks were considered off protocol.

Pharmacokinetic Sample Acquisition and Handling

Blood samples (5 to 10 mL each patient) were drawn via an indwelling peripheral catheter or peripheral venipuncture, into tubes containing heparin. Tetrahydrouridine (Calbiochem-Novabiochem Corp La Jolla Ca), a cytidine deaminase inhibitor, was then added (0.1 ml of a 10 mg/ml solution) to prevent *ex vivo* Gemcitabine deamination. Samples were collected 30 minutes before Gemcitabine infusion, at 30, 60 and 80 minutes during the infusion, at the end of the infusion, and at 5, 30, 90, 180 and 240 minutes after the completion of the infusion.

Blood samples were immediately centrifuged at room temperature for 10 minutes at 1000 rpm. The resulting plasma was frozen and stored at -20°C until analysis.

Determination of Gemcitabine and dFdU

All the analysis was performed at the Regina Elena National Cancer Institute, Rome, Italy. Gemcitabine and dFdU plasma levels were determined using the hyphenated technique HPLC-MS/MS (high performance liquid chromatography tandem mass spectrometry). Gemcitabine (Ly188011) and dFdU (Ly198791) were kindly supplied by Eli Lilly Co, (Indianapolis, IN), 2'-deoxycytidine (dC) was purchased at Sigma Aldrich. 10 µl of Internal Standard (20γ/ml**)** were added to 0,2 ml of each plasma sample and the mixture was extracted with 200µl of Isopropilic Alchool and then 400µl of Ethyl Acetate. Samples were vortexed and then centrifuged for 10 minutes. The supernatant was transferred to a glass tube and the organic phase evaporated to dryness under nitrogen stream. 200µl of HPLC grade Water with 0.5% Acetic Acid, were added to each sample to reconstitute the dried residue and the mixture was vortexed and then centrifuged for ten minutes at 4000g. 20 µL of the reconstituted solution were injected into HPLC system.

HPLC analysis was performed by using an Agilent 1100 series system (Agilent Technologies, Palo Alto, CA, USA) equipped with a binary pump, an automatic injector and vacuum degasser. The separation was carried out on a Symmetry C18 (4.6*250mm I.D, 5µm particle size) protected by a sentry guard column Symmetry C18 (3.9*20mm). Mobile Phase: A, 0.5% Acetic Acid in Water; B, 0.5% Acetic Acid in Acetonitrile. Gradient elute procedure: B 2% for 2 min, B 2-50% in 10 min, B 50-70% in 1 min, B 70% for 4 min, B 2% in 2 min, B 2% for 3 min. The flow-rate was 1 mL/min and the HPLC output was directly interfaced to the ESI ion source, the LC/MSD ion

trap mass spectrometer 1100 (Agilent Technologies). The mass spectrometer was equipped with an ESI source and operated in the positive ion mode. The ESI conditions were the following: capillary voltage -3.5 kV; end plate offset voltage-500 V; capillary exit voltage 110.9 V; nebulizer pressure 70 psi; drying gas flow 12 L min-1; temperature 350°C.

The ESI-MS analyses were MRM (multiple reaction monitoring) experiments, performed by ion fragmentation (Gemcitabine: 264→112 m/z, dC (2'-deoxycytidine)): 228→112 m/z; dFdU: 265→ 113 m/z) and the scan range was from m/z 100–300. In these analytical conditions, retention times for dC, Gem and dFdU were respectively 2.3, 3.8 and 6.5 minutes.

The extraction and the analysis were carried on modifying previously published methods [17,18].

Quant Analysis software was used to process the quantitative data. Plasma concentrations for Gemcitabine and dFdU were calculated from the ratio of the Gemcitabine and dFdU peaks area to the area of Internal Standard using least squares linear regression. Lower limit of quantitation was for both Gemcitabine and dFdU was 0.05 μg/ml and linearity was assessed from 0.078 μg/ml and 15 μg/ml. Within-day and between-day variability (measured as coefficient of variation) was < 12.00%.

Pharmacokinetic Analysis

Principal PK parameters were estimated for each patient by non-compartmental method analysis; parameters include: plasmatic peak concentration (Cmax, μg/mL), determined graphically from the observed experimental values; experimental area under the plasma concentration-time curve (AUC_{exp}, μg*h/ml), calculated according to the trapezoidal rule, from the first to the last sampling time; infinite AUC (AUC_{inf} μg*h/ml) area under plasma concentration-time curve extrapolated to infinity; total plasma clearance (Cl, L*h/m^2), calculated as ratio of dose in μg and AUC; rate of elimination (K, h^{-1}),calculated as the negative slope estimated from the log-linear regression of the terminal part of the plasma concentration–time curve; terminal half life ($t_{1/2}$) defined as ln2/K. The pharmacokinetics of gemcitabine was described by all the above parameters; for dFdU only Cmax and AUCexp have been calculated according to the sampling period performed (until 4 hours after the completion of the infusion) and the documented terminal half life of the metabolite, reported to be >10 h [5].

Statistical Analysis

Summary statistics are presented as mean, standard deviation, coefficient of variation, median and range or frequency for descriptive purposes. Differences between cohort I and II were analyzed with analysis of variance (ANOVA) for continuous variables at the 1st cycle. The normality assumptions for ANOVA were assessed with the tests available. If the normality assumption was violated, the Mann-Whitney U non-parametric test was used. Paired t tests were used to compare Cmax, AUCexp, AUCinf, $t_{1/2}$, clearance and K at different time for a given group. A repeated measures ANOVA for all PK parameters using patient, cohort and cycle factors as variables has

been performed. The Kaplan-Meier method was used to calculate overall survival and progression-free survival, reported with their 95% confidence interval. All analyses were done with SPSS 11.0. Degree of myelosuppression, defined by %G, was defined as ([pretreatment granulocyte number – granulocyte numbed after week 1] /pretreatment granulocyte number) x 100%.

RESULTS

Thirteen patients were enrolled into this study; all of them were assessable for toxicity and pharmacokinetic analysis at cycle one. The characteristics of the 13 patients are listed in Table 1. Seven of them were females and the median age was 63 years (range, 27 to 75 years). Seven patients had locally advanced or metastatic pancreatic adenocarcinoma, three had biliary tree carcinoma and the remainder three presented advanced gallbladder adenocarcinoma. None of them received prior chemo- or radiotherapy, and liver was the major site of metastatic disease. The median ECOG performance status was 1 (range 0-2). Four patients had normal hepatic function with serum bilirubin <1.6 mg/dl, and AST, ALT <2 upper normal limit (UNL (cohort I); nine patients had hepatic dysfunction with serum bilirubin >1.6 mg/dl, and/or AST, ALT >2 UNL (cohort II). All patients received gemcitabine 1000 mg/m^2/min at FDR days 1,8,15 every 4 weeks. One patient in the control arm had a 25% dose reduction at the second cycle due to hematological toxicity, while two patients in the experimental arm never started the second cycle, one for disseminated intravascular coagulation (DIC) after the first cycle and the other for deterioration of general conditions (rapid worsening of his performance status). The baseline laboratory parameters are listed in Table 2. The only statistical significant difference in the baseline laboratory values between the two cohorts was in two hepatic function parameters, total bilirubin level (p=0,04) and AST level (p=0,01), whereas no significant difference was observed for ALT level (p=0,16) and for all other blood parameters reported on Table 2. . Only the total bilirubin level had statistical significant decrease from the first to the second cycle in cohort II (5,29 mg/dl vs 1,90 mg/dl, p= 0.03), while all other laboratory values had comparable means between the first two cycles in both groups of patients.

The main toxicities were reported after the first cycle and detailed on Table 3. Although more patients in cohort II experienced grade 3 toxicities, this difference did not result to be statistically significant (figure 1); moreover patient with bilirubin and/or transaminases elevation did not require dose reduction of gemcitabine. Even though no patient experienced grade 4 toxicity, hematological toxicity represented the major side effect. Two patients experienced grade 3 neutropenia in the control arm, one patient grade 3 thrombocytopenia and one patient grade 3 anaemia in the cohort II. Laboratory toxicities were low in both groups, although two episodes of transient grade 3 elevation in serum bilirubin and transaminases from baseline values were seen in one patient in cohort II. Other toxicities concerned mainly asthenia and fever. A decrease in

variation of %G after 1 week (mean ± SD) was greater for the cohort II (10% ± 13) compared to the cohort I (2% ± 13).

All patients met criteria for measurable disease; one complete response was observed in the control group, three patients had partial response, two stable disease and six patients experienced progressive disease. One patient was not evaluable for response due to a serious adverse event (DIC) after the first cycle. At a median follow-up of 19 weeks (1- 167) the median progression-free survival was 15 weeks (95% C.I. 9-22) and the median overall survival was 20 weeks (95% C.I. 12-50).

Pharmacokinetic Results

Pharmacokinetic analysis was performed on 13 patients at the first cycle and on 11 patients at the second cycle. Two of the patients never started the second cycle due to adverse events. All patients were studied at dose of 1000 mg/m2 at the fixed dose rate infusion of 10 mg/m^2 per minute (FDR). Patients in cohort I had normal hepatic function (serum bilirubin <1.6 mg/dl, and AST, ALT <2 UNL), and patients in cohort II had impaired liver function (serum bilirubin >1.6 mg/dl, and/or AST, ALT >2 UNL). A descriptive analysis of the pharmacokinetic results is listed in Table 4. With normal or impaired hepatic function, the mean of the maximum gemcitabine concentration was similar in the two groups: 6,83 μg/ml (± 0,73) and 7,76 μg/ml (± 1,77) respectively (Figure 2). The variability in peak plasma concentration was not very high, ranging from 6.0 to 7.7 μl/ml for gemcitabine and from 6.5 to 12.2 μl/ml for dFdU. The peak plasma concentration of dFdU was measured in all patients at the end of gemcitabine infusion (after 100 minutes from the start of infusion) or after 5 minutes from the end of infusion. After the end of fixed-rate infusion the plasma concentration of gemcitabine declined rapidly in all patients (Figure 3). The overall mean clearance (± SD) of gemcitabine was 88.12 (± 18.65) and 127.27 (± 37.43) L h/m2 in cohort I and II respectively, with no significant difference between the two groups. The clearance of gemcitabine in the two groups is reported in Figure 4, whereas the relationship between clearance and bilirubin level is illustrated in Figure 5. No relationship has been found between serum bilirubin concentration and gemcitabine clearance. A regression analysis has been performed for other variables of hepatic function, such as transaminases, alkaline phosphatase, total bilirubun, PT, PTT, but none of them was statistically significant. The mean of expected total area under the plasma concentration-time curve for gemcitabine was higher in patients with normal hepatic function (11,75 μg*h/ml) than in patients with impaired liver function (8,43 μg*h/ml), this difference results statistically significant (p=0.04). The results of AUCexp in the two cohorts is illustrated in Figure 6. When the area under the plasma concentration-time curve of gemcitabine was extrapolated from zero to infinite, the mean values results 12,13 μg*h/ml and 8,87 μg*h/ml for cohort I and II, respectively (p=0.07). The mean of dFdU AUCexp for cohort I was 37,70 μ

g*h/ml and for cohort II was 25,14 μg*h/ml; the difference between the two AUC values was statistically significant, p=0.01. There were no significant differences in the terminal half-life of gemcitabine in both cohorts. Similarly, there were no significant differences among the cohorts in the elimination rate constant for gemcitabine (3,35 h^{-1} in control group and 5,41 h^{-1} in patients with altered liver function).

In 11 out of 13 patients the pharmacokinetic analysis was performed also at the second cycle, in order to evaluate the variability of the PK parameters in two consecutive cycles. No statistical difference was verified for all the parameters analyzed between cycle 1 and cycle 2 in the two groups (Table 5). The linkage of gemcitabine clearance and dFdU AUCexp between cycle 1 and 2 is reported in Figure 7.

Finally we investigated whether pharmacokinetic alterations could be associated with any altered toxicity profile. We identified four patients with grade ≥3 myelotoxicity, two in the control arm and two in the experimental arm; only one patient in cohort II had grade ≥3 hyperbiliribinemia. The Cmax of dFdU resulted significantly higher (p=0.02) in patients with grade 3 hematological toxicity. The patient with hepatic side effects presented an higher dFdU AUCexp value when compared with all the other patients in the same cohort (AUCexp 34,63 μg*h/ml vs 28,5 μg*h/ml)

DISCUSSION

The pharmacokinetics and the toxicity profile of chemotherapeutic agents are usually evaluated in phase I studies and in patients with normal organ function. This methodology precludes the possibility to evaluate specific dose recommendations in patients with organ dysfunctions. Gemcitabine is a drug with a broad spectrum of activity and a favorable toxicity profile. Literature data reported an increased incidence of transient hepatic toxicity in patients with liver metastases [19] and a phase I escalation study of gemcitabine over 30 minutes recommend to reduce the dose to 800 mg/m^2 in patients with elevated bilirubin level[15].

Gemcitabine infusion at the FDR of 10 mg/m2/min has been demonstrated to maximize the rate of triphosphate accumulation, its major intracellular metabolite [8,9]. Despite this robust pharmacological data, several phase II and III studies comparing different doses of gemcitabine in standard 30 minutes and FDR infusion, have failed to demonstrate a substantial clinical benefit for the main outcome

Based on these data, we were interested in evaluating the hepatic toxicity of gemcitabine at FDR infusion in patients already affected by impaired liver function. This is a frequent condition in patients with pancreatic and biliary tree carcinoma: hepatic function is compromised directly by cancer. We decided to use gemcitabine at 1000 mg/m2 in patients with pancreatic and biliary tree carcinoma, based on a current lack of evidence that gemcitabine activity is improved by increasing its dose [20].

Our primary aim was to evaluate the safety of gemcitabine starting from the same dose administered at FDR infusion in patients with hepatic dysfunction compared with those displaying normal liver function. The secondary end-point was to assess whether a dose adjustment was required in this subset of patients. We observed grade 3 myelosuppression in both cohorts of patients and a slight increased incidence of non-hematological toxicity in patients with hepatic dysfunction. The only dose reduction was performed in a patient with normal hepatic function. Although the limited number of patients included does not allow us to extrapolate any tolerability data in patients with impaired hepatic function, we can conclude that in our series all toxicities occurred were manageable and patients experienced grade 3 side effects in cohort II did not require dose adjustment . In spite of this clinical data, a major variation of %G was observed in cohort II, when compared with cohort I (10% vs 2% vs in decrease of %G variation). Moreover we have not identified a PK parameters that correlate with a pharmacodynamic outcome, such as myelosuppression.

The pharmacokinetic analysis revealed no significant difference for Cmax, Cl and $t_{1/2}$ between the two cohorts, but reveals a significant low AUCexp for gemcitabine and dFdU in patients with impaired liver function when compared to control group. Although the sample size is too small to confirm or refuse a meaningful difference of this parameter, the overall drug exposition is lower in patients with hepatic dysfunction. Another aim of this study was to verify and confirm the repeatability of the pharmacokinetic parameters analyzed within the same patient in two different cycles. For all the variables analyzed, no one appears significantly different from cycle 1 to cycle 2, therefore, despite the considerable inter-patient variability in both cohorts, the intra-patient variability results small.

Finally, we investigated whether patients with increased toxicity, compared with patients with a better tolerability, presented a different pharmacokinetic disposition of gemcitabine and/or dFdU. Actually, our analysis failed to reveal statistically significant difference in the pharmacokinetics of both agents in patients with altered toxicity profile, except for the AUCexp of gemcitabine and its inactive metabolite. This observation may reflect the fact that gemcitabine is not the active drug but a pro-drug, that requires a series of activations to be transformed into its triphosphate form. Therefore, more accurate relationship between toxicity and triphosphate disposition should provide some interesting correlation between pharmacodynamic and pharmacokinetic properties of this drug. This simple correlation between plasma gemcitabine/triphosphae form and toxicity seems to be unlikely, as prospected by other studies[21]. For example, it has been demonstrated that high dose of gemcitabine (2,800 mg/m2) is not correlated with a corresponding high grade of toxicity. This is possibly explained by the saturable mechanism of accumulation of gemcitabine triphosphate into the cells. A weak relationship between plasma gemcitabine levels and its triphosphate form has been reported also recently by Grimson et al.[15]. Moreover these Authors

observed an autoinduction of dFdCTP accumulation during the second week infusion, underlying the importance to perform pharmacological study beyond week one.

Only one patient presented a transient elevation of bilirubin and transaminases in cohort II. This singular evidence is not enough to confirm the transient hepatic toxicity observed in the Tempero's study[13] in the FDR arm, and the reason of the temporary hepatic dysfunction remains unclear. The analysis of the gemcitabine and dFdU disposition in this specific patient revealed, compared with all other patients included, a significant high level of the inactive metabolite in the blood,and a faster clearance of the gemcitabine. . We are unable to extrapolate this information from the only case observed, but we are currently analyzing other patients with transient hepatic toxicity in order to confirm this data.

Although the small sample size of our control group, the PK parameters analyzed are not dissimilar from the same data reported in the literature. In fact, the AUC of gemcitabine administered at 1000 mg/m2 range from 9.5 μg h/ml and 3.8 μg h/ml [5] and our analysis demonstrated a range from 9.11μg h/ml to 15.22 μg h/ml; similarly terminal half life and clearance of gemcitabine reported in the literature range from 5 to 11 minutes and from 39 to 1,239 L/h-m2[5].

Our results seem to exclude a possible increased toxicity of gemcitabine when administered at FDR infusion in patients with impaired hepatic function. Nevertheless, we believe that patients with organ dysfunction do require specific studies to verify the correct drug dose and tolerability. These data can not be extrapolated from conventional phase I trials and deserve further specifically designed investigations.

REFERENCES

1. Stadler WM, Kuzel T, Roth B, et al: Phase II study of single-agent gemcitabine in previously untreated patients with metastatic urothelial cancer. J Clin Oncol 1997;15: 3394-3398

2. Moore MJ, Tannock IF, Ernst DS, et al: Gemcitabine: A promising new agent in the treatment of advanced urothelial cancer. J Clin Oncol 1997;15: 3441-3445

3. Heinemann V, Hertel LW, Grindey GB, Plunkett W: Comparison of the cellular pharmacokinetics and toxicity of 2',2'-diflurodeoxycitidine and 1β-D-arabinofuranosylcytosine. Cancer Res 1988;48: 4024-4031

4. Grunewald R, Kantarjian H, Keating MJ, et al. Pharmacologically directed design of the dose rate and schedule of 2,2-diflouorodeoxycytidineadministration in leukaemia, Cancer Res 1990;50: 6823-6826

5. Abbruzzese JL, Grunewald R, Weeks EA, et al: A phase I clinical, plasma and cellular pharmacology study of Gemcitabine. J Clin Oncol 1991;9:491-498

6. Heinemann V, Xu YZ, Chubb S, et al: Inhibition of ribonucleotide reduction in CCRF-CEM cells by 2,2-diflouorodeoxycytidine. Mol Pharmacol 1990;38:567-572

7, Gandhi V.: Questions about gemcitabine dose rate: answered or unanswered? J Clin Oncol 2007;25(36): 5691-5694

8,Grunewald R, Abbruzzese JL, Tarassoff P, et al: Saturation of 2',2'-difluorodeoxycytidine 5'-triphosphate accumulation by mononuclear cells during a phase I trial of Gemcitabine. Cancer Chemother Pharmacol 1991;27:258-262

9. Grunewald R, Kantarjian H, Du M, et al. Gemcitabine in leukaemia: A phase I clinical, plasma, and cellular pharmacology study of gemcitabine. J Clin Oncol. 1991;9:491-498

10. Patel SR, Gandhi V, Jenkins J, et al. Phase II clinical investigation of Gemcitabine in advanced soft tissue sarcomas and window evaluation of dose rate on Gemcitabine triphosphate accumulation. J Clin Oncol 2001;19:3483–3489

11. Brand R, Capadano M, Tempero M. A phase I trial of weekly Gemcitabine administered as a prolonged infusion in patients with pancreatic cancer and other solid tumors. Invest New Drugs 1997;15:331–341

12. Grunewald R, Kantarjian H, Du M, et al. Gemcitabine in leukemia: A phase I clinical, plasma, and cellular pharmacology study. J Clin Oncol 1992;10:406–413

13. Tempero M., Plunkett W., Ruiz Van Haperen V., Hainsworth J., Hochester H., Lenzi R., Abbruzzese J. Randomized Phase II Comparison Of Dose Intense Gemcitabine: Thirty Minute Infusion And Fixed Dose Rate Infusion In Patients With Pancreatic Adenocarcinoma. J Clin Oncol. 2003;21: 3402-8

14. Grimison P., Galettis P., Manners S., et al.: Randomized crossover study evaluating the effect of gemcitabine infusion rate: evidence of autoinduction of gemcitabine accumulation. J Clin Oncol 2007;25(36): 5704-5709

15. Venook A,. Egorin M J, Rosner G, Hollis D, Mani S, Hawkins M, Byrd J, Hohl R, Budman D, Meropol N.J, Ratain MJ Phase I and Pharmacokinetic Trial of Gemcitabine in Patients With Hepatic or Renal Dysfunction: Cancer and Leukemia Group B 9565; J Clin Oncol. 2000;18:2780-2787

16. Therasse P, Arbuck SG, Eisenhauer EA, Wanders J, Kaplan RS, Rubinstein L, Verweij J, Van Glabbeke M, van Oosterom AT, Christian MC, Gwyther SG. New guidelines to evaluate the response to treatment in solid tumors. European Organization for Research and Treatment of Cancer, National Cancer Institute of the United States, National Cancer Institute of Canada. J Natl Cancer Inst. 2000;92(3):205-16

17. Sottani C, Massimo Zucchetti M, Zaffaroni M et al.:Validated procedure for simultaneous trace leveldetermination of the anti-cancer agent gemcitabine and its metabolite in human urine by high-performance liquid chromatography with tandem mass spectrometry. Rapid Commun. Mass Spectrom 2004;18:1017-1023

18. Fogli S., Danesi R., Gennai A., Donati S., Conte P.F., Del Tacca M. Gemcitabine, epirubicin and paclitaxel: pharmacokinetic and pharmacodynamic interactions in advanced breast cancer. Ann Oncol. 2002;13(6):919-27

19. Sessa C., Aamdal S., Wolff I., et al.: Gemcitabine in patients with advanced malignant melanoma or gastric cancer: Phase II studies of the EORTC Early Clinical Trias group. Ann Oncol 1994;5: 471-472

20. Gelibter A., Malaguti P., Di Cosimo S., et al.: Fixed dose-rate gemcitabine infusion as first-line treatment for advanced-stage carcinoma of the pancreas and biliary tree. Cancer. 2005;104(6): 1237-1245

21. Fossella F.V., Lippman S.M., Shin D.M., et al.: Maximum-tolerated dose defined for single-agent gemcitabine: A phase I dose.escalation study in chemotherapy-naïve patients with advanced non-small-cell-lung cancer. J Clin Oncol 1997;15:310-316

Table 1. Patient Characteristic

Characteristic	Cohort I	Cohort II
Patients entered	4	9
Age, median, years	59	67
Sex, n. of patients		
Male	1	5
Female	3	4
WHO PS		
0-1	3	7
2	1	2
Diagnosis, no of patients		
Pancreas	2	5
Biliary tree	2	1
Cholecyst	-	3
Locally advanced disease	1	6
Metastatic disease	3	3

Table 2. Baseline Laboratory Values

Parameters	Cohort I		Cohort II	
	Mean (±SD)	Range	Mean (±SD)	Range
WBC count, x10^{3}cells/µL	6,27 (2,06)	4,81-9,30	11,86 (7,08)	5,90- 28,00
PLT count, x10^{3}cells/µL	159,000 (65,15)	96,000-236,000	369,000 (232,55)	146,000-775,000
Hgb, g/dL	11,7 (1,91)	10,3- 14,5	11,16 (1,43)	9,3- 14,0
Total bilirubin level, mg/dl	0,80 (0,35)	0,55-1,33	5,29 (3,83)	0,66-14,24
Direct bilirubin level, mg/dl	0,39 (0,39)	0,15- 0,85	2,58 (1,41)	0,22-4,52
AST level, U/L	32 (14)	16- 46	70 (48)	23- 168
ALT level, U/L	39 (18)	17-62	92 (32)	43-134
AP level, U/L	710 (487)	365-1055	1278 (625)	420-2258
Creatinine level, mg/dl	0,72 (0,08)	0,66-0,85	0,73 (0,35)	0,05-1,21
Total protein, g/dl	6,50 (0,60)	6,10-7,20	6,58 (0,72)	5,10-7,50
PT time, %	99 (6,4)	95-107	97 (9,8)	86-115
PTT, time, sec	31 (2,6)	29-34	32 (4,2)	28-41

Abbreviations: WBC: white blood cells; PLT: platelet; AST: aspartate transaminase; ALT: alanine transaminase; AP: alkaline phosphatase; PT: prothrombin time; PTT: partial thromboplatin time; SD: standard deviation

Table 3. Toxicity Summary (n. of patients)

Toxicity per Patient	Cohort I		Cohort II	
	Grade 2	Grade 3	Grade 2	Grade 3
Anemia	1	-	1	1
Neutropenia	-	2	1	-
Thrombocytopenia	-	-	-	1
AST/ALT	1	-	-	1
Bilirubinemia	-	-	-	1
Asthenia	1	-	-	1
Fever	-	-	1	-
Nausea/vomiting	-	-	1	-

Table 4. Pharmacokinetic results

	Cmax (µ g/ml)		**AUCexp** (µg h/ml)		**AUCinf** (µg h/ml)	**t1/2** (h)	**Cl** (L h/m2)	**K** (h^{-1})
	Gem	dFdU	Gem	dFdU	Gem	Gem	Gem	Gem
Cohort I								
Mean cy1	6,82	11,07	11,75	37,70	12,13	0,92	88,12	3,35
Range	6,00-7,70	8,80-12,40	9,11-15,22	34,01-41,83	9,20-16,42	0,08-2,77	65,70-109,80	0,25-8,27
SD	0,73	1,58	2,61	3,74	3,12	1,25	18,65	3,62
Cohort II								
Mean cy1	7,76	8,93	8,43	25,14	8,87	0,18	127,27	5,41
Range	6,50-12,20	5,40-14,0	5,06-12,54	13,80-35,14	5,15-13,17	0,06-0,35	79,76-197,59	0,30-12,18
SD	1,77	2,39	2,29	8,12	2,50	0,10	37,43	4,11

Cmax: plasmatic peak concentration; *AUCexp*: experimental area under the plasma concentration-time curve; *AUCinf*: infinite area under the plasma concentration-time curve; $t_{1/2}$:terminal half life; *Cl*: total plasma clearance; K: rate of elimination (*K); Cy1*: cycle 1; *SD*: Standard Deviation.

Table 5. Total pharmacokinetic results at cycle I and cycle II

	Cmax (µ g/ml)		**AUCexp** (µg h/ml)		**AUCinf** (µg h/ml)	**t1/2** (h)	**Cl** (L h/m2)	**K** (h^{-1})
	Gem	dFdU	Gem	dFdU	Gem	Gem	Gem	Gem
Mean cy1	7,47	9,59	9,45	29,00	9,88	0,41	115,22	4,77
Mean cy2	7,26	8,73	8,14	27,01	8,73	0,25	128,45	5,36

Cmax: plasmatic peak concentration; *AUCexp*: experimental area under the plasma concentration-time curve; *AUCinf*: infinite area under the plasma concentration-time curve; $t_{1/2}$: terminal half-life; *Cl*: total plasma clearance; K: rate of elimination (*K); Cy1*: cycle 1; *Cy2*: cycle 2.

Figure 1. Cumulative grade 2 and 3 toxicity in patients for cohort I and II

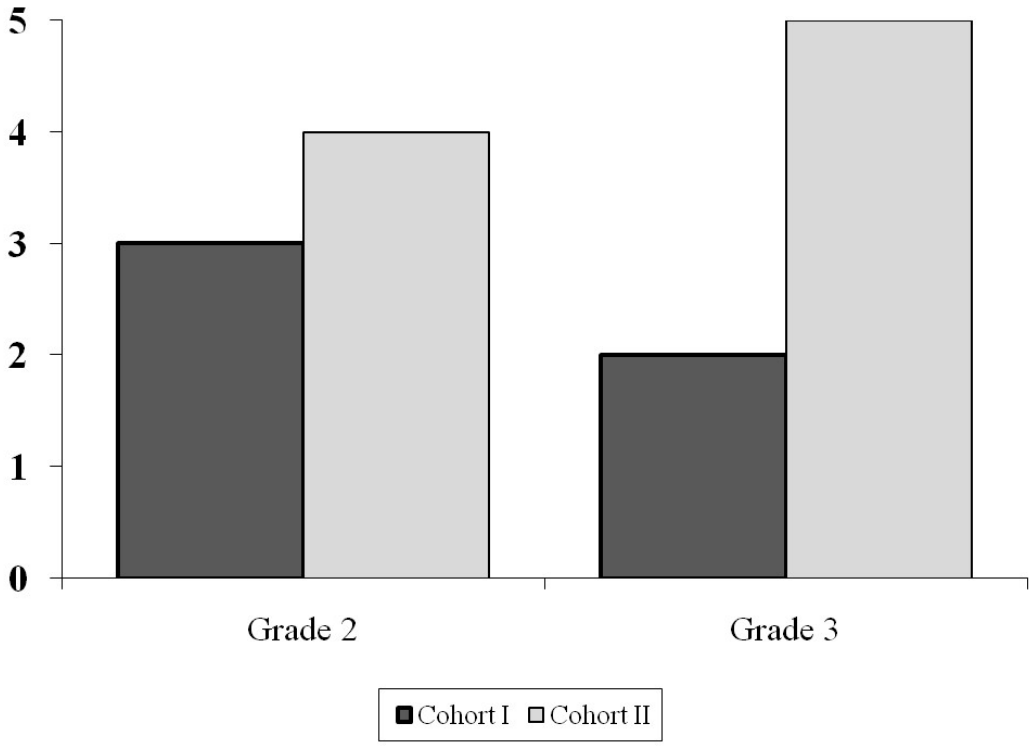

Figure 2. The maximum concentration (Cmax) of gemcitabine (dFdC) and its metabolite (dFdU) in cohort I and II

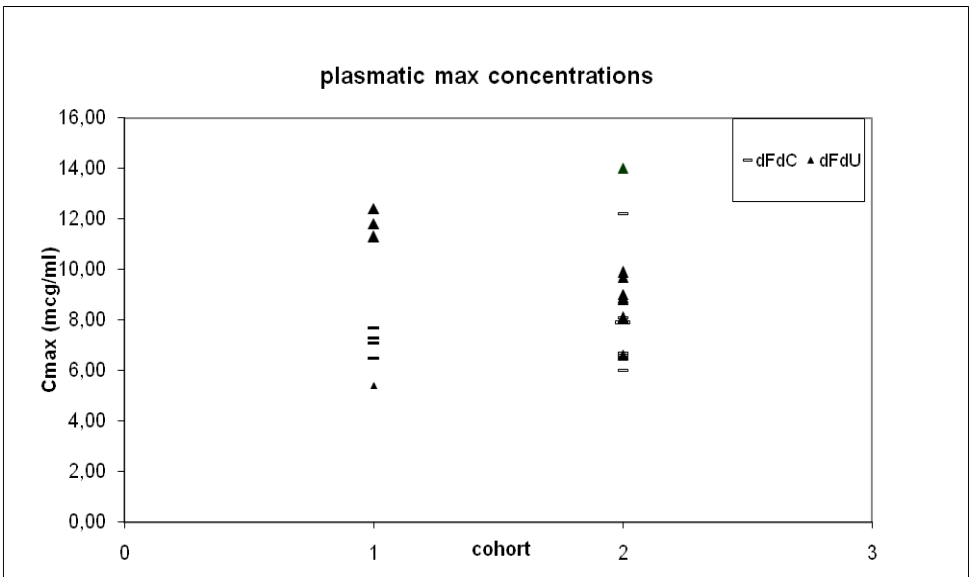

Figure 3. .Plasma concentration-time profile of gemcitabine (dFdC) (a) and of dFdU (b) at the first cycle in patient with normal hepatic function (cohort I) and in patients with altered hepatic function (cohort II)

Fig.3a

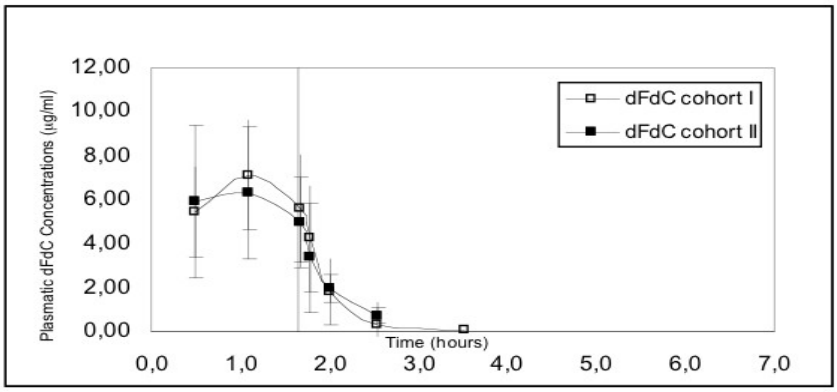

Fig.3b

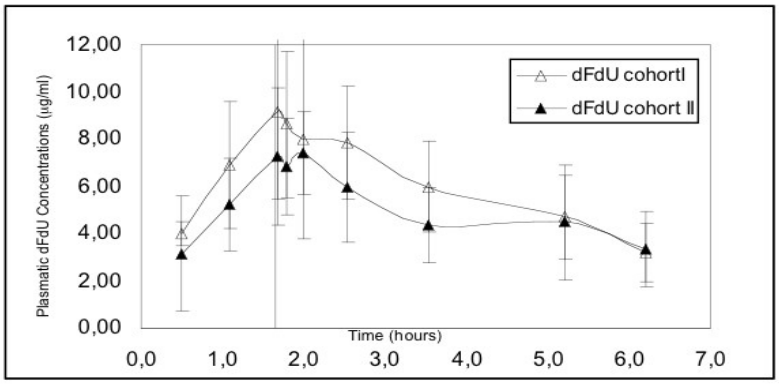

Figure 4. Clearance of gemcitabine in cohort I and II

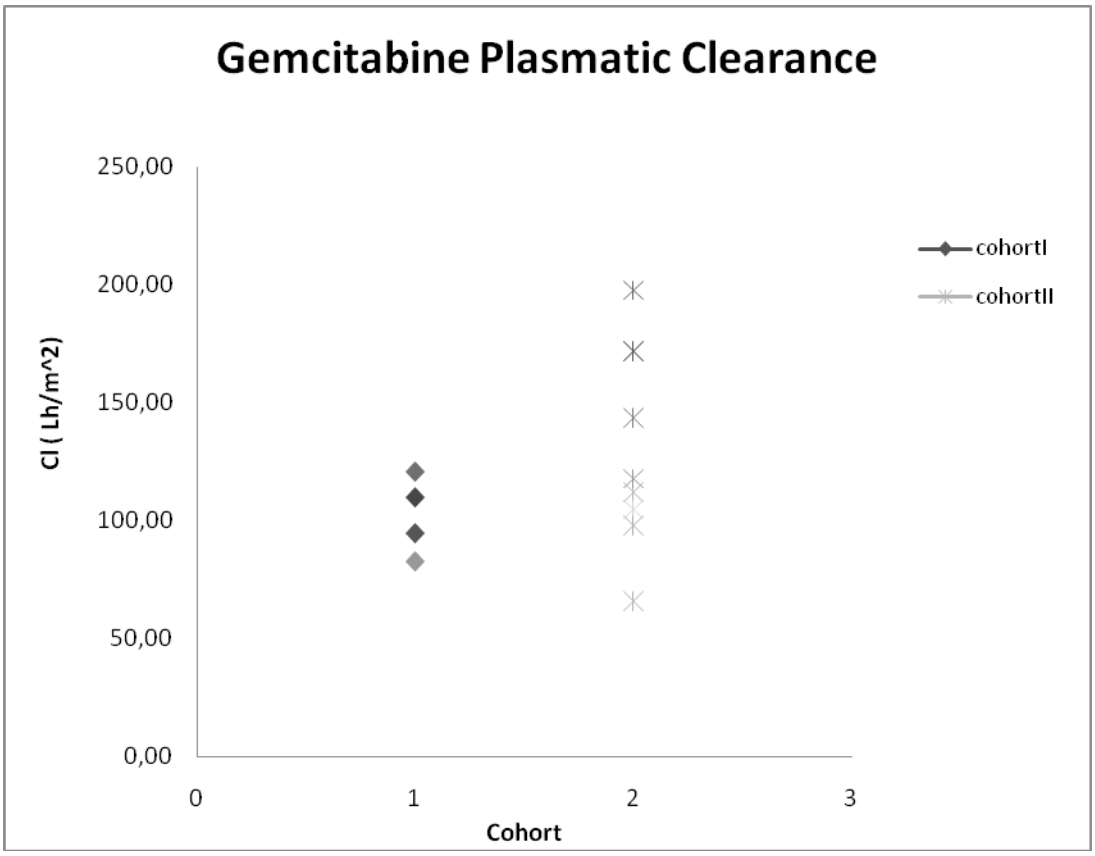

Figure 5. Regression of dFdC (gemcitabine) and dFdU clearance as function of total bilirubin

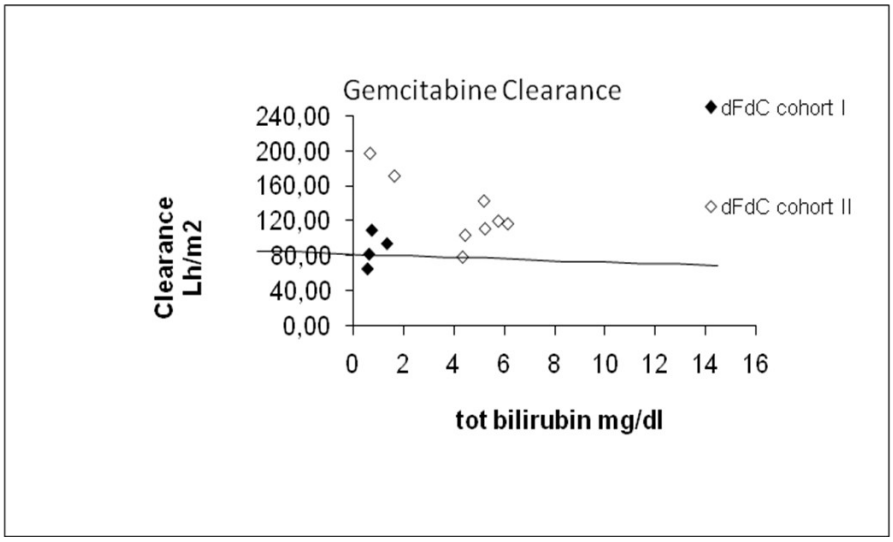

Figure 6. AUCexp of gemcitabine and dFdU in cohort I and II

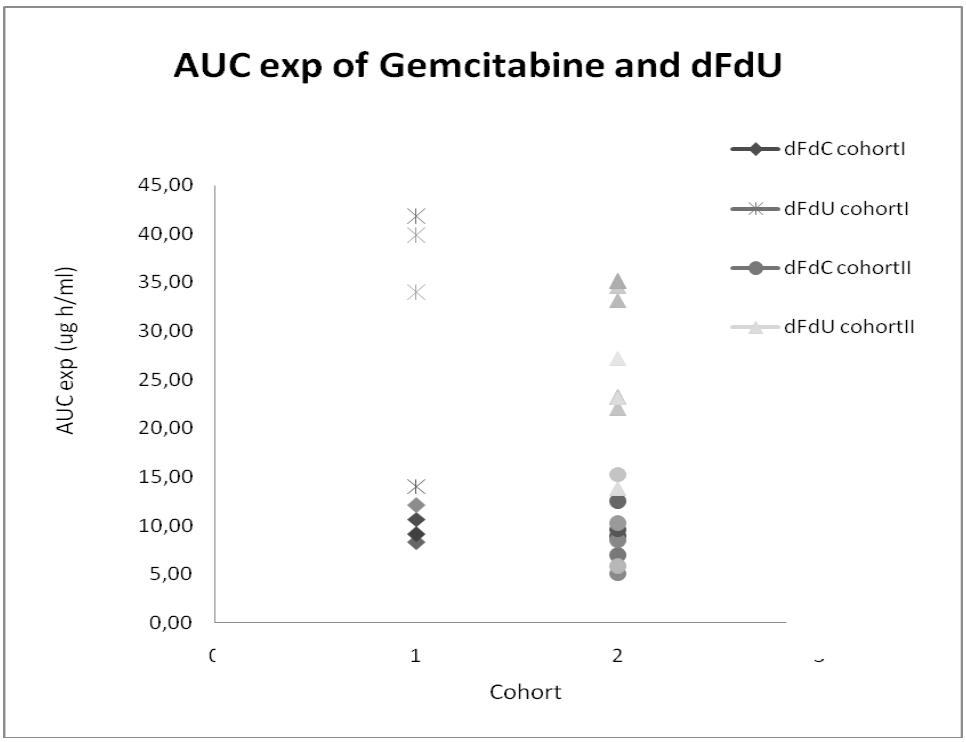

Figure 7. Relationship of gemcitabine clearance and dFdU AUC in cycle 1 and 2

Analytical Considerations for Mass Spectrometry Profiling in Serum Biomarker Discovery.
Clinics in Laboratory Medicine. In press.

Gordon R. Whiteley, Ph.D., M.Sc.[1], Simona Colantonio[1,2], Andrea Sacconi[1,2], Richard G. Saul, Ph.D., B.S.[1].

[1]Clinical Proteomics Reference Lab, Advanced Technology Program, SAIC-Frederick, Inc., NCI-Frederick, Frederick, MD USA and [2]Regina Elena National Cancer Institute, Rome, Italy

Key Words: Biomarkers, Proteomic Patterns, MALDI, Bioinformatics

Abstract:

The potential of using mass spectrometry profiling as a diagnostic tool has been demonstrated for a wide variety of diseases. Various cancers and cancer related diseases have been the focus of much of this work due to both the paucity of good diagnostic markers as well as the knowledge that early diagnosis is the most powerful weapon in treating cancer. However, the implementation of mass spectrometry as a routine diagnostic tool has proven to be difficult, primarily because of the stringent controls that are required for the method to be reproducible. Because this technology had not been studied for factors that could influence the end result, there was a need to examine a series of conditions including sample bias, pre-processing, instrument controls, environmental conditions, post-analysis classification to name a few. When these were examined, it became clear that while the method was feasible, implementation of mass spectrometry as a routine clinical testing method was unlikely. In the meantime, however, the method is evolving as a powerful guide to the discovery of biomarkers that could, in turn, be utilized either individually or in an array or panel of tests for early disease detection. Using proteomic patterns to guide biomarker discovery and the

possibility of deployment in the clinical lab environment on current instrumentation or in a hybrid technology has the possibility of being the early diagnosis tool that is needed.

Proteomic patterns are revealed:

The potential of mass spectrometry (MS) patterns as a diagnostic tool was first described in 2002 [33] and was hailed as a breakthrough in diagnostic medicine. While this first report was a concept paper, many interpreted it as a completed test ready for commercialization. A resulting storm of controversy criticizing the concept was based largely on theoretical concerns [5,12]. At the same time proteomic patterns for a long list of additional diseases were reported[9,15,46] and the debate continued. Indeed, there are still reports of proteomic patterns that are being discovered for diseases but with a heavy focus on early cancer detection [41,42] . There was and still is a lack focus on the true development of a method that is well understood and controlled and could be used in a clinical study to determine the true feasibility of this technology as a diagnostic tool. There are however several breakthroughs both in the understanding of proteomic patterns from the laboratory testing of samples and in the bioinformatics analysis that will result in clinically useful information for diagnosis and further understanding of the disease process.

The role of SELDI in proteomics awareness:

The term proteomics first appeared in the early 1990's but did not become common in the scientific literature until much later in that decade[1]. At about the same time, the SELDI (surface enhanced laser desorption ionization) system was introduced by Ciphergen (Fremont, CA now BioRad). This technique was a fusion of sample fractionation and

MALDI (matrix assisted laser desorption ionization) mass spectrometry. The company had made both the sample preparation and instrumentation simple to use and convenient for processing large numbers of samples. For the first time, it was possible for scientists in the biological sciences to investigate mass spectrometry in their laboratories without having to tackle the complexities of the other mass spectrometer instruments available. The SELDI arrays were designed with an increased surface area within a series of 8 circles surrounded by a hydrophobic membrane (see figure 1). Samples were processed on 12 arrays that were held in a device that gave the standard 96 configuration of a 96 well microtiter plate. This allowed for high throughput processing and adaptation to robotic platforms designed for ELISA (enzyzme linked immunosorbant assay) tests. The arrays were then read by the compact (for that time) mass spectrometer instrument. A user friendly software gave presentation of results in formats familiar to biologists such as the "gel view" graphic representation of spectra in a density plot [33,40].

In a ground breaking report, Petricoin *et al* reported the use of this system to test a group of ovarian cancer patient samples and a group of samples that were free of ovarian cancer[33]. Once the spectra had been collected from the sample sets, a genetic algorithm and self-organizing cluster analysis was used to find differences in the spectral patterns between the two groups. Masked samples were then used to test the discovered patterns and the results gave a startling sensitivity and specificity of 100% and 95% respectively. This report was followed rapidly by reports from many authors finding patterns for other cancers and diseases and new patterns are being reported even now[2,16,25,41,42].

SELDI goes high resolution:

One of the disadvantages of the SELDI system is that the resolution is not sufficient for identification of peptides. This was overcome when Ciphergen produced a SELDI front-end to a high resolution instrument, the ABI Q-star. It allowed the SELDI arrays to be read with higher resolution but the throughput was low and did not allow for large sample sets to be easily processed. As biologists became more comfortable with mass spectrometry, profiling was evaluated on this platform with results that appeared to be absolutely accurate compared to the original results found on the Ciphergen instrumentation[10](table 1). There were a total of 4 models that gave 100% sensitivity and specificity but it was noted that there were several peaks common to all of the algorithms that gave high accuracy results. As both excitement and criticism grew over the possibility of using this technology for early detection of cancer and other diseases, the need for evaluation of reproducibility, robustness, control and understanding of the mechanism of the method became more urgent.

Principle of the test:

The most fundamental issue before dealing with reproducibility and robustness was the question of the principle of the test and what exactly was being measured. What was curious in the initial reports was that the potential biomarkers being measured could be detected by a mass spectrometer whose sensitivity is some 2 orders of magnitude less than the standard ELISA technique (Saul, RG and Whiteley, GR unpublished data, 2005). It just did not seem possible to measure products of small primary stage tumors in the large volume of plasma using this technique. However, this was soon explained by the possibility that biomarkers were being collected and concentrated in the serum by high

abundance carrier proteins such as albumin [29]. Albumin is known to be a carrier protein and one with a relatively long half life of 19 days [20]. Traditional mass spectrometry concentrated on the removal of the high abundance proteins in order to detect the low concentration peptides and proteins in serum hoping that these would yield biomarkers for disease. However, the revolutionary thought that the biomarkers may indeed be discarded with the removal of the carrier proteins led to the discovery that there were ion species correlating with cancer such as ovarian cancer associated with these carrier proteins. By isolating the albumin and then dissociating low molecular weight peptides and proteins, a further large number of cancer related proteins and peptides along with new unique peptides were also found [27]. This discovery was instrumental in the development and approach of other studies that have since shown patterns of albumin associated peptides for Alzeheimer's disease [25], ovarian cancer [26], cutaneous T-cell lymphoma, [23] and breast cancer [8]. It has also provided the basis for the isolation and concentration of peptides that are now being studied as potential biomarkers.

Automation of the process:

One of the earliest tools for making the SELDI and other MALDI platforms more robust was automation of sample preparation thereby eliminating bias introduced by person to person technique variability. Early in the proteomic profiling studies using the Ciphergen system, automation was a key to both ease of high throughput processing and reproducibility. The Beckman Biomek system was originally packaged with the Ciphergen system and sold as part of the system. This microplate processor platform was easy to program and the design of the 96 spot microplate layout made the adaptation of

the system simple. However, we had observed that the matrix application timing was critical to reproducibility and this observation was confirmed by others [18]. Furthermore, we had found that the drying time of the sample on the arrays was also critical and this finding was also observed by others [3]. These factors needed to be taken into account when selecting a robotics system.

The weak point of the original Biomek system was that the matrix application was done one spot at a time and it took close to one hour to apply matrix to all 96 positions. We later converted to the Tecan Genesis system (TecanAG, Switzerland) and had programmed a system of serpentine matrix application that substantially reduced the application time. This along with the installation of the robot in a laboratory that was both temperature (±2°C) and humidity (± 5%) controlled led to an improvement in the robustness of the technology [8]. Our final adaptation to robotic processing was done using the Hamilton Star robot (Hamilton, Reno, NV). This robot utilizes a unique method to pick up pipette tips and has a 96 head pipettor capable of application of 1µl of matrix to all positions with great precision. That allowed the simultaneous application of matrix and eliminated the matrix addition timing as a potential source of variability. This robot became the basis for both SELDI and MALDI studies done within our lab [11,23].

Reproducibility and robustness factors:

While the adaptation of sample processing was an important factor in stabilizing reproducibility, it was only one of many factors that were key. Indeed, many of the top level requirements were outlined in an editorial in 2005 (table 2) [17]. This sobering reality brought attention beyond the analytical platform to issues of sample acquisition and

handling along with the data processing, both critical components of technology robustness.

The influence of pre-sampling factors on the human proteomic pattern has not been thoroughly studied. There are studies emerging on the manipulation of the proteome through factors such as diet in fish [28] and and rats[37] with the expected result that there are changes in the proteome induced by diet changes. Some of the identified proteins involved are apolipoprotein A and aldolase both of which have been identified as potential sentinels of disease [4]. One can also assume that other factors such as medication, diet and hormonal status could disrupt the human proteome and therefore must be either accounted for or diluted out in studies of disease through proteomic patterns [35]. The careful selection of patient populations becomes a critical part of these studies especially during the validation of any proteomic pattern [6].

The next set of issues involves the acquisition, handling processing of samples before testing. Here there are some studies that have been done on various aspects but no standard procedure has been set. A comparison of serum and plasma as sources demonstrated expected differences in the two samples [7]. It was also observed by Banks *et al* that there was significant alteration of the profiles when there was a delay in the time between sample acquisition and processing. Clotting time for serum was found to be significant and it was suggested that a time greater than 30 minutes was necessary for all of the changes resulting from clotting were at a steady state. There has also been an observation that the many possible additives to tubes show potential for differences in observed ions [13] and the only tubes that appeared to be suitable for serum were glass tubes without additives. Storage is another issue. Freezing was shown to not impact the

patterns [43]. We had also found that freezing and thawing did not impact the patterns but time stored refrigerated did show a significant drop in the an area of the spectra around the 3800 to 4000 m/z range (Shand, WB and Whiteley, GR unpublished data). Additional studies done in animals also demonstrate the issues of sample handling and processing and their impact on spectra [47].

Sample preparation for mass spectrometry can have yet a further impact on the spectra. We had found that temperature and humidity were critical issues for the drying of samples and matrix [8] and these findings were confirmed in a more formal study [43]. The influence of pH, buffer concentration and surface selected can also cause shifts in proteomic pattern [5] and these can be misinterpreted as lack of reproducibility [21]. What is clear is that there needs to be definition of not only the factors that can influence reproducibility but also the limitations of each of these factors. Controls or indicators of these factors can assist researchers in guiding data interpretation so that patterns can be reliably reproduced.

Demonstrations of reproducibility:

Despite all of the above issues, there have been very promising demonstrations of the power and reproducibility of proteomic patterns. The earliest comprehensive report appeared in 2005 where 6 sites were asked to prepare and test samples using a standard protocol after a rigorous calibration with known proteins (insulin and IgG) a standardized pooled sample. Known peaks were evaluated for intensity, resolution and signal to noise ratio. After this, sites were asked to test 14 prostate cancer and 14 non-cancer samples and analyze the data using a standardized method. Their results showed that, under these

conditions, they were able to show agreement between laboratories to a high degree of confidence [38]. Another study demonstrated reproducibility of a pattern for breast cancer over a 14 month period using the same instrumentation, method and highly controlled conditions [8]. This was the first time that the potential of patterns being stable over time had been reported. Within patient stability of profiles has also been demonstrated [39]. In this study, individual patient samples taken over a three year period were examined. Although some peaks showed high CV values, the authors concluded that there were sufficient peaks with good reproducibility that the spectra from this group of patients were stable. It should be noted however that these samples were all run at the same time, thus reducing the issues regarding control of the sample processing and instrumentation listed above.

The use of Bioinformatics to find patterns

The complexity of mass spectra compounded with a significant number of samples within each of a "training group" dictates that sophisticated computer analysis methods be employed to find patterns that correlate with disease. Most of the techniques used were originally designed for other purposes involving pattern recognition to extract information from surveillance and other data. The first mass spectrometry patterns were revealed wih the use of genetic algorithms and self-organizing maps[33]. Since that time, a number of programs have been developed by mass spectrometry manufacturers such as the Cipergen Biomarker Wizard® software. An earlier version of this software was used to identify biomarkers for ovarian cancer[34] and these are the basis for a series of markers now in clinical evaluations by Vermillion that has been filed with the FDA (http://ir.ciphergen.com/preview/phoenix.zhtml?c=121814&p=irol-

newsArticle&ID=1169372&highlight=). The same types of software have also been used in the world of genetic analysis to reveal gene patterns that are indicative of disease [45]. However, mass spectra are so complex that before analysis there must be some processing of the data. This involves the separation of true signal from noise that can be the result of both chemical and / or spectral baseline noise. Each of these can in themselves cause problems with the data analysis unless particular care is taken. One of the great assets of mass spectral data is its high dimensionality but this is also one of the great issues in efficient data mining. In order to reduce the dimensionality, binning of data is usually done. This can be done by the addition of peaks at fixed distances along the spectrum but is much better performed when the data is binned in a growing window taking advantage of the higher resolution of instruments at the lower mass / charge (m/z) range and compensating for the lower resolution at the high m/z end of the spectrum. Algorithms for binning have also been developed using only areas between two valleys in the spectrum[23]. This method helps preserve peaks and avoid loss of resolution due to the accidental addition of separate peaks because of their location within a fixed m/z range. Once this is done, pattern analysis can be performed.

Our approach has been to simplify or have redundant analysis as much as possible in order to have confidence in patterns that were observed in order to avoid the pitfalls of each of the methods that are well documented. The method is described in detail in the publication by Liu *et al* [23]. Briefly, peaks that showed significant intensity differences between disease and non-disease groups were selected. Then three classification methods were used: partial least square regression, support vector machine and the C5.0 decision tree. Each of the test samples were classified by the three methods and then a

voting scheme was used for the final classification. Where disagreement occurred, the samples were classified as unknown. The classification showed that complex patterns existed showing differences between these two groups. However, a simpler approach took advantage of the true power of mass spectrometry – the ability to detect very small differences in a molecule caused by a post-translational modification. Using this method, an algorithm of peak pair ratios selected peak pairs correlating with post-translational modifications associated with cancer that showed significant differences between patients with ovarian cancer and patients without disease. The result was that 4 peak pairs (8 peaks) could differentiate between these two groups in a test group of samples. This finding showed that there were potential biomarkers of disease markers to be discovered in these samples.

Proteomic patterns as potential diagnostic tools

This appears to be extremely challenging and will probably require significant breakthroughs in all areas: mass spectrometry, computer software, understanding of sample issues and methods of controlling all aspects of testing. Despite this, we did assess the feasibility of the technology using a set of patient samples and the algorithm developed above. The original algorithm was developed from samples collected at Northwestern University under their protocol. Samples were stored at -80°C until testing. A set of blinded samples were collected and processed at a second institution (Duke University). There was no review of the sample collection and processing protocol to make it consistent with that of Northwestern University. The samples were also frozen at -80°C before testing. The method for sample preparation and testing was consistent in the laboratory and all tests were done on the same instrumentation under the

same conditions. The spectra were processed and classified according to the algorithm above. The final results had been blinded up until this point. The results showed that there was a significant agreement between the classification and clinical diagnosis when un-blinded although the sensitivity and specificity were much lower than in the test group (table XXXX). While this clearly shows that the methodology needs substantial development before it could be used in a clinical trial, it does demonstrate that there are potential biomarkers that should be investigated.

Guided biomarker discovery using proteomic patterns:

Once a pattern has been found, it is not a trivial task to identify the proteins that are the source of the pattern. However, using high resolution MALDI results such as those obtained above, it is conceivable to sort through the spectra of the sample collection and select individual samples with high intensities of the peaks of interest as well as samples with extremely low intensities of these same peaks. Using these samples, the process of fractionation and the search for the identity begins with the knowledge that the MALDI database identification can confirm a more definitive methodology.

Several methods have been successfully used to identify proteins. These include conventional chemical methods such as Edman's degradation but the more sophisticated and less laborious mass spectrometry techniques are now more commonly used.

Probably the most important aspect of mass spectrometry in proteomics is the possibility to obtain tandem mass spectrometry experiments (MS/MS or MS^n) on selected instruments. In tandem mass spectrometry inducing ion fragmentation is possible and the m/z of the daughter ions can be measured. The capability of this method has been largely explored since the early 1990's especially in ion traps [14,22,24], although also FT ICR [36,48] and MALDI TOF–TOF have shown interesting results [19].

Generally, a fractionation of the complex protein mixture is done that would mimic the fractionation done before the original spectral patterns are generated. This is then followed by further fractionations to reduce the complexity of the samples. These fractionations can be done using methods such as electrophoresis (either 1 or 2 dimensional) or liquid chromatography followed by mass spectrometry on either digested fragments or the intact material.

Deployment of patterns into the clinical laboratory:

The migration of this technology to the clinical environment will not be an easy task. There are, however, several possibilities that could accommodate the knowledge gained by these studies and merge them with technology that is currently accepted or could be adapted to the clinical lab environment. Certainly the immunoassay in its many forms is a well understood and accepted platform for clinical sample testing. Techniques such as the ELISA (enzyme linked immunosorbant assay) have exquisite sensitivity. However, they do not have the capability of easily and accurately detecting small changes in molecules that are possible markers of disease. Mass spectrometry has the capacity to detect these very minor changes but lacks the sensitivity of the immunoassay techniques. It would therefore seem logical to explore the fusion of these techniques.

Exploration of the affinity concentration and mass spectrometry techniques has been done as a way of biomarker definition and discovery. Several different solid phases have been used in a basic scheme as outlined in figure 2. These have included magnetic beads [44], affinity pipette tips [31] and gold surfaces[30]. In each case, antibodies were used as

affinity capture reagents to fractionate and concentrate proteins and peptides from more complex solutions. In the case of the magnetic beads and affinity pipette tips, the process was automated on a robotic system and proteins captured by the antibodies were eluted and analyzed by mass spectrometry. The results show that these two techniques together are powerful and provide an information rich output that not only shows different isoforms of proteins but also quantitative information.

The use of gold surfaces adds yet another dimension [30,32]. This allows for the label free detection of proteins captured through SPR (surface plasmon resonance) and then utilizing the same surface the proteins can be encapsulated in matrix and MALDI mass spectrometry interrogation can be performed. Thus, samples can be tested to see if they contain a particular binding partner to the affinity surface and then the form of the protein can be determined by mass spectrometry. The sensitivity of SPR is somewhat less than more sensitive amplification methods. However, this type of hybrid technology increases the value of the data collected through the addition of another dimension of separation and detection.

Summary:

Mass spectrometry patterns are a rich source of potential biomarkers for a wide variety of diseases. Although they have been described more than 5 years ago, the understanding of the source of the patterns and the identity of the majority of the proteins remains largely unknown. The host of factors that must be considered when using these patterns for biomarker discovery or potential diagnostic testing is extensive and still largely unexplored. However, the enormous potential for this technology in both discovery and

early diagnosis is clear. The path forward will require a tremendous amount of development work and careful clinical validation. The promise of new insight into disease mechanisms and early detection using the technique or hybrid forms with other synergistic technologies calls for additional time and effort that will result in positive patient benefit.

Acknowledgement:

This project has been funded in whole or in part with federal funds from the National Cancer Institute, National Institutes of Health, under contract number N01-CO-12400. The content of this publication does not necessarily reflect the views or policies of the Department of Health and Human Services, nor does mention of trade names, commercial products, or organizations imply endorsement by the U.S. Government. This research was supported [in part] by the Developmental Therapeutics Program in the Division of Cancer Treatment and Diagnosis of the National Cancer Institute.

References:

1. Abbott G: Proteomics, transcriptomics; what's in a name? Nature 202:715, 1999
2. Adam BL, Qu Y, Davis JW, et al: Serum protein fingerprinting coupled with a pattern-matching algorithm distinguishes prostate cancer from benign prostate hyperplasia and healthy men. Cancer Res 62:3609, 2002
3. Aivado M, Spentzos D, Alterovitz G, et al: Optimization and evaluation of surface-enhanced laser desorption/ionization time-of-flight mass spectrometry (SELDI-TOF MS) with reversed-phase protein arrays for protein profiling. Clin Chem Lab Med 43:133, 2005
4. Anderson NL, Polanski M, Pieper R, et al: The human plasma proteome: a nonredundant list developed by combination of four separate sources. Mol Cell Proteomics 3:311, 2004
5. Baggerly KA, Morris JS, Coombes KR: Reproducibility of SELDI-TOF protein patterns in serum: comparing datasets from different experiments. Bioinformatics 20:777, 2004
6. Banks RE: Preanalytical influences in clinical proteomic studies: raising awareness of fundamental issues in sample banking. Clin Chem 54:6, 2008
7. Banks RE, Stanley AJ, Cairns DA, et al: Influences of blood sample processing on low-molecular-weight proteome identified by surface-enhanced laser desorption/ionization mass spectrometry. Clin Chem 51:1637, 2005
8. Belluco C, Petricoin EF, Mammano E, et al: Serum Proteomic Analysis Identifies a Highly Sensitive and Specific Discriminatory Pattern in Stage 1 Breast Cancer. Ann Surg Oncol, 2007
9. Bhattacharyya S, Siegel ER, Petersen GM, et al: Diagnosis of pancreatic cancer using serum proteomic profiling. Neoplasia 6:674, 2004
10. Conrads TP, Fusaro VA, Ross S, et al: High-resolution serum proteomic features for ovarian cancer detection. Endocr Relat Cancer 11:163, 2004
11. Cowen EW, Liu, C., Steinberg, S.M., Kang, S., Vonderheid, E.C., Kwak, H.S., Booher, S., Petricoin, E.F., Liotta, L.A., Whiteley, G., Hwang, S.T.: Differentiation of tumor-phase mycosis fungoides, psoriasis vulgaris, and normal controls in a pilot study using serum proteomic analysis. Brit. J. Derm., 2007
12. Diamandis EP: Analysis of serum proteomic patterns for early cancer diagnosis: drawing attention to potential problems. J Natl Cancer Inst 96:353, 2004
13. Drake SK, Bowen RA, Remaley AT, et al: Potential interferences from blood collection tubes in mass spectrometric analyses of serum polypeptides. Clin Chem 50:2398, 2004
14. Ducret A, Van Oostveen I, Eng JK, et al: High throughput protein characterization by automated reverse-phase chromatography/electrospray tandem mass spectrometry. Protein Sci 7:706, 1998
15. Grizzle WE, Adam BL, Bigbee WL, et al: Serum protein expression profiling for cancer detection: validation of a SELDI-based approach for prostate cancer. Dis Markers 19:185, 2003

16. Honda K, Hayashida Y, Umaki T, et al: Possible detection of pancreatic cancer by plasma protein profiling. Cancer Res 65:10613, 2005
17. Hortin GL: Can mass spectrometric protein profiling meet desired standards of clinical laboratory practice? Clin Chem 51:3, 2005
18. Jock CA, Paulauskis JD, Baker D, et al: Influence of matrix application timing on spectral reproducibility and quality in SELDI-TOF-MS. Biotechniques 37:30, 2004
19. Julie H: Protein sequence information by matrix-assisted laser desorption/ionization in-source decay mass spectrometry, in, 2007, Vol 26, pp 672
20. Liotta LA, Ferrari M, Petricoin E: Clinical proteomics: written in blood. Nature 425:905, 2003
21. Liotta LA, Lowenthal M, Mehta A, et al: Importance of communication between producers and consumers of publicly available experimental data. J Natl Cancer Inst 97:310, 2005
22. Little DP, Speir JP, Senko MW, et al: Infrared multiphoton dissociation of large multiply charged ions for biomolecule sequencing. Anal Chem 66:2809, 1994
23. Liu C, Shea N, Rucker S, et al: Proteomic patterns for classification of ovarian cancer and CTCL serum samples utilizing peak pairs indicative of post-translational modifications. Proteomics 7:4045, 2007
24. Loo JA, Edmonds CG, Smith RD: Primary sequence information from intact proteins by electrospray ionization tandem mass spectrometry. Science 248:201, 1990
25. Lopez MF, Mikulskis A, Kuzdzal S, et al: High-resolution serum proteomic profiling of Alzheimer disease samples reveals disease-specific, carrier-protein-bound mass signatures. Clin Chem 51:1946, 2005
26. Lopez MF, Mikulskis A, Kuzdzal S, et al: A novel, high-throughput workflow for discovery and identification of serum carrier protein-bound Peptide biomarker candidates in ovarian cancer samples. Clin Chem 53:1067, 2007
27. Lowenthal MS, Mehta AI, Frogale K, et al: Analysis of albumin-associated peptides and proteins from ovarian cancer patients. Clin Chem 51:1933, 2005
28. Martin SA, Vilhelmsson O, Medale F, et al: Proteomic sensitivity to dietary manipulations in rainbow trout. Biochim Biophys Acta 1651:17, 2003
29. Mehta AI, Ross S, Lowenthal MS, et al: Biomarker amplification by serum carrier protein binding. Dis Markers 19:1, 2003
30. Nedelkov D: Development of surface plasmon resonance mass spectrometry array platform. Anal Chem 79:5987, 2007
31. Nedelkov D: Mass spectrometry-based immunoassays for the next phase of clinical applications. Expert Rev Proteomics 3:631, 2006
32. Nedelkov D, Nelson RW: Surface plasmon resonance mass spectrometry for protein analysis. Methods Mol Biol 328:131, 2006
33. Petricoin EF, Ardekani AM, Hitt BA, et al: Use of proteomic patterns in serum to identify ovarian cancer. Lancet 359:572, 2002
34. Rai AJ, Zhang Z, Rosenzweig J, et al: Proteomic approaches to tumor marker discovery. Arch Pathol Lab Med 126:1518, 2002

35. Rifai N, Gillette MA, Carr SA: Protein biomarker discovery and validation: the long and uncertain path to clinical utility. Nat Biotechnol 24:971, 2006
36. Roepstorff P, Fohlman J: Proposal for a common nomenclature for sequence ions in mass spectra of peptides. Biomed Mass Spectrom 11:601, 1984
37. Santos-Gonzalez M, Gomez Diaz C, Navas P, et al: Modifications of plasma proteome in long-lived rats fed on a coenzyme Q10-supplemented diet. Exp Gerontol 42:798, 2007
38. Semmes OJ, Feng Z, Adam BL, et al: Evaluation of serum protein profiling by surface-enhanced laser desorption/ionization time-of-flight mass spectrometry for the detection of prostate cancer: I. Assessment of platform reproducibility. Clin Chem 51:102, 2005
39. Tworoger SS, Spentzos D, Grall FT, et al: Reproducibility of proteomic profiles over 3 years in postmenopausal women not taking postmenopausal hormones. Cancer Epidemiol Biomarkers Prev 17:1480, 2008
40. von Eggeling F, Junker K, Fiedle W, et al: Mass spectrometry meets chip technology: a new proteomic tool in cancer research? Electrophoresis 22:2898, 2001
41. Wang J, Zhang X, Ge X, et al: Proteomic studies of early-stage and advanced ovarian cancer patients. Gynecol Oncol, 2008
42. Wei YS, Zheng YH, Liang WB, et al: Identification of serum biomarkers for nasopharyngeal carcinoma by proteomic analysis. Cancer 112:544, 2008
43. West-Nielsen M, Hogdall EV, Marchiori E, et al: Sample handling for mass spectrometric proteomic investigations of human sera. Anal Chem 77:5114, 2005
44. Whiteaker JR, Zhao L, Zhang HY, et al: Antibody-based enrichment of peptides on magnetic beads for mass-spectrometry-based quantification of serum biomarkers. Anal Biochem 362:44, 2007
45. Whiteley G: Bringing diagnostic technologies to the clinical lab: rigor, regulation and reality. Proteomics In Press, 2008
46. Whiteley GR: Proteomic patterns for cancer diagnosis-promise and challenges. Mol Biosyst 2:358, 2006
47. Zhong L, Taylor DL, Whittington RJ: Proteomic profiling of ovine serum by SELDI-TOF MS: Optimisation, reproducibility and feasibility of biomarker discovery using routinely collected samples. Comp Immunol Microbiol Infect Dis, 2008
48. Zubarev RA: Electron-capture dissociation tandem mass spectrometry. Curr Opin Biotechnol 15:12, 2004

Figure 1: The SELDI array consisting of 8 spots (sliver) surrounded by a hydrophobic membrane (brown). Twelve of these arrays can be held together in a configuration that has the footprint of a microtiter plate.

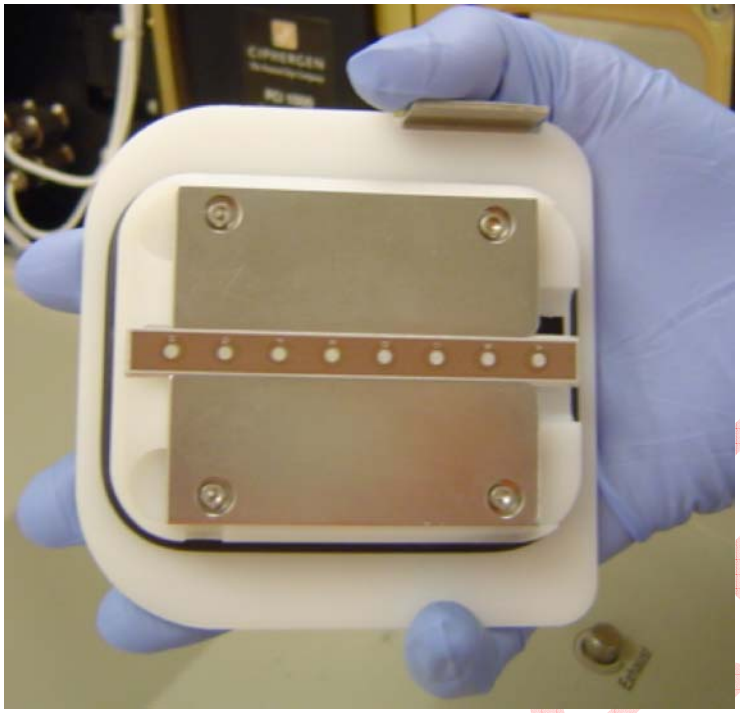

Table 1: Four computer models that identified test sets of samples with ovarian cancer with a sensitivity and specificity of 100%. Note the repeating ions that appear in more than one of the models. Adapted from [10].

Model 1

Test Specificity	100%
Test Sensitivity	100%
Validation Sensitivity	100%
Validation Specificity	100%

Result Breakdown

State	Testing Results	Validation Results
Normal	30/30 (100%)	37/37 (100%)
Ovarian Cancer	57/57 (100%)	40/40 (100%)
STAGE I	17/17 (100%)	12/12 (100%)

Distinguishing *m/z* values

1	1276.8612
2	2374.2444
3	4292.9
4	7060.121
5	8605.678
6	8706.065
7	9870.9375

Model 2

Test Specificity	100%
Test Sensitivity	100%
Validation Sensitivity	100%
Validation Specificity	100%

Result Breakdown

State	Testing Results	Validation Results
Normal	31/31 (100%)	37/37 (100%)
Ovarian Cancer	63/63 (100%)	40/40 (100%)
STAGE I	22/22 (100%)	12/12 (100%)

Distinguishing *m/z* values

1	818.4801
2	6352.7227
3	6548.771
4	7060.121
5	7096.9224
6	8540.536
7	8605.678
8	8706.065

Model 3

Test Specificity	100%
Test Sensitivity	100%
Validation Sensitivity	100%
Validation Specificity	100%

Result Breakdown

State	Testing Results	Validation Results
Normal	31/31 (100%)	37/37 (100%)
Ovarian Cancer	63/63 (100%)	40/40 (100%)
STAGE I	22/22 (100%)	12/12 (100%)

Distinguishing *m/z* values

1	1144.7963
2	4260.4033
3	7046.018
4	8602.237
5	8664.385

Model 4

Test Specificity	100%
Test Sensitivity	100%
Validation Sensitivity	100%
Validation Specificity	100%

Result Breakdown

State	Testing Results	Validation Results
Normal	31/31 (100%)	37/37 (100%)
Ovarian Cancer	63/63 (100%)	40/40 (100%)
STAGE I	22/22 (100%)	12/12 (100%)

Distinguishing *m/z* values

1	1001.6544
2	1255.5934
3	4377.8535
4	6004.4165
5	7060.121
6	7202.716
7	8605.678
8	8709.548
9	9367.113

Table 2: **Recommended practices for clinical applications of protein profiling by matrix-assisted laser desorption/ionization time-of-flight mass spectrometry. (Adapted from Hortin[28])**

Preanalytical

- Evaluate optimum patient preparation
- Identify optimum procedures for specimen collection and processing
- Analyze specimen stability
- Develop criteria for specimen acceptability

Analytical

- Prepare calibrators for mass, resolution, and detector sensitivity
- Use internal standards
- Automate specimen preparation
- Optimize methods to yield highest possible signals for peaks of interest
- Identify sequences of peaks of interest
- Develop calibration materials for components of interest
- QC: prepare/identify at least two concentrations of control material
- Evaluate reproducibility (precision)
- Evaluate limits of detection and linearity
- Evaluate reference intervals
- Evaluate interferences such as hemolysis, lipemia, renal failure, acute-phase responses
- Develop materials or programs for external comparison/proficiency testing of analyzers

Postanalytical

- Analyze each spectrum to identify peaks before applying diagnostic algorithms
- Develop criteria for the acceptability of each spectrum based on peak characteristics
- Use peaks rather than raw data as the basis for diagnostic analysis
- Use caution in interpretation of peaks with $m/z<1200$
- Select peaks with high intensities and sample stability for diagnosis
- Select approximately equal numbers of peaks that increase and decrease in intensity as diagnostic discriminators
- In developing a training set for diagnosis, careful clinical classification of patients is essential
- Clinical validity depends on having a typical rather than highly selected population of patients
- The number of training specimens should be at least 10 times the number of measured values
- Any clinical application should use a fixed training set and algorithm for analysis
- Any analysis should provide a numerical value
- Diagnostic performance should be evaluated with ROC curves to select cutoffs
- A sensitivity analysis should be performed of the necessary precision for accurate diagnostic performance
- There should be QC procedures for daily verification of software performance

Table 3: Classification of blinded samples from study site 2 using a classification system derived from samples collected at study site 1. Classification was done using the peak pair algorithm and involved 4 peak pairs (8 peaks total)[23]. Note the high number of "unknown" results.

	Classification		
	Normal	Cancer	Unknown
Clinical Diagnosis			
Normal n=30	23	2	5
Cancer n=29	4	20	5

Sensitivity: 83%
Specificity: 92%

Figure 2: Immunocapture of proteins from more complex solutions followed by the analysis of the captured material by MALDI mass spectrometry. The mass spectrometry can be done directly on the same surface or in a more concentrated fashion by elution of the captured material.

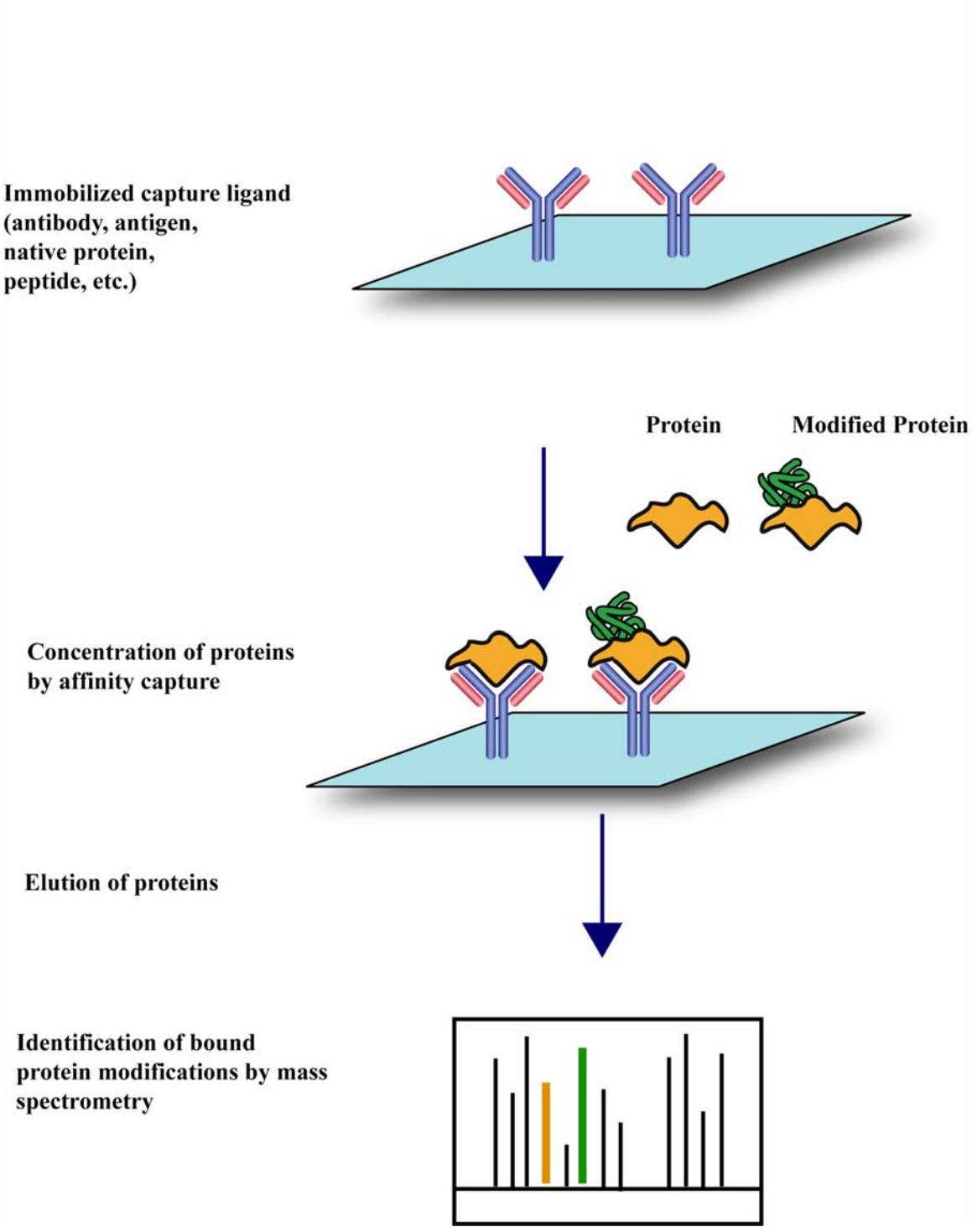

APPENDIX B

Proceedings

Background: Amplification of the HER-2/neu gene (HER-2), overexpression of the HER-2 protein, or both, occur in 20% to 30% of primary breast cancers (BC) and have been correlated with high histologic grade, increased mitotic activity, negative estrogen-receptor (ER) status. Fluorescence *in situ* hybridization (FISH) is used to detect HER-2 amplification. The FDA-approved PathVysion test includes a second probe for the centromeric region of chromosome 17 (CEP17) and allows a correction of the HER-2 gene copy number to the number of copies of chromosome 17 (HER-2/CEP17 ratio). PathVysion test is positive (HER-2 amplified) when HER-2/CEP17 ratio is >2 but a wide variability in the ratio of amplification can be observed in clinical practice.

Methods: Our evaluation was performed on 28 female early stage BC patients (pts) treated with curative surgery at Istituto Clinico Humanitas from August 2001 to January 2005, randomly taken from the archives of Pathology. Patients characteristics were: median age: 55 (range: 36–73); invasive ductal carcinoma: 24 (86%), invasive lobular: 3 (11%); mixed (ductal and lobular) type: 1 (3%).

Results: Seventeen pts had HER-2 amplification with HER-2/CEP17 ratio ranging 2.1–8.5, whereas 11 FISH negative pts represented the control group. Patients with FISH positive were divided into two groups according to the HER-2/CEP17 ratio of HER-2 amplification: low-level HER-2 amplification (HER-2/CEP17 ratio 2.1–3.9) and high-level HER2 amplification (ratio 4–8). Relevant histopathologic features of tumors in the three groups (no amplification/low-amplification/high-amplification, respectively) were as follows: high histologic grade (G3): 36/33/63% (P 0.07 Mantel–Haentzel test); vascular invasion present: 45/44/75%, high proliferative MIB-1 index (MIB-1 protein >20%): 27/44/63%. No significant difference was observed for ER and/or progesterone-receptor status.

Conclusions: This is the first observation of a possible correlation between the level of HER-2 amplification and some relevant histopathological features of BC. Basing on this pivotal experience conducted on a small numbers of pts, we think that the level of HER-2 amplification may have a prognostic role in pts with early stage BC.

C10 A PHARMACOKINETIC STUDY OF GEMCITABINE AT FIXED DOSE RATE INFUSION IN PATIENTS WITH IMPAIRED HEPATIC FUNCTION

Felici A[1,2], Di Segni S[2], Colantonio S[2], Milella M[1], Ciccarese M[1], Cecere FL[1], Nuvoli B[2], Ferretti G[1], Citro G[2] & Cognetti F[1]
[1]Divisione Oncologia Medica A, Istituto Nazionale Tumori Regina Elena, Roma; [2]Laboratorio di Farmacocinetica, Istituto Nazionale Tumori Regina Elena, Roma, Italy

The aim of this study was to evaluate if hepatic dysfunction leads to increased toxicity at fixed dose rate of gemcitabine (gem), and to characterize the pharmacokinetic (PK) of gem and its major metabolite (2′,2′-difluorodeoxyuridine- 2dFdU) in patients with normal and altered liver function. Eight patients with metastatic solid tumor were treated with: gem 1000 mg/m^2 at 10/mg/m^2/min fixed rate days 1, 8, and 15 every 28 days for a maximum of six cycles. Three pts had normal serum bilirubin and AST level (Cohort I); four pts had bilirubin level from 1.6 to 7.0 mg/dl and normal AST level, one pt had bilirubin level less than 1.6 mg/dl and AST level greater than two times the ULN (Cohort II). Patients characteristics were: median age 62 yrs (range 28–75), male/female 4/4, median cycle cohort I: 6 cycle (3–6), median cycle cohort II: 3 cycle (1–5), median follow-up: 30 weeks (range 3–79) and median weeks of treatment: 14 (1–25). The rate of dose reduction was the same in the two cohorts, as the rate of omitted administration. Patients with liver dysfunction tolerated gem without increased toxicity and neither AST nor bilirubin elevation was observed after drug administration. Analysis was performed by HPLC/MS.

The pharmacokinetic results are shown in the table below:

	No pts	C max (μg/ml)		AUC exp (μg h/ml)		t 1/2 (h)		Cl p (L h/m^2)	
		Gem	2dFdU	Gem	2dFdU	Gem	2dFdU	Gem	2dFdU
COHORT I									
Mean cy1	3	6.18	63.00	8.09	138.48	0.15	4.24	124.38	7.29
Mean cy2	3	5.81	49.90	5.60	107.46	0.05	3.00	181.73	10.62
COHORT II									
Mean cy1	5	6.74	52.47	7.81	117.65	0.11	3.14	179.05	8.59
Mean cy2	3	5.88	100.53	5.86	205.54	0.21	1.74	175.32	7.92
Mean CV%*	6	2.09	−17.34	198.38	47.80	29.94	2.83	−33.78	20.82

*Coefficient of variability; cy, cycle; Cl p, plasmatic clearance.

The PK of gem at fixed dose rate in patients with impaired liver function seems similar to control and PK data are comparable between cycles in both cohorts; no difference in terms of toxicity and dose reduction was required for this subset of patients.

C11 EFFECTIVENESS OF THE CRCAPRO PROGRAM IN IDENTIFYING PATIENTS SUSPECTED FOR HNPCC

Galizia E, Bianchi F, Bracci R, Belvederesi L, Loretelli C, Giorgetti G, Ferretti C, Bearzi I, Porfiri E & Celerino R
Istituto di Medicina Clinica e Biotecnologie Applicate, Oncologia Medica, Università Politecnica delle Marche, Ancona, Italy

Background: Subjects affected by Hereditary Non-Polyposis Colorectal Cancer (HNPCC) exhibit a high susceptibility to colon and extracolonic (particularly endometrial) tumours, due to MisMatch Repair genes (MMR) defects. Revised Bethesda criteria are used to select patients candidates to genetic tests. For hereditary breast and ovarian cancer, BRCAPRO is a useful tool in selecting patients to be studied: recently the CRCAPRO model has been developed, based on family history of colorectal and endometrial cancers. Our study aims to evaluate the reliability of CRCAPRO in identifying mutation carriers.

Patients and methods: We used CRCAPRO program to evaluate carrier probability risk in 99 patients fulfilling Amsterdam or Bethesda guidelines. *MLH1* and *MSH2* were studied by direct sequencing in all the 99 patients and, when tumour tissue was available, the study of microsatellite instability and of MMR proteins expression was performed.

Results: Nine *MLH1* and 9 *MSH2* germline mutations were identified. Five out of the 9 patients with *MLH1* mutation showed a CRCAPRO risk evaluation of less than 20%. The same happened for 4 out of nine patients with *MSH2* mutation. On the other hand, of the 17 patients with an estimated risk superior to 80%, only 4 harboured a mutation, all in the *MSH2* gene. The highest risk calculated by the CRCAPRO system in the 9 carriers of a *MLH1* mutation has been 31.7%.

Conclusion: Sensitivity and specificity of the CRCAPRO program appears to be low in our experience but needs to be further evaluated in larger samples.

C12 REVERSE TRANSCRIPTASE INHIBITORS INDUCE CELL DIFFERENTIATION AND ENHANCE THE IMMUNOGENIC PHENOTYPE IN HUMAN RENAL CELL CARCINOMA

Landriscina M[1], Altamura SA[1], Roca L[3], Piscazzi A[1], Fabiano A[2], Maiorano N[1], Ranieri E[3], Barone C[4] & Gesualdo L[3]
[1]Medical Oncology and [2]Endicrinology Units, Department of Medical Science; [3]Nephrology Unit, Department of Biomedical Sciences; School of Medicine, University of Foggia, Foggia; [4]Medical Oncology Unit, Catholic University, School of Medicine, Rome, Italy

Two classes of repeated genomic elements, retrotransposons and endogenous retroviruses, encode for endogenous non-telomeric RT, a gene which is down-regulated in differentiated cells, but is highly expressed in embryonic and transformed tissues. Two non-nucleosidic RT inhibitors such as efavirenz and nevirapine, widely used in the therapy of HIV infection, have been shown to reversibly down-regulate tumor growth and induce differentiation in several human tumor cell models. Since renal cell carcinoma (RCC) is an aggressive neoplasm, poorly responsive to anticancer treatments, we evaluated efavirenz and nevirapine as a differentiating molecular-targeted treatment to enhance the immunogenic phenotype in RCC Shaw cells as well as in primary cultures of human RCC. We observed that the two RT inhibitors reversibly down-regulated cell proliferation by 70–80%, without inducing either apoptotic or necrotic cell death. Interesting, pharmacological inhibition of RT activity correlated with the appearance of a more differentiated phenotype and with the up-regulation of the vitamin D receptor, a gene which is known to co-regulate cell proliferation, differentiation and apoptosis in RCC. Interestingly, RT inhibitors induced the protein expression of HLA-I and CD40, two molecules involved in antigen presentation and T-lymphocytes stimulation. Indeed, co-cultures of nevirapine-treated RCC cells and autologous T lymphocytes as well as the evaluation of PBMC-specific interferon-γ release by ELISPOT demonstrated a significant T cell lymphocytes activation, with the up-regulation of the CD3/CD56/CD16 NK subpopulation and the down-regulation of CD3/CD4/CD25 T-reg cells, which are involved in the suppression of the immune response. These data suggest that the pharmacological inhibition of RT may represent a new strategy able to enhance the sensitivity to immune therapy in human RCC.

C13 THE PROGNOSIS OF BRCA1/2 RELATED CANCERS. ANALYSIS OF 70 CASES DIAGNOSED AT MODENA CANCER CENTER FOR FAMILIAL BREAST AND OVARIAN CANCER

Cortesi L[1], Calista F[2], Ruscelli S[1], Cavazzini G[3], Artioli F[4], Turchetti D[5], Pasini G[6], Medici V[1], Rashid I[1] & Federico M[1]
[1]Dipartimento di Oncologia ed Ematologia Università di Modena e Reggio Emilia; [2]U.O. Oncologia Medica Università degli Studi L'Aquila; [3]Oncologia Medica Ospedale C. Poma, Mantova; [4]Servizio di Oncologia, Ospedale Carpi; [5]Cattedra ed U.O. Genetica Medica Policlinico S. Orsola–Malpighi Bologna; [6]U.O.Oncologia ed Oncoematologia, Ospedale Infermi Rimini, Italy

The BRCA1 breast cancer (BC) are often characterized by an aggressive tumor phenotype with a worse prognosis for BRCA1 than BRCA2 carriers. To assess the behavior of BRCA related cancers we performed a comparison between BRCA and sporadic BC observed at the Modena Cancer Registry (MCR). Between 1996 and 2005, 403 index cases were analyzed for BRCA1/2 mutations at our center. Out of 403 analysis, 80 (20%) were found carriers, of which 16 were ovarian cancers. Out of the 64 BRCA related BC, 40 resulted BRCA1 and 24 BRCA2 carriers. All the patients were analyzed for clinical–pathological profile and 5-year survival rates were compared with a series of 5587 sporadic BC registered by the MCR in the same time frame. The median age at diagnosis was 38 in the BRCA group and 61 years in the control one ($P < 0.001$). The most frequently hystotype was DCI (72%) as in the control group (75%). The

Journal of Clinical Oncology, 2006 ASCO Annual Meeting Proceedings (Post-Meeting Edition).
Vol 24, No 18S (June 20 Supplement), 2006: 12009

A pharmacokinetic study of gemcitabine at fixed dose rate infusion in patients with impaired hepatic function

A. Felici, S. Di Segni, S. Colantonio, M. Milella, M. Ciccarese, F. Cecere, B. Nuvoli, G. Ferretti, G. Citro and F. Cognetti

Regina Elena National Cancer Institute, Rome, Italy

12009

Background: The aim of this study was to evaluate if hepatic dysfunction leads to increased toxicity of gemcitabine (gem) at fixed dose rate, and to characterize the pharmacokinetic (PK) of gem and its major metabolite (2`,2`-difluorodeoxyuridine- 2dFdU) in patients (pts) with normal and altered liver function. **Methods:** Eight pts with metastatic pancreatic or biliary tract cancer were treated with the followed schedule: gem 1000 mg/m2 at 10/mg/m2/min fixed rate days 1,8, and 15 every 28 days for a maximum of six cycles. Three pts had normal serum bilirubin level and AST level less than two times the upper limit of normal (ULN) (Cohort I); four pts had bilirubin level from 1.6 to 7.0 mg/dL and normal AST level, one pt had serum bilirubin level less than 1.6 mg/dL and AST level greater than two times the ULN (Cohort II). The PK parameters measured were: plasmatic peak concentration (*Cmax)*, area under the plasma concentration-time curve (*AUCexp*), total plasma clearance (*Cl p*) and half life ($t_{1/2}$). **Results:** Patient characteristics were: median age 62 yrs (range 28–75), male/female 4/4, median cycles cohort I: 6 cycles (3–6), median cycles cohort II: 3 cycles (1–5), median follow-up: 30 weeks (range 3–79) and median weeks of treatment: 14 (1–25). The rate of dose reduction was the same in the two cohorts, as the rate of omitted administrations. Patients with liver dysfunction tolerated gemcitabine without increased toxicity and neither AST nor bilirubin elevation was observed after drug administration. PK parameters were calculated at the first cycle and the results are presented below (see table). **Conclusions:** The pharmacokinetics of gemcitabine at fixed dose rate in patients with impaired liver function seems similar to control; no difference between the two cohorts was observed in terms of toxicity and dose reduction.

APPENDIX C

Oral Presentations

The results of the proteomics profiling studies have been presented in two different occasions.

The oral presentation "*A comparison of SELDI and High Resolution MALDI serum profiling with CA-125 in High Risk and confirmed Ovarian Cancer samples*" has been held on July 10th, 2007 at the Workshop Italy-USA Program on Oncoproteomics, in Rome at the Istituto Superiore di Sanità.

"*Advances in Proteomic Profiling for Biomarker Discovery*" was presented at the NCI-Frederick, MD, USA as an event part of Advanced Technology Program Staff Seminar Series in January 30th, 2008.